FISEVIER

Contents lists available at ScienceDirect

# Progress in Oceanography

journal homepage: www.elsevier.com/locate/pocean



# Carbon cycling in the Sargasso Sea water column: Insights from lipid biomarkers in suspended particles



R. Pedrosa-Pàmies<sup>a,\*</sup>, M.H. Conte<sup>a,b</sup>, J.C. Weber<sup>a</sup>, R. Johnson<sup>b</sup>

- <sup>a</sup> The Ecosystems Center, Marine Biological Laboratory, Woods Hole, MA, USA
- <sup>b</sup> Bermuda Institute of Ocean Science, St. Georges GE01, Bermuda

#### ARTICLE INFO

Keywords:
Suspended particulate matter
Lipid biomarkers
Particle cycle
Hurricanes
Sargasso Sea
Bermuda
Carbon cycle

#### ABSTRACT

This study compares lipid biomarker and bulk constituents (organic carbon and  $\delta^{13}$ C, nitrogen and carbonate) in particles (30–4400 m depth) collected at the Oceanic Flux Program site in the northern Sargasso Sea off Bermuda during three periods of contrasting oceanographic conditions: following the spring bloom (April 2015), during the low productivity period (November 2015), and two weeks after the passage of the Category 3 Hurricane Nicole (October 2016). Lipids biomarkers were used to evaluate the contributions of phytoplankton, zooplankton and bacterial sources to the particulate organic carbon (POC), diagenetic transformations of suspended POC throughout the water column and within the nepheloid layer, and seasonal and non-seasonal temporal variability, including the impact of an extreme weather event.

Depth profiles of lipid concentration and molecular composition showed seasonal and non-seasonal variability in particle composition throughout the water column. Higher lipid concentrations in April versus November 2015 reflected differences in plankton productivity, while relative abundances in diagnostic phytosterols,  $C_{18}$  polyunsaturated fatty acids and alkenones reflected differences in phytoplankton community structure. A rapid decrease in lipid biomarker concentrations below the euphotic zone was accompanied by a marked transition in lipid composition, e.g. increases in the relative percentages of cholesterol,  $C_{16}$ - $C_{18}$  fatty alcohols, odd- and branched- chain fatty acids. This reveals the intense remineralization of algal-derived carbon and fresh inputs of organic materials from zooplankton and microbial production within the upper mesopelagic zone. Particulate lipids within the bathypelagic zone reveal a close connectivity of deep particulate carbon composition with upper ocean properties, while compositional heterogeneity with depth reflects continuous particle turnover and *de novo* particle production throughout the deep water column. Additionally, depth trends in the within-class composition of fatty alcohols and bacterial fatty acids were observed, suggesting depth zonation of zooplankton and microbial community structure.

Hurricane Nicole (October 2016) strongly impacted upper ocean physics and nutrient supply, resulting in a transient phytoplankton bloom/flux event that increased concentrations of fresh particulate phytodetritus (e.g.,  $C_{18}$  polyunsaturated fatty acids) throughout the mesopelagic and upper bathypelagic zones. Concurrent increases in zooplankton and bacterial lipid biomarkers (e.g.,  $18:1\omega9$ , odd- and branched-chain fatty acids, cholesterol) indicated that this transient pulse of labile carbon stimulated mesopelagic zooplankton and microbial activity, resulting in an enrichment of labile materials in the suspended particle pool throughout the deep ocean. Our study demonstrates that extreme weather events can have a major impact on carbon flux and particle cycling in the deep ocean, with pronounced implications for the ocean carbon pump and deep ocean ecosystems.

# 1. Introduction

The transfer of particulate organic carbon (POC) from the surface ocean to deep waters plays a key role in the global carbon cycle. Only a small fraction of the carbon fixed by marine plankton is exported as sinking particles to the deep ocean (Henson et al., 2012; Wakeham and

Lee, 1989), but this fraction drives the sequestration of carbon dioxide from the atmosphere, supplies the energy that fuels life within the ocean interior (Sanders et al., 2016) and seafloor (Gooday, 2002; Tyler, 2003) and controls the global cycling and ocean distributions of nutrients and many elements (Martiny et al., 2014; Weber et al., 2016). Improved understanding of the oceanic particle cycle and how it is impacted by

E-mail address: rpedrosa@mbl.edu (R. Pedrosa-Pàmies).

<sup>\*</sup> Corresponding author.

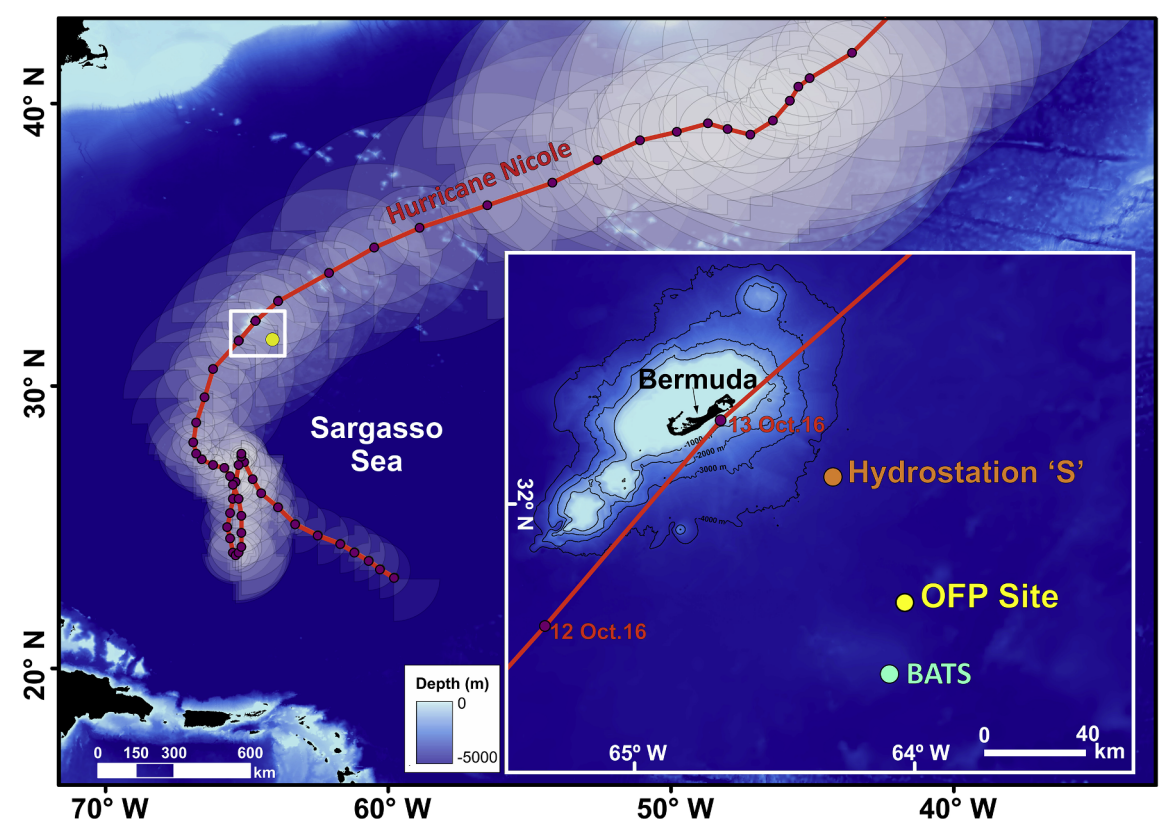


Fig. 1. Map of the study region and insert showing the Bermuda Time-Series Site and locations of the OFP, BATS and Hydrostation S time-series. The track of Category 3 Hurricane Nicole (4–18 October 2016) is also shown (red line). (For interpretation of the references to colours in this figure legend, the reader is referred to the web version of this paper.)

seasonal and non-seasonal forcing by upper ocean physics and biology is crucial to evaluate feedbacks between the carbon cycle and the climate system. This is particularly urgent in oligotrophic gyres, which comprise roughly 75% of the ocean area (Lewis et al., 1986), and contribute over 30% of the global marine carbon fixation (Marañón et al., 2003).

The amount of POC exported from the surface waters is controlled by biological processes, such as surface primary and secondary production and remineralization by microbial and zooplankton communities (Cavan et al., 2017; Herndld and Reinthaler, 2013), but also by physical processes such mixing and advection (Levy et al., 2013). Mesoscale eddies in oligotrophic waters play an important role in nutrient supply, thus stimulating phytoplankton production and, in turn, increasing the oceanic carbon export flux (Benitez-Nelson et al., 2007; Buesseler et al., 2008; Conte et al., 2003; McGillicuddy et al., 1998; Oschlies, 2002; Shih et al., 2015; Stukel et al., 2017).

Physical forcing of the upper water column by large storms and hurricanes also affects biogeochemical processes in the upper ocean. These events dissipate large amounts of energy into the surface ocean, locally enhancing vertical mixing and causing cooling and nutrient enrichment (e.g., Price, 1981; Jacob et al., 2000; Walker et al., 2005). Due to difficulties of shipboard data collection in extreme weather conditions, the direct impacts of extreme weather events have been poorly studied (Chen et al., 2013; Hung et al., 2009). Advances in non ship-based sampling platforms such as gliders and autonomous floats, remote sensing and in modeling are beginning to provide a better understanding of how extreme weather events influence the upper ocean carbon cycle (e.g., Hodson, 2013; Guan et al., 2014; Domingues et al., 2015; Bishop et al., 2016; Shropshire et al., 2016; Goni et al., 2017), but we still have a very limited understanding of how extreme weather events might influence the particle flux and deep ocean ecosystems (Fröb et al., 2016; Pedrosa-Pàmies et al.,

# 2016; Smith et al., 2013, 2009).

The composition of suspended POC within the water column reflects contributions from a variety of sources (phytoplankton, bacteria, zooplankton tissue and excreta, or organic detritus), diagenetic alterations of primary materials by microbial and animal particle processing, and exchanges with the sinking and dissolved/colloidal organic carbon pools (Abramson et al., 2010; Boyd et al., 1999; Dong et al., 2010; Hannides et al., 2013; Lee et al., 2004; Volkman and Tanoue, 2002). Despite the fact that over 90% of particulate material in the deep water column is suspended, this POC pool remains relatively understudied in terms of its sources, chemical composition, and processing by deep water ecosystems.

Due to their structural diversity and source specificity, lipid compounds are valuable tools for identifying organic matter (OM) sources, fate, diagenesis and reactivity in marine environments (e.g., Lee et al., 1988; Meyers, 1997; Wakeham et al., 1997; Volkman, 2006). However, there are few studies that have used lipid biomarkers to characterize the suspended OM pool (Abramson et al., 2010; Close et al., 2014; Conte, 1990; Conte et al., 1995; Gašparović et al., 2018, 2017, 2016; Loh et al., 2008; Sheridan et al., 2002; Tolosa et al., 2003, 2013; Wakeham, 1995).

In this paper we present a detailed study of lipid biomarkers in particle profiles collected at the Bermuda Time-series Site in the northern Sargasso Sea during three contrasting time periods: post spring bloom (April 2015), minimum productivity (November 2015), and following passage of a Category 3 hurricane (Hurricane Nicole, October 2016). The Bermuda Time-series site is among the most intensively studied open ocean regions in the world, yet there have been few compositional studies of suspended POC below the euphotic zone (Cavagna et al., 2013; Gundersen et al., 2001), and in particular only limited investigation of organic composition (Ittekkot, 1993).

#### 2. Material and methods

#### 2.1. Study area

The Bermuda Time-Series Site is located in the oligotrophic northern Sargasso Sea gyre about 75 km southeast of the island of Bermuda (Fig. 1). Water depth is 4500 m. Currents in the area are generally weak, with mean velocities of 5 cm s<sup>-1</sup> at 500 m depth decreasing to < 1 cm s<sup>-1</sup> below 1500 m depth (Gust et al., 1994; McKee et al., 1981). The Site hosts several ongoing multi-decadal time-series: the Hydrostation S (since 1954) time-series of hydrographic parameters (Michaels and Knap, 1996; Phillips and Joyce, 2007; Steinberg et al., 2001), the Oceanic Flux Program (OFP, since 1978) time-series of deep ocean fluxes (Conte et al., 2001a; Conte and Weber, 2014; Deuser, 1986), the Bermuda Atlantic Time-series Study (BATS, since 1988) time-series of upper ocean biogeochemistry (Lomas et al., 2013; Michaels and Knap, 1996; Steinberg et al., 2001) and previously the Bermuda Testbed Mooring (BTM, 1995–2007, Dickey et al., 2001) time-series of upper ocean physics and optics.

The seasonal patterns in mixed layer dynamics and primary production in the area have been previously described (Lomas et al., 2013; Phillips and Joyce, 2007; Steinberg et al., 2001). Convective mixing in the late fall and winter generates a deep winter mixed layer, which reaches a maximum depth of between 150 and 300 m in February. With the onset of seasonal stratification in late February- early March, a short-lived phytoplankton bloom develops. Increasing solar stratification in late spring reduces vertical mixing and nutrient supply, limiting primary productivity. A shallow ( $< 20\,\mathrm{m}$ ), strongly stratified mixed layer is present in summer and fall, resulting in a minimum in primary production.

Significant inter-annual variability is present in upper ocean biogeochemical parameters, the seasonal cycle of production (Lomas et al., 2013; Steinberg et al., 2001), and the deep particle flux (Conte et al., 2001a; Conte and Weber, 2014). Part of the non-seasonal seasonal variability arises from mesoscale physical variability, driven by eddies and fronts, which alters nutrient influx into the euphotic zone and in turn phytoplankton production (Babin et al., 2004; Conte et al., 2003; Dickey et al., 2001; Krause et al., 2010; McGillicuddy et al., 1998; McNeil et al., 1999; Shropshire et al., 2016; Siegel et al., 1999). Synoptic-scale weather systems, such as the passage of strong storms and hurricanes, alter upper-ocean heat loss and mixing (Jacob et al., 2000; Price, 1981) and also contribute to short-lived variability. Dickey et al. (1998) and Black and Dickey (2008) describe the upper ocean response after the passage of hurricanes over the Bermuda Testbed Mooring, including the generation of large inertial currents, a decrease in sea surface temperature, a deepening of the mixed layer and upwelling of nutrients stimulating phytoplankton production.

#### 2.2. Sample collection

Suspended particle profiles were collected using McLane WST-LV *in situ* pumps (McLane Laboratories Inc., Falmouth, MA, USA) at the OFP Site during three time periods: one month following the spring bloom (15–19 April 2015), in the late fall when phytoplankton productivity is low (13–17 November 2015), and two weeks after passage of a Category 3 Hurricane (Nicole, 25–29 October 2016). The pumps were fitted with dual filter holders for simultaneous collection of particles for organic and elemental analysis (not presented here). Ten to fifteen depths were sampled on each cruise, targeting the epipelagic (30–100 m), the upper mesopelagic (200–500 m), the lower mesopelagic (500–1000 m), the upper bathypelagic (1000–2500 m), the lower bathypelagic (> 2500 m) and the nepheloid (4400 m) layers (Table 1). Time constraints in November 2015 limited sampling to the mixed layer and below 650 m.

Samples collected for lipid analysis filtered between 160L and 2200 L (based on depth) through a pre-combusted (380  $^{\circ}$ C), 142 mm diameter

Table 1

Suspended collection depths in April 2015, November 2015 and October 2016, and abbreviations used in this paper for the epipelagic (30–100 m), upper mesopelagic (250–500 m), lower mesopelagic (700–1000 m) upper bath-ypelagic (1000–2500 m), lower bathypelagic (> 2500 m) and nepheloid (4400 m) layers.

	Depths sampled (m)								
Depth layer	April	November	October						
Epipelagic (EL)	30, 80, 100	30, 80	30, 80, 100						
Upper Mesopelagic (Up. ML)	200, 250, 450, 500	-	200, 250, 500						
Lower Mesopelagic (L. ML)	-	650, 850	700, 800, 850, 1000						
Upper Bathypelagic (Up. BL)	1500, 1700, 2300, 2500	2300, 2500	1500, 1700						
Lower Bathypelagic (L. BL)	3200, 3400, 4200	3200, 4200	3200, 4200						
Nepheloid (NL)	4400	4400	4400						

GF/F filter (Millipore, nominal 0.7  $\mu$ m pore size). After recovery, subsamples (22 mm diameter) were immediately taken from each filter for organic carbon/nitrogen and carbonate analyses and frozen at  $-30\,^{\circ}$ C. The remaining filter, designated for lipid analysis, was immersed in 2:1 CHCl<sub>3</sub>-MeOH (Optima grade, ThermoFisher Scientific) and stored at  $-30\,^{\circ}$ C

OFP, BATS and Hydrostation S cruises collected data on oceanographic conditions before and during pump sampling dates. Temperature, salinity, oxygen, fluorescence and beam attenuation profiles were obtained from CTD casts made during BATS and OFP cruises. CTD bottle data for nitrate (NO<sub>3</sub>), nitrite (NO<sub>2</sub>), POC and phytoplankton pigments were obtained from BATS CTD casts on 9 April 2015 (7 days before suspended particle collection), 29 November 2015 (15 days after suspended particle collection), and 19 October 2016 (7 days before suspended particle collection). Current profiles of the upper 280 m of the water column were obtained from the Acoustic Doppler Current Profiler (ADCP, 150 KHz RDI Quarter Master) located at the top of the OFP mooring.

# 2.3. Analytical methods

#### 2.3.1. Phytoplankton pigments

Samples for phytoplankton pigment analyses were taken from 12 depths in the upper 250 m at the BATS site and processed using standard BATS protocols (Knap et al., 1997). At each depth 4 L of seawater were filtered under vacuum onto 25 mm Whatman GF/F filters and then flash frozen in liquid nitrogen. In the laboratory, filter samples were extracted in 100% acetone and analyzed by both standard fluorometric (Turner AU10) and high performance liquid chromatography (HPLC) techniques using the method of Bidigare (1991). The HPLC analyses were performed on an Agilent 1100 series instrument. Pigment concentrations were quantified from instrument response and retention times previously standardized using commercial pigment standards from the Danish Hydraulic Institute, Denmark.

#### 2.3.2. Bulk carbon, nitrogen, carbonate and stable isotopes

Filter subsamples for bulk analyses were oven dried at 60 °C. Carbonate was measured by automated coulometric titration of carbon dioxide (Engleman et al., 1985; Huffman, 1977) using a Coulometrics model 5011 coulometer equipped with a System 140 module for inorganic carbon determination. Subsamples for organic carbon/nitrogen were decalcified by fuming overnight with concentrated HCl and then drying at 60 °C. Particulate organic carbon (POC) and total nitrogen (N) concentration and isotopic composition were analyzed at the MBL Stable Isotope Laboratory using a Europa 20-20 continuous-flow isotope ratio mass spectrometer interfaced to a Europa ANCA-SL elemental analyzer. All samples were analyzed in duplicate.

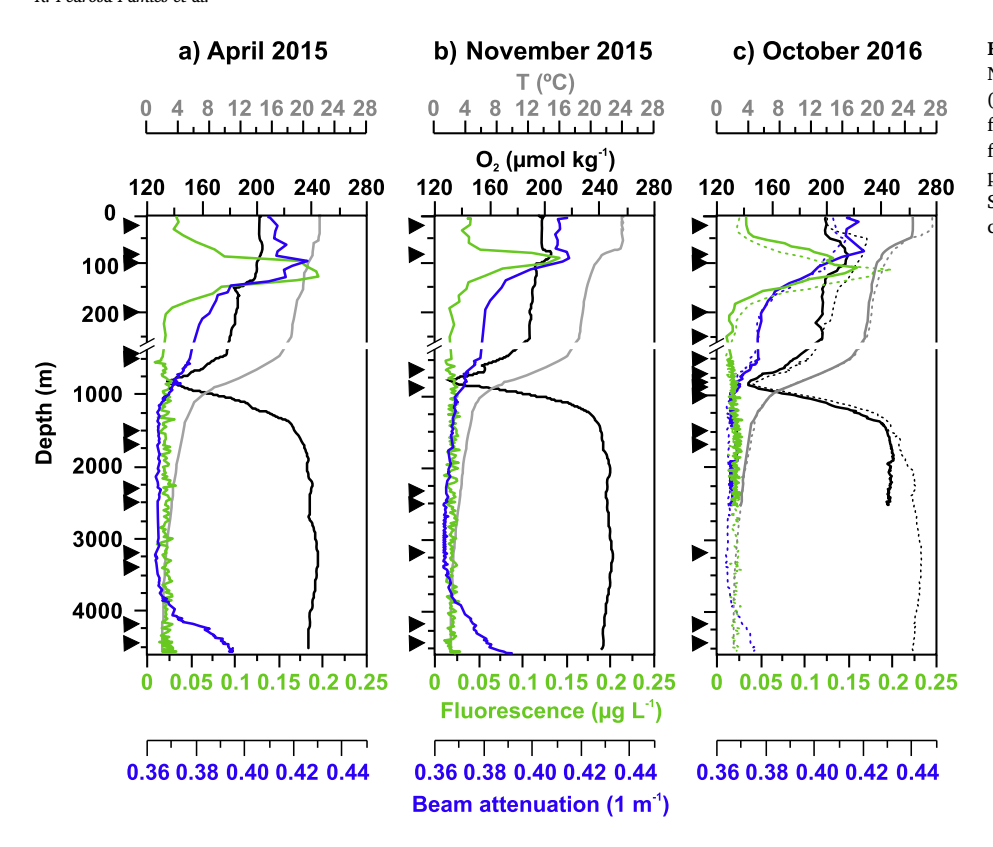


**Fig. 2.** Water column properties in April and November 2015 and in October 2016: Temperature (T,  $\,^{\circ}$ C), oxygen concentration ( $O_2$  µmol kg $^{-1}$ ), fluorescence (µg L $^{-1}$ ) and beam attenuation coefficient (1 m $^{-1}$ ) (0–4600 m). The October 2016 profiles show water column properties before (30 September, dashed lines) and after (25 October, continuous lines) Hurricane Nicole.

#### 2.3.3. Lipid biomarkers

Lipids were extracted from the GF/F filters using a modification of the method detailed in Conte et al. (2003). Briefly, an internal standard mixture consisting of n-C<sub>21:0</sub> fatty alcohol, n-C<sub>23:0</sub> fatty acid, 5α-cholestane and n- $C_{36:0}$  alkane was added to the samples prior to lipid extraction. Lipids were then ultrasonically extracted using 2:1 CHCl3-MeOH (~120 W, 2 min). Salts and non-lipid components were removed from the extracts using the cleanup procedure of Folch et al. (1957). The lipid extracts were concentrated to just dryness using a rotoevaporator, resuspended in CHCl3, and passed through a short bed of combusted, anhydrous Na<sub>2</sub>SO<sub>4</sub> to remove residual water. The purified sample extract was then transesterified using anhydrous 10% methanolic HCl (55 °C, 12 h), following the procedure of Christie (1982). The transesterified lipid products were extracted into hexane and passed through a short bed of Na<sub>2</sub>SO<sub>4</sub> to remove residual water. The hexane was evaporated using a Savant SpeedVac (SC110) and resuspended in CH<sub>2</sub>Cl<sub>2</sub>. Just prior to gas chromatography-mass spectrometry (GC-MS), sample extracts were transferred to GC-MS autosampler v-vials, evaporated under a stream of N2 and TMS-derivatized under N2 using 25 µL pyridine and 25 μL of N,O-Bis (trimethylsilyl)triof fluoroacetamide + 1% Trimethylchlorosilane (BSTFA + 1% TMCS) (55 °C, 1 hr.). The TMS reagents were evaporated under N2 and the samples resupended in CH<sub>2</sub>Cl<sub>2</sub>.

The transesterified, trimethylsilyl derivatives were analyzed on an Agilent 7890A GC coupled to a 5975C MS equipped with triple-axis MS and FID detectors. A Varian CPSil 5CB low bleed MS column (60 m  $\times$  0.25 mm diameter  $\times$  0.25 µm film thickness) was used to separate the lipid compounds. The temperature programming was 50 °C (2 min hold), 10 °C/min to 150 °C, 4 °C/min to 320 °C and then held for 35 min. Compounds were identified by their mass spectra and were quantified from their FID response relative to the internal standard.

#### 2.4. Multivariate analysis

Principal component analysis (PCA) was performed to reduce the multidimensionality of the data set and to identify the dominant factors

contributing to the variance. A total of 39 observations (depth intervals) and 86 variables were selected, using the most abundant compounds or lipid groups. PCA was performed using XLSTAT, an add-in software package for Microsoft Excel (Addinsoft Corp.) All variables were normalized prior to PCA analysis. A Varimax rotation was applied to the first three principal components to simplify the visual interpretation of data in PCA projections while preserving the trends.

#### 3. Results

#### 3.1. Water column properties and elemental composition

**April 2015.** April was typical of late-spring conditions (Steinberg et al., 2001), with depth-integrated primary production of 543 mg C m $^{-2}$  d $^{-1}$ . There was a weakly stratified 40 m mixed layer depth and a broad well-developed subsurface fluorescence maximum between 95 and 130 m (Fig. 2). Nutrient profiles (Fig. 3) show NO<sub>3</sub> depletion in the mixed layer and a strong NO<sub>2</sub> subsurface max. (0.25 μmol L $^{-1}$ ) at 120 m, typical of stratified conditions (Lomas and Lipschultz, 2006). POC concentrations averaged 18 μg L $^{-1}$  in the mixed layer and increased to  $\sim$  27 μg L $^{-1}$  between 40 and 80 m before declining to concentrations less than 10 μg L $^{-1}$  below 120 m depth.

Pigment data (Fig. 3) showed a strong deep Chl a maximum of  $\sim$  340 ng L $^{-1}$  at 80 m depth. The haptophyte pigment 19-hexanoyloxyfucoxanthin (Hex-fuco) and the pelagophyte/dictyochophyte pigment 19-butanoyloxyfucoxanthin (But-fuco) had similar concentration profiles as Chl a, with maximum concentrations of 120 ng L $^{-1}$  and 40 ng L $^{-1}$ , respectively, at 80 m depth. The concentration maximum of the chlorophyte/prasinophyte pigment a+b Carotene (a+b Car, 30 ng L $^{-1}$ ) was shallower, occurring at 60 m depth. The diatom/haptophytes/pelagophytes/dictyochophytes/dinoflagellates pigment diadinoxanthin (data not shown) had a shallow surface peak at 1–10 m (9 ng L $^{-1}$ ), and maximum concentrations at 80 m (11 ng L $^{-1}$ ), before declining to 1 ng L $^{-1}$  by 140 m depth.

Suspended POC, N and CaCO<sub>3</sub> profiles collected by *in situ* pumps one week later are shown in Fig. 4. In the upper 250 m, POC concentrations

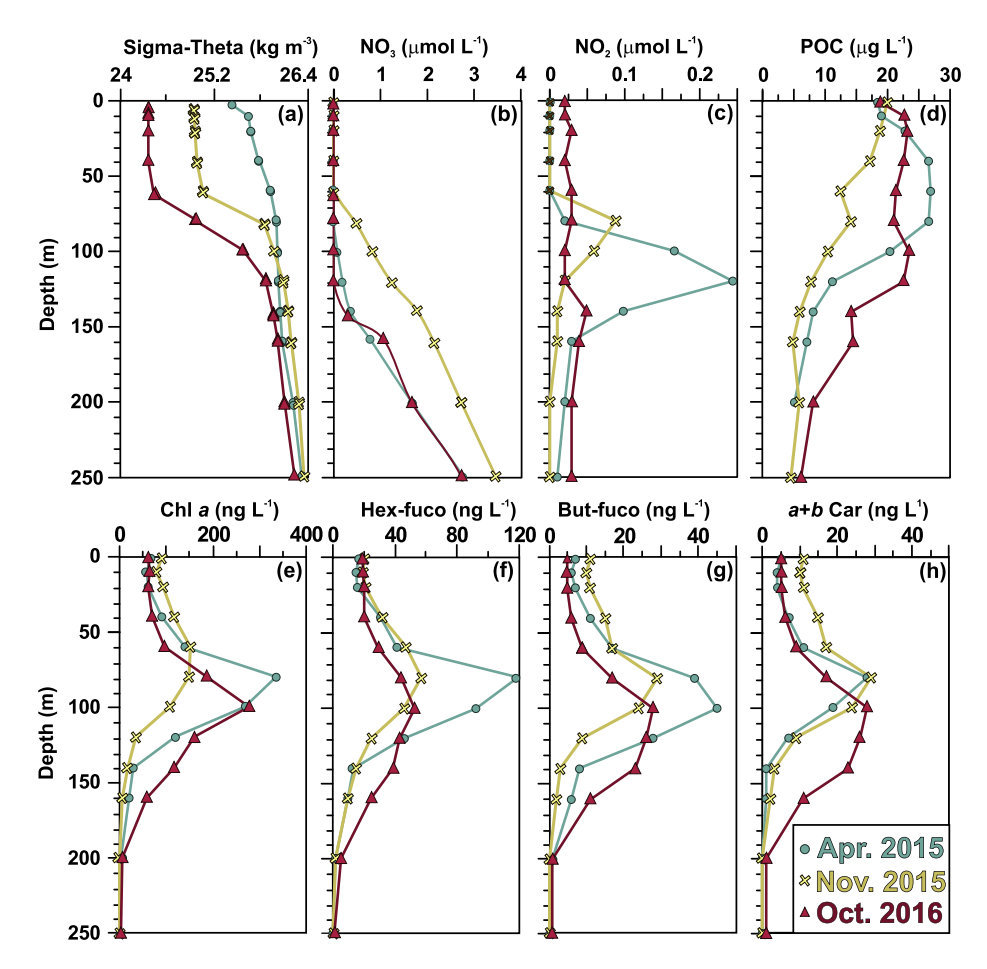


**Fig. 3.** Vertical profiles of density (kg m<sup>-3</sup>), nutrient concentration ( $\mu$ mol L<sup>-1</sup>) and pigment concentrations (ng L<sup>-1</sup>) measured on 9 April 2015, 29 November 2015 and 18 October 2016, five days after passage of Hurricane Nicole. (a)  $\sigma_b$  (b) nitrate (NO<sub>3</sub>) and nitrite (NO<sub>2</sub>), (c) POC, (d) Chlorophyll a (Chl a), e) 1,9-Hexanoyloxyfucoxanthin (Hex-fuco), (f) 19-Butanoyloxyfucoxanthin (But-fuco), and (g) a+b Carotene (a+b Car).

were similar to the BATS bottle data (Fig. 3). POC concentrations decreased with depth to 0.8  $\mu g \; L^{-1}$  at 1500 m and then remained constant deeper in the water column. The  $\delta^{13}C$  of the POC decreased from -24.0% at 30 m to a minimum of -24.8% at 100 m, and then increased to -22.5% at 250 m. Between 450 and 3400 m depths,  $\delta^{13}$ C averaged -22.2% with no apparent depth trend. A sample collected at 2300 m had a depleted  $\delta^{13}$ C value of -23.4%, suggesting fresher, more lipid rich  $(\delta^{13} \mbox{C depleted})$  material in this sample. The C/N molar ratio was highest at the surface (7.6) and rapidly declined with depth to values of 5.0-5.5 below 100 m. No depth trend was observed in the deep water column. CaCO<sub>3</sub> concentrations within the mixed layer averaged 8.0 µg L<sup>-1</sup> and increased by nearly a factor of three to a maximum (22  $\mu$ g L<sup>-1</sup>) at deep chlorophyll maximum, indicating high coccolithophore concentration.  $CaCO_3$  concentrations then rapidly declined to 6.3 µg  $L^{-1}$  at 200 m depth and continued to decline deeper in the water column, with a small increase ( $\sim$ 5 µg  $L^{-1}$ ) observed between 450 and 500 m. CaCO<sub>3</sub> concentrations decreased a further 50% between 500 and 1500 m depths and then remained constant deeper in the water column.

Increase in beam attenuation below 3800 m depth indicated the presence of a weak nepheloid layer, with maximum beam attenuation at 4500 m depth (Fig. 2a). Within the nepheloid layer, POC concentrations increased by 20% between 4200 m (0.5  $\mu g~L^{-1}$ ) and 4400 m (0.6  $\mu g~L^{-1}$ ), C/N molar ratio decreased from 5.2 to 4.8, and CaCO $_3$  concentrations increased by 50%, from 2.1  $\mu g~L^{-1}$  to 3.4  $\mu g~L^{-1}$ .

**November 2015.** November 2015 was characterized by very low productivity conditions at Bermuda (Steinberg et al., 2001), with depthintegrated primary production of 106 mg C m $^{-2}$  d $^{-1}$ , 20% of that in April. A narrow fluorescence peak was centered at 80 m depth (Fig. 2b). Nutrients were depleted in the mixed layer and showed a weak NO<sub>2</sub> subsurface max (0.09 µmol L $^{-1}$ ) at the fluorescence maximum (Fig. 3).

POC concentrations were highest at the surface ( $\sim 20~\mu g~L^{-1}$ ) and gradually declined to concentrations of  $\sim 5~\mu g~L^{-1}$  below 100 m depth. The deep maximum in Chl a concentration in November (150 ng  $L^{-1}$ ) was only  $\sim 45\%$  that in April, reflecting the low primary production. Similarly, peak concentrations of Hex-fuco and But-fuco were also lower by  $\sim 50\%$  and  $\sim 30\%$ , respectively. In contrast, the subsurface maximum for a+b Car and fucoxanthin (data not shown), were similar to concentrations observed in April. Diadinoxanthin (data not shown) concentrations were highest at the surface ( $\sim 6~n g~L^{-1}$ ) and declined to 1 ng  $L^{-1}$  at 140 m. Although pigment concentrations within the deep chlorophyll maximum were lower in November than in April, mixed layer concentrations of Chl a, But-fuco and a+b Car were higher and suggested a recent surface production event.

POC concentrations two weeks later (Fig. 4) were similar to those in the BATS bottle data (Fig. 3). POC  $\delta^{13}C$  within the mixed layer was -23.0% and decreased to a minimum at the deep fluorescence maximum (-24.0%). C/N molar ratio also decreased, from 6.6 within the mixed layer to 6.0 at the deep fluorescence maximum. In contrast, CaCO3 concentrations were similar at 30 m and 80 m ( $\sim 5~\mu g~L^{-1}$ ). Below 600 m, POC concentrations,  $\delta^{13}C$  and C/N ratios were similar to those observed in April. POC concentrations decreased from  $1.4~\mu g~L^{-1}$  at 650 m to 0.6  $\mu g~L^{-1}$  at 3200 m, and  $\delta^{13}C$  values ranged between -21.2% to -22.9% with no consistent depth trend. CaCO3 concentrations decreased with depth, from  $\sim 4~\mu g~L^{-1}$  between 650 m and 850 m, to  $\sim 3~\mu g~L^{-1}$  between 2300 and 2500 m, to  $\sim 2~\mu g~L^{-1}$  at 3200 m depth.

Beam attenuation in November also indicated the presence of a weak nepheloid layer below 3800 m with maximum particle concentrations at 4550 m depth (Fig. 2b). Between 4200 m and 4400 m depth, POC concentrations increased by ~20%, from  $0.6\,\mu g~L^{-1}$  to  $0.7\,\mu g~L^{-1}$ , while the POC  $\delta^{13}$ C decreased from -21.1% to -21.6%

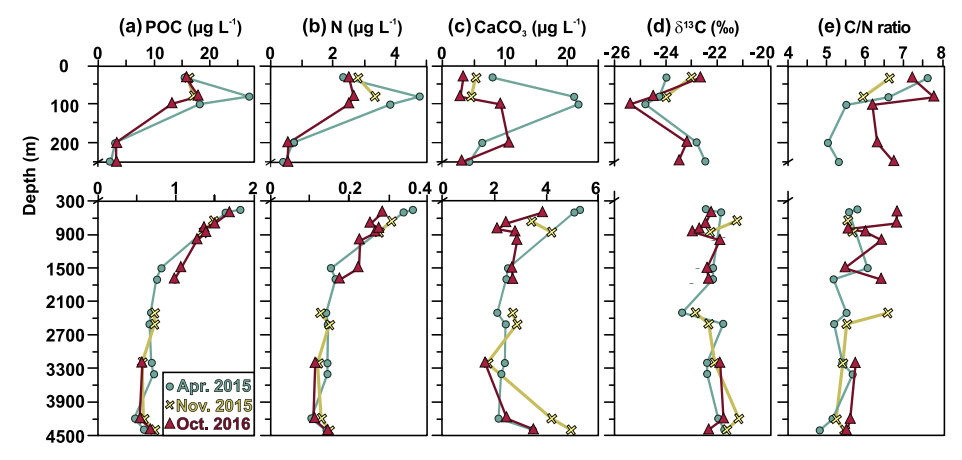


Fig. 4. (a) Particulate organic carbon content (POC,  $\mu$ g L<sup>-1</sup>), b) nitrogen content (N,  $\mu$ g L<sup>-1</sup>), (c) carbonates content (CaCO<sub>3</sub>,  $\mu$ g L<sup>-1</sup>), d)  $\delta^{13}$ C of POC (‰), (e) C/N molar ratios in the suspended particles collected in April and November 2015 and October 2016.

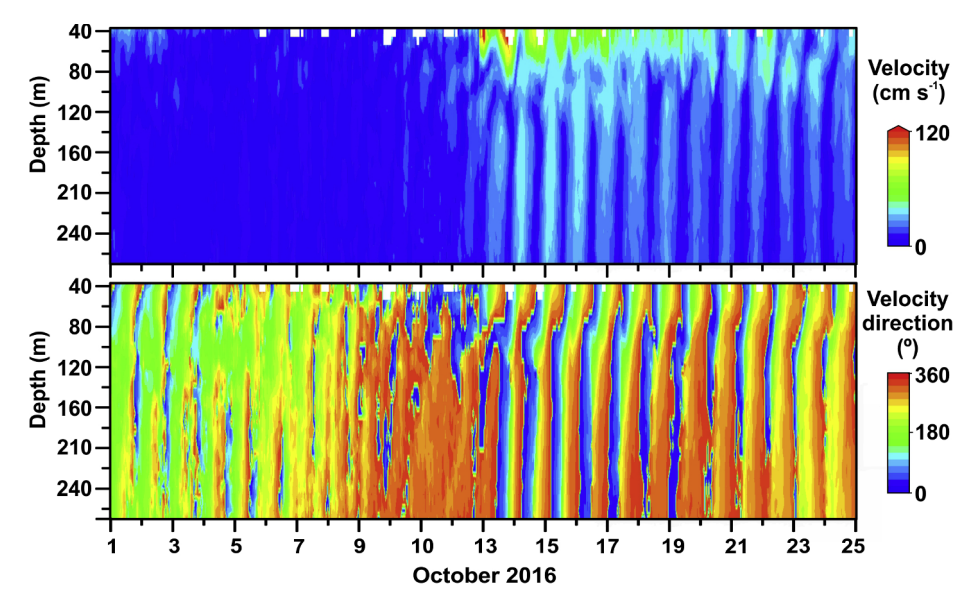


Fig. 5. Profiles (0–280 m) of current magnitude (cm s<sup>-1</sup>) and direction (<sup>0</sup>) before, during and after passage of Hurricane Nicole (13 October 2016, closest approach to site).

(Fig. 5).  $CaCO_3$  concentrations at 4200 m (4.2  $\mu g~L^{-1}$ ) and 4400 m (4.9  $\mu g~L^{-1}$ ) were almost twice that observed at 3200 m and were 50% higher than in the nepheloid in April.

*October 2016.* Hurricane Nicole, a Category 3 hurricane, passed just northwest of the study site in October, with its closest approach on 12–13 October (Fig. 1). Nicole generated large inertial currents (up to  $100 \, \mathrm{cm \, s^{-1}}$  at  $70 \, \mathrm{m}$ ), which persisted for more than two weeks after passage (Fig. 5). CTD profiles collected 10 days prior to the passage of Nicole showed a 30 m mixed layer with a temperature of 27 °C (dashed grey line, Fig. 2c). Five days after Nicole, the mixed layer had deepened to 62 m and the temperature had decreased 2 °C to 25 °C (BATS data, not shown). By 26 October, the mixed layer had shoaled to 40 m depth although the mixed layer temperature remained at 25 °C. A broad fluorescence maximum was centered at 100 m depth.

Five days after Nicole's passage (18 October), the depth-integrated primary production was  $366\,\mathrm{mg\,m^{-2}}~d^{-1}$ , which is typical of the average depth-integrated primary production in October (346 mg m $^{-2}$ d $^{-1}$ ). However, the primary production measured between 100 m and 145 m (57 mg m $^{-2}$ d $^{-1}$ ) was the highest recorded by the BATS timeseries since 1990 and five-fold higher than the average depth-integrated primary production below 100 m (19 mg m $^{-2}$ d $^{-1}$ ). POC, nutrient and pigment concentrations indicated that the strong mixing generated by Nicole had induced a deep phytoplankton bloom (Fig. 3). Near uniform

physical and biogeochemical properties were observed within the 60 m mixed layer. In contrast to April and November, there was detectable  $NO_2$  within the mixed layer (0.03  $\mu mol\ L^{-1}$ ) but no subsurface  $NO_2$  concentration maximum. POC concentrations ( $\sim\!23\,\mu g\ L^{-1}$ ) were constant from the surface to 120 m depth before gradually declining.

Between 120 m and 250 m depths, POC and pigment concentrations (Fig. 3) were significantly higher than observed in either April or November and pigment concentrations at these depths were the highest in October at BATS since 1992. Diadinoxanthin and fucoxanthin concentrations also showed deep subsurface maxima of  $\sim\!4$  ng  $L^{-1}$  between 100 and 120 depth and high concentrations up to 160 m depth ( $\sim\!2$  ng  $L^{-1}$ ). These deep pigment concentrations were comparable to those observed in October 1999 following the passage of Hurricane Gert, another Category 3 hurricane with a similar track, and indicated a deep penetration of labile phytoplankton-derived organic material.

Suspended POC profiles collected two weeks after Hurricane Nicole's passage (25–29 October 2016) showed a weak subsurface maximum of 18  $\mu g\,L^{-1}$  at 80 m depth with a gradual decrease deeper in the water column. The  $\delta^{13} C$  values decreased from -22.7 % within the mixed layer to a minimum of -25.4 % at the fluorescence maximum before increasing again to  $\sim -23.0 \%$  below 200 m depth. C/N ratios in the mixed layer were similar to that observed in April, but C/N ratios between 100 and 500 m (6.0–6.5) were significantly higher than those

**Table 2**Compound abbreviations used in this paper.

Biomarker	Abbreviation
Fatty acids	
C <sub>12</sub> -C <sub>28</sub> saturated even	SFA
C <sub>14:1</sub> -C <sub>22:1</sub> monosaturated even	MUFA
C <sub>12</sub> -C <sub>21</sub> odd and C <sub>14</sub> -C <sub>18</sub> saturated iso- anteiso-branched	Odd/br FA
C <sub>16</sub> -C <sub>20</sub> diunsaturated	DUFA
C <sub>16</sub> -C <sub>20</sub> polyunsaturated	PUFA
Fatty alcohols	
C <sub>14</sub> -C <sub>18</sub> saturated even	Short-chain SFAI
C <sub>20</sub> -C <sub>24</sub> saturated even	Long-chain SFAL
C <sub>15</sub> -C <sub>19</sub> saturated odd	Odd FAL
C <sub>16:1</sub> -C <sub>22:1</sub> monosaturated even	MUFAL
Sterols	
Cholest-5-en-3β-ol (cholesterol)	$C_{27}\Delta^5$
24-Nor-cholesta-5,22-dien-3β-ol <sup>*</sup>	$C_{26}\Delta^{5,22}$
27-nor-24-methylcholesta-5,22-dien-3β-ol®	$C_{por27}\Delta^{5,22}$
Cholesta-5,22-dien-3β -ol <sup>*</sup>	$C_{27}\Delta^{5,22}$
24-Methylcholesta-5,22-dien-3β-ol*	$C_{20}\Lambda^{5,22}$
24-Methylcholesta-5,24(28)-dien-3β-ol*	$C_{28}\Delta^{5,24(28)}$
24-Methylcholest-5-en-3β-ol <sup>*</sup>	$C_{28}\Delta^{5}$
24-Ethylcholesta-5,22-dien-3β-ol <sup>*</sup>	$C_{29}\Delta^{5,22}$
24-Ethylcholest-5-en-3β-ol*	$C_{29}\Delta^5$
24-Propylcholesta-5,24(28)-dien-3β-ol*	$C_{30}\Delta^{5,24(28)}$
The state of the s	$4\alpha C_{30}\Delta^{22}$
4α,23,24-Trimethyl-5a-cholest-22-en-3β-ol	4αC <sub>30</sub> Δ
Stanols	2
24-Nor-5α-cholest-22-en-3β-ol	$C_{26}\Delta^{22}$
5α-Cholesta-22-en-3β-ol	$C_{27}\Delta^{22}$
24-Methyl-5α-cholest-22-en-3β-ol	$C_{28}\Delta^{22}$
24-Ehtyl-colesta-22-en-3β-ol	$C_{29}\Delta^{22}$
5α-Cholestan-3β-ol	$C_{27}\Delta^0$
24-Methyl-colestan-3β-ol	$C_{28}\Delta^{o}$
24-Ethyl-5α-cholestan-3β-ol	$C_{29}\Delta^0$
4α,23S,24R-trimethyl-5α(H)-cholestan-3β-ol	$4\alpha C_{30}\Delta^{0}$
Saturated 4-methyl steroidal ketones	SK
C <sub>37</sub> –C <sub>39</sub> methyl ketones (alkenones)	LCK
C <sub>30</sub> alkan-1,15-diol	C <sub>30</sub> diol
Hopanoids	
C <sub>27</sub> hopanone 22,29,30-trisnorhop-17(21)-ene	HOP-a
C <sub>31:1</sub> hopene	HOP-b
C <sub>30</sub> triterpanol	HOP-c
C <sub>31</sub> hopanol ββ-homopan-31-ol	HOP-d
C <sub>33</sub> hopanoic acid	НОР-е
Hydroxy fatty acids	
3- hydroxy acids	β-ОН
(ω-1)-hydroxy acids	ω-ΟΗ
1-O-alkylglycerols	AG

<sup>\*</sup> Phytosterols

in April. CaCO $_3$  concentrations increased three-fold between the mixed layer (3 µg L $^{-1}$ ) and 100–200 m (average  $\sim$  10 µg L $^{-1}$ ), before declining again to  $\sim$  3 µg L $^{-1}$  by 250 m depth. Within the bathypelagic water column, POC,  $\delta^{13}$ C, and CaCO $_3$  concentrations in October were similar to those in April and November (Fig. 4).

Beam attenuation in October also indicated the presence of a weak nepheloid layer below 3800 m, but the maximum beam attenuation was only about 50% that observed in April and November (Fig. 2c). As observed in April and November, POC, PON and CaCO $_3$  concentrations increased by ~20% from 4200 m to 4400 m.  $\delta^{13}$ C values were comparable to those in April, and declined between 4200 m (~21.8%) and 4400 m (~22.3%) depths.

#### 3.2. Lipid biomarkers

Abbreviations used for the lipid classes and individual compounds are provided in Table 2.

#### 3.2.1. Total extractable lipids

Concentration profiles of total extractable lipids (TEL) in suspended particles are shown in Fig. 6 and summarized in Table 3. In April, TEL concentrations declined by almost three orders of magnitude from the epipelagic to lower bathypelagic layers. There was a strong subsurface TEL concentration maximum ( $\sim 4900 \text{ ng L}^{-1}$ , 18% of POC) at the depth of the chlorophyll maximum. TEL concentrations then rapidly declined to 240 ng  $L^{-1}$  (11% of POC) by 250 m depth, and continued to decline an additional 60% to 160 ng  $L^{-1}$  (9.2% of POC) by 450 m depth. TEL concentration declined another ~ 70% through the deep mesopelagic and upper bathypelagic layer to  $\sim 5 \text{ ng L}^{-1}$  (6.9% of POC) at 1700 m depth, and then remained rather constant deeper in the water column. OC-normalized TEL concentrations (ng ugOC<sup>-1</sup>) decreased by about 40% between the epipelagic layer (170 ng μgOC<sup>-1</sup>) and the lower bathypelagic layer (99 ng μgOC<sup>-1</sup>), consistent with high lability of fresh lipids in comparison to bulk OC. Within the deep water column, OC-normalized TEL concentrations varied 10-20%, indicating significant heterogeneity in the OM richness of deep suspended pool. Peaks in TEL concentration, ~20-30% higher than the average deep water TEL concentration, were observed in samples collected at 2300 m, 3200 m and 4200 m depths, indicating more lipid-rich suspended materials at these depths.

In November, TEL concentrations in the mixed layer ( $\sim\!2300\,ng\,L^{-1},\,15\%$  of POC) were 50% lower than in April, reflecting the low surface water productivity. There was also no evidence of a subsurface maximum at the depth of the deep chlorophyll maximum. TEL concentrations within the mesopelagic water column were also lower than in April, and even within the bathypelagic layer TEL concentrations were about half those in April. OC-normalized TEL concentrations followed a similar depth trend as in April, decreasing by 50% from the epipelagic layer (119 ng  $\mu g O C^{-1}$ ) to the lower bathypelagic layer (56 ng  $\mu g O C^{-1}$ ). OC-normalized TEL concentrations in the mesopelagic and bathypelagic layers were about half those observed in April, consistent with the lower absolute concentrations and indicating a significantly more refractory suspended POC pool throughout the water column in November.

In October 2016 following Hurricane Nicole, absolute TEL concentrations (Fig. 6) showed a weak maximum at the depth of the deep chlorophyll maximum, consistent with the increase in Chl a concentrations (Fig. 3). Between 100 and 250 m depth, OC-normalized TEL concentrations were similar to those in April, again indicative of the increased phytoplankton productivity following Nicole. However, within the upper 1000 m, both absolute and OC-normalized TEL concentrations were 50% higher than those in April and indicated a large increase in lipid-rich suspended materials in the mesopelagic layer following Hurricane Nicole. Within the bathypelagic layer, TEL concentrations were lower than in April but still ~25% higher than in November. Within the nepheloid layer, absolute TEL concentrations were similar those observed in April, although OC-normalized concentrations were intermediate between those observed in April and November (Table 3).

# 3.2.2. Fatty acids

Fatty acids (FA) were the most abundant lipid class and comprised between 53 and 84% of total TEL (Table 3). Total FA concentration profiles were similar to those of TEL (Fig. 6). In April 2015, there was a strong subsurface maximum in FA concentration at the depth of the deep chlorophyll maximum (4200 ng  $\rm L^{-1}$ ). FA concentrations then decreased by an order of magnitude by 200 m depth and continued to decline with depth to 1500 m depth ( $\sim 30~\rm ng~L^{-1}$ ). Concentrations were variable but with no apparent depth trend in the deep bathypelagic layer. In November 2015, no subsurface concentration maximum was apparent, and concentrations in mesopelagic and bathypelagic waters were only  $\sim 30$ –50% those observed in April. In October 2016 two weeks after passage of Hurricane Nicole, FA concentrations also showed a small subsurface peak of 2000 ng  $\rm L^{-1}$  at the deep chlorophyll

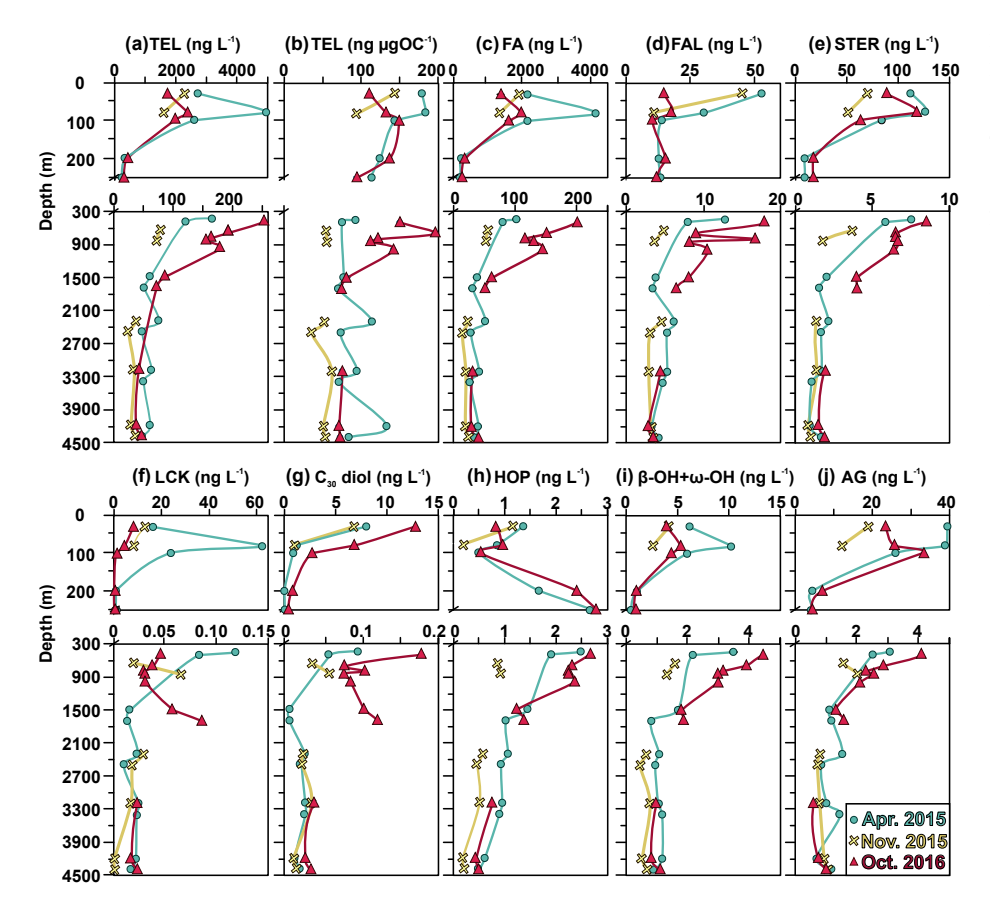


**Fig. 6.** Lipid biomarker concentrations in suspended particles collected in April 2015, November 2015 and October 2016. (a) Total extractable lipid (TEL) concentration (ng  $L^{-1}$ ), (b) OC-normalized TEL concentration (ng  $\mu gOC^{-1}$ ), (c) concentrations (ng  $L^{-1}$ ) of total (c) fatty acids (FA), (d) fatty alcohols (FAL), (e) sterols + stanols (STER), (f) alkenones (LCK), (g)  $C_{30}$  alkan-1,15-diol ( $C_{30}$  diol), (h) hopanoids (HOP), (i) β-and ω-OH hydroxy acids, and 1-O-alkylglycerols (AG) in the suspended particles collected in April and November 2015 and October 2016.

maximum and then rapidly declined to  $\sim\!250\,\mathrm{ng}\;\mathrm{L^{-1}}$  by 200 m depth. Between 450 and 1700 m depth, FA concentrations in October were three times greater than observed in April, again indicative of the strong lipid enrichment in suspended POC within the mesopelagic and upper bathypelagic layers following Hurricane Nicole.

FA concentrations in this study are compared with FA concentrations observed in the northwestern Sargasso Sea in August 1982 (Conte 1990), in the Sargasso Sea core waters of a newly formed Gulf Stream eddy in October 1982 (Conte 1990) and at BATS in June 2000 (Loh et al. 2008) (Fig. 7). In the upper water column, FA concentrations in August and October 1982 were lower than in November 2015. Deeper in the water column, FA concentrations in August and October 1982 were similar to those in April and November 2015. In contrast, FA concentrations in October 2016 were more than double. Additionally, FA concentration at 1500 m in October was also 50% higher than that measured at 1500 m in June 2000 (Loh et al. 2008).

OC-normalized (ng µgOC-1) FA concentration profiles are presented in Fig. 8. OC-normalized FA concentrations were highest in April (120–150 ng µgOC<sup>-1</sup>) with a strong subsurface maximum at the depth of the chlorophyll maximum. Concentrations then declined to  $\sim 50 \, \mathrm{ng}$ μgOC<sup>-1</sup> by 500 m depth. At bathypelagic depths, OC-normalized FA concentrations were variable and ranged from 35 to 85 ng  $\mu$ gOC<sup>-1</sup>, indicating significant compositional heterogeneity of suspended POC within the deep-water column. In November, OC-normalized FA concentrations were highest at 30 m depth (115 ng µgOC<sup>-1</sup>). The concentration at 80 m was only about 60% that in April, consistent with the lower productivity in November. Within the deep water column, OCnormalized FA concentrations were lower and less variable than in April (20–35 ng  $\mu gOC^{-1}$ ), indicating a more refractory and homogenous composition of suspended POC in the deep waters. In October, OC-normalized FA concentration profiles again showed the significant FA enrichment in suspended POC within the mesopelagic layer, and unlike April or November, remained high down to 1000 m depth with

no apparent depth trend below 1500 m. OC-normalized FA concentrations within the mesopelagic layer were variable, ranging between 70 and 150 ng  $\mu g O C^{-1}$ , and indicated high compositional heterogeneity in the suspended POC. Deeper in the water column, OC-normalized concentrations were less variable and averaged  $\sim\!50$  ng  $\mu g O C^{-1}$ , similar to April deep water concentrations.

Saturated fatty acids (SFA). Saturated, even-chain  $C_{12}$ - $C_{28}$  fatty acids comprised between 15 and 42% of the TFA (Fig. 8, Table 3). In April, the SFA contribution to TFA ranged from  $\sim$  40% in the epipelagic layer to  $\sim$  30% in the bathypelagic layer. The SFA contribution to TFA was lower in November and October ( $\sim$ 15% of TFA). N- $C_{16:0}$  was the most abundant compound, comprising 50–60% of the total SFA. N- $C_{14:0}$  and n- $C_{18:0}$  were the next most abundant SFAs.

Depth trends were observed in the SFA composition (Fig. 8). N-C<sub>14:0</sub> was most abundant in the epipelagic layer, comprising up to 40% of the SFA, but its contribution declined to  $\sim$ 20% of the SFA in the mesopelagic and continued to decline to only  $\sim$ 15% of the total SFA in the bathypelagic layers. In contrast, the relative contribution of n-C<sub>18:0</sub> increased with depth, from  $\sim$ 5% the total SFA in the epipelagic layer to  $\sim$ 10% of the total SFA in the mesopelagic layer. The transition in SFA composition with depth is clearly observed in the 14:0/16:0 ratio which averages 0.8–0.9 in the epipelagic layer and 0.2–0.3 in the bathypelagic layer (Table 3). The 14:0/16:0 ratio in the deep water column and nepheloid layer in October was about 50% higher than in April or November, suggesting a greater relative abundance surface-derived OC in the deep water column in October.

The relative contributions of the individual SFA compounds also differed among the three sampling periods (Fig. 8). N-C<sub>18:0</sub> was more abundant in the mesopelagic layer in April, whereas n-C<sub>14:0</sub> was more abundant following Hurricane Nicole in October. In April, OC-normalized n-C<sub>18:0</sub> concentrations increased by a factor of four with depth, from  $2.3 \text{ ng } \mu\text{gOC}^{-1}$  at 100 m to  $8.1 \text{ ng } \mu\text{gOC}^{-1}$  at 4200 m. This pattern was not observed in either November or October. The highest OC-

Table 3 Absolute (ng  $L^{-1}$ ) and OC-normalized (ng  $\mu$ gOC $^{-1}$ ) concentrations of total extractable lipids (TEL) and total fatty acids (TFA) in the epipelagic layer (EL), mesopelagic layer (ML), upper and lower bathypelagic layers (Up. BL and L. BL, respectively) and the nepheloid layer (NL). The data are average concentrations within each layer. See Table 2 for compound abbreviations. Symbols "+" indicate concentrations < 0.01 ng  $L^{-1}$  or < 1%, and symbol "-" indicate not detected.

			A	pril 2015				No	vember 2	015				Octobe	r 2016		
		EL	Up. ML	Up. BL	L. BL	NL	EL	L. ML	Up. BL	L. BL	NL	EL	Up. ML	L. ML	Up. BL	L. BL	NL
TEL (ng L <sup>-1</sup> )		3431	227	59.6	58.9	48.9	1949	77.2	31.6	32.0	37.1	2027	327	174	79.9	40.2	48.8
TEL (ng μgOC <sup>-1</sup> )		1699	101	83.1	99.3	83.4	119	54.5	43.6	56.0	52.6	131	127	143	77.7	72.9	72.1
Total FA (ng L <sup>-1</sup> Total FA (ng μgO		2846 139	148 66.2	37.4 52.2	36.1 61.6	34.2 58.3	1629 99.4	55.1 38.9	19.7 27.1	20.0 34.9	25.6 36.3	1657 107	258 101	136 112	57.0 55.4	29.1 52.8	36.2 53.5
SFA (ng L <sup>-1</sup> )		1112	55.7	10.1	10.5	5.23	689	17.7	4.26	3.43	3.89	689	91.3	49.7	13.0	5.0	5.6
SFA (ng μgOC <sup>-1</sup> ) (%SFA):	) 12:0	54.7 1	24.7 1	14.1 +	18.0 1	8.92 -	42.3 +	12.4 1	5.87 1	5.99 +	5.50 +	44.5 +	36.2 +	40.9 +	12.6 +	8.98 1	8.33 1
	14:0	41	20	13	12	13	41	18	14	13	15	43	20	20	19	16	22
	16:0	51	62	61	55	61	51	62	61	61	59	49	66	67	63	60	57
	18:0 20:0	6 1	14 1	21 1	29 1	20 1	6 1	16 1	17 2	20 2	20 1	5 1	11 1	10 1	12 1	17 1	15 1
	22:0	+	1	1	1	2	+	1	3	2	2	+	1	1	2	2	2
	24:0	+	1	1	1	2	+	1	3	1	1	+	1	1	2	2	1
	26:0	+	+	+	1	1	+	+	1	1	1	+	+	+	1	1	1
. 1.	28:0	-	-	-	+	+	+	+	+	+	-	+	-	-	-	-	-
MUFA (ng L <sup>-1</sup> ) MUFA (ng μgOC	<sup>-1</sup> )	628 30.8	35.3 16.0	13.7 19.2	13.1 22.5	16.5 28.2	355 21.6	16.9 12.0	7.79 10.7	8.30 14.5	11.35 16.1	372 24.2	65.1 26.1	42.3 34.5	20.5 19.9	12.1 22.0	15.7 23.2
(%MUFA):	14:1	4	1	_	+	+	5	1	1	1	1	5	1	1	1	1	1
	Σ16:1	53	35	34	37	44	59	32	37	47	52	57	35	25	40	44	52
	16:1ω7	45	29	28	20	4	59	27	31	40	45	45	28	9	4	5	5
	18:1ω7 18:1ω9	10 27	17 33	18 33	22 26	27 20	10 20	14 41	18 31	25 17	28 11	11 21	12 44	9 57	16 32	21 20	25 13
	20:1ω9	1	33 1	33 2	20	20	1	2	3	1	1	1	1	1	2	20	13
	22:1ω11	1	4	5	4	2	1	2	2	2	2	1	1	1	2	2	1
	22:1ω9	2	6	7	7	4	3	7	6	6	3	2	4	4	6	8	5
$DUFA (ng L^{-1})$		88.3	2.10	0.56	0.57	0.55	45.3	1.21	0.36	0.28	0.35	37.8	4.49	2.88	0.92	0.40	0.37
DUFA (ng µgOC	<sup>-1</sup> )	4.37	0.93	0.79	0.98	0.93	2.79	0.87	0.50	0.49	0.50	2.40	1.83	2.37	0.89	0.71	0.54
(%DUFA):	16:2	2	-		7	28	2	6	8	17	28	2	5	4	10	8	8
	18:2ω6 20:2ω6	94 4	89 11	85 15	80 14	60 12	93 6	85 9	80 12	69 13	58 14	93 5	87 7	91 6	79 11	76 16	76 17
PUFA (ng L <sup>-1</sup> )	20.200	938	31.92	6.77	5.20	5.80	484	13.4	4.04	3.66	4.08	498	67.0	28.2	14.2	5.75	6.63
PUFA (ng µgOC	<sup>-1</sup> )	45.4	13.8	9.39	8.53	9.89	29.4	9.48	5.56	6.40	5.77	32.2	25.1	23.4	13.8	10.4	9.79
(%PUFA):	16:4ω3	1	1	-	-	-	1	1	1	1	1	1	+	1	+	+	1
	18:3ω6	5	1	2	3	2	6	3	4	5	6	3	1	1	+	+	+
	18:3ω3	12	3	3	3	1	9	4	3	3	5	8	3	3	2	6	8
	18:4ω3 18:5ω3	15 16	6 4	- 5	8	- 6	14 12	- 4	1 2	2	2	16 11	9 4	5 3	2 1	1	1
	18:6ω3	1	+	-	-	-	1	_	_	_	_	1	+	+	_	_	_
	20:3ω6	+	1	1	1	1	+	1	1	1	1	+	+	+	+	1	+
	20:4ω6	1	7	9	8	7	2	7	8	7	7	2	7	6	8	8	8
	20:4ω3	1	1	1	2	1	1	1	2	1	1	1	1	1	1	1	1
	20:5ω3 22:4	10 +	22 +	22	23	29 -	12 +	21 1	27 -	26 -	25 1	12 +	19 -	20	27 -	27 -	29 -
	22:5ω3	2	2	2	2	2	3	6	2	3	4	2	1	2	3	2	1
	22:6ω6	2	8	9	8	4	2	5	5	6	7	3	6	5	4	4	3
	22:6ω3	33	44	45	39	48	35	45	44	45	39	41	47	51	50	49	47
Odd/br FA (ng L		78.4	23.3	6.28	6.70	6.10	56.0	5.91	3.25	4.35	5.97	59.9	30.1	12.8	8.4	5.9	7.9
Odd/br FA (ng με		4.02	10.7	8.72	11.5	10.4	3.41	4.17	4.47	7.57	8.45	3.86	11.4	10.6	8.16	10.7	11.7
(%odd/br FA):	13:0 14:0br	2	2	+ 1	2	1	2	2	2	1	1	2	2	2	2	1	1
	i15:0	14	14	10	10	10	12	10	8	8	9	13	12	9	9	9	9
	a15:0	8	8	10	10	9	6	6	7	6	6	7	6	6	8	7	7
	15:0	23	16	13	12	9	23	14	11	8	7	23	15	13	13	10	9
	i16:0 a16:0	7 +	9	10	9	7	15 -	10 1	10 2	8 2	6 1	9 1	9 1	8 2	9 1	7 1	6 +
	i17:0	+	3	5	6	8	_	2	6	8	9	+	3	3	4	7	8
	a17:0	1	4	4	4	6	1	5	4	6	4	+	1	1	1	3	5
	17:0	19	11	9	10	7	17	10	9	7	7	15	10	9	6	7	5
	17:1	13	16	16	12	14	17	17	16	10	10	12	14	17	16	11	10
	i18:0	-	2	2	2	2	- 1	4 2	3	2	1	4 3	6 4	8	6	3 2	2
	a18:0 19:0	1	- 7	- 11	- 13	- 15	1	6	+ 12	+ 13	- 17	3	4 11	5 11	3 14	2 20	2 19
	19:1	6	5	7	8	12	1	4	8	17	20	4	4	4	6	10	12
	21:0	2	1	2	1	-	1	2	1	1	1	2	1	1	1	1	-
Ratios:	14:0/16:0	0.81	0.32	0.22	0.22	0.21	0.81	0.28	0.23	0.21	0.26	0.89	0.30	0.31	0.30	0.27	0.39
	18:1ω9/18:1ω7	2.67	1.97	1.94	1.20	0.73	1.85	2.92	1.76	0.74	0.39	2.12	4.02	6.53	2.03	1.00	0.52
	20:5ω3/22:6ω3	0.30	0.49	0.49	0.58	0.61	0.34	0.47	0.62	0.57	0.64	0.30	0.41	0.40	0.53	0.59	0.62
	C <sub>13-15</sub> /C <sub>19-21</sub> odd/br FA	5.48	3.13	1.72	1.48	1.06	18.9	2.82	1.34	0.78	0.64	8.00	2.18	1.85	1.57	0.87	0.92

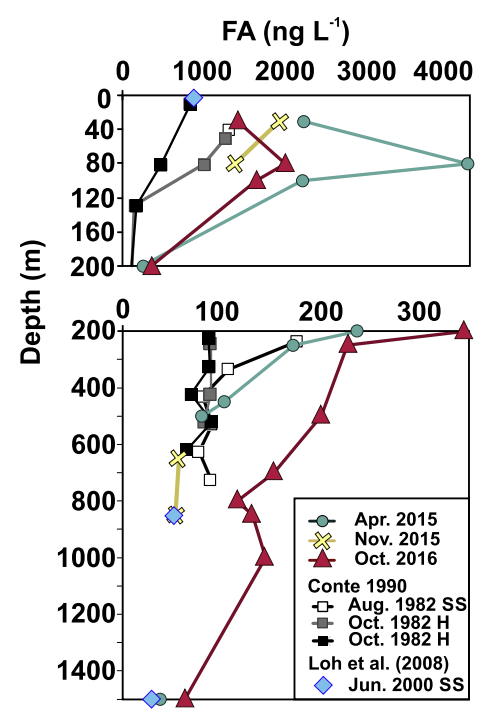


**Fig. 7.** Comparison of fatty acid concentration (FA, ng L<sup>-1</sup>) in the suspended particles collected in this study with FA concentration of suspended material collected previously in the Sargasso Sea by Conte (1990) and Loh et al (2008).

normalized concentrations of n-C<sub>16:0</sub> were observed in the epipelagic layer in April and November ( $\sim$ 25% of the total FA). In contrast, in October the highest OC-normalized concentrations ( $\sim$ 40  $\mu$ gOC<sup>-1</sup>) were observed in the mesopelagic layer ( $\sim$ 26% of the total FA). These concentrations were roughly four times higher than observed in the mesopelagic layer in either April or November.

Long-chain n-C $_{20}$  to n-C $_{28}$  SFA were present in much lower concentrations (Table 3). The highest absolute concentrations of the long-chain SFA were found in the epipelagic layer. N-C $_{20:0}$ , n-C $_{22:0}$  and n-C $_{24:0}$  were also more abundant in the epipelagic layer in April, whereas n-C $_{26:0}$  was more abundant in October post hurricane. In April and November, OC-normalized SFA concentrations decreased by an order of magnitude between the epipelagic and the mesopelagic layers, whereas in October OC-normalized SFA concentrations remained high down to 1000 m depth, consistent with the enrichment observed in TFA within the upper 1000 m (Fig. 8).

Total SFA concentration within the nepheloid layer at 4400 m depth was  $\sim\!40\%$  lower in November (3.9 ng L $^{-1}$ , 5.5 µgOC $^{-1}$ ) than in April (5.2 ng L $^{-1}$ , 8.9 µgOC $^{-1}$ ) or October (5.6 ng L $^{-1}$ , 8.3 µgOC $^{-1}$ ) (Table 3). In November and October, total SFA concentrations at 4400 m were about 20% higher than at 4200 m, whereas in April total SFA concentration was higher at 4200 m depth, as result of elevated concentrations of  $n\text{-C}_{16:0}$  and  $n\text{-C}_{18:0}$ .

Monounsaturated and diunsaturated fatty acids (MUFA and DUFA). Monounsaturated, even chained  $C_{14}$ - $C_{22}$  compounds comprised ~ 20% of the TFA in the epipelagic layer and increased to ~ 35–40% of TFA in the deep water column (Table 3). The most abundant MUFA were 16:1 isomers (16:1ω7, 16:1ω10, 16:1ω5), 18:1ω9, and 18:1ω7. 16:1ω7 is a particularly abundant FA in phytoplankton (Dalsgaard et al., 2003; Volkman et al., 1989), and concentrations of 16:1ω7 in the euphotic zone followed a similar trend as Chl  $\alpha$ , with a maximum at the depth of the deep chlorophyll maximum. Concentrations decreased by an order of magnitude through the water column to < 5% of epipelagic concentrations at bathypelagic depths. 18:1ω9 is a major FA in zooplankton and also highly enriched in fecal material (Harvey et al., 1987; Wakeham and Canuel, 1988). The relative contribution of 18:1ω9 to

total MUFA was lowest within the chlorophyll maximum ( $\sim\!20\text{--}25\%$ ) and highest within the mesopelagic layer (30–55%) in all months (Fig. 8). The contribution of 18:1 $\omega$ 9 within the mesopelagic layer in October was twice that observed in April or November, indicating a much higher contribution of animal-derived lipids in the suspended POC within the mesopelagic layer following Hurricane Nicole. The contribution of 18:1 $\omega$ 9 decreased in the deep bathypelagic and nepheloid layers, particularly in November where 18:1 $\omega$ 9 comprised only 11% of the total. 18:1 $\omega$ 7 is a major FA in bacteria but is also present in zooplankton, presumably sourced from enteric bacteria (Volkman et al., 1980c). The relative contribution of 18:1 $\omega$ 7 was lowest at the deep chlorophyll maximum ( $\sim$ 10% of the MUFA) and increased with depth to a maximum contribution in the lower bathypelagic and nepheloid layers of between 20 and 30% of MUFA.

 $20:1\omega 9,\ 22:1\omega 9$  and  $22:1\omega 11$  are important components of zoo-plankton wax esters (Lee et al., 2006) and were present in low concentrations ( $\sim\!1\text{--}3\%$  of MUFA). As observed for  $18:1\omega 9$ , the contribution of long-chain MUFA was lowest in the epipelagic layer and increased with depth, from <1.3% of TFA in the epipelagic layer to 3.5–6.0% within the lower bathypelagic layer. The relative abundances of these compounds differed among the sampling periods, with  $22:1\omega 9$  being far more abundant than  $20:1\omega 9$  or  $22:1\omega 11$  in November and October.

Within the nepheloid layer, total MUFA concentrations at 4400 m were  $\sim 10\text{--}20\%$  higher than in the bathypelagic layer (Table 3). This increase was due to higher  $16\text{:}1\omega7$  and  $18\text{:}1\omega7$  concentrations in the nepheloid layer, as concentrations of  $18\text{:}1\omega9$  and the  $C_{20}$  and  $C_{22}$  MUFAs were all lower. The MUFA compositional shift indicated an increase in the contribution of microbe-sourced lipids in the nepheloid layer. Differences among sampling periods were also observed, with concentrations were about 30% lower in November as compared with April or October.

The major diunsaturated fatty acid (DUFA) was  $18:2\omega6$ , which comprised > 90% of the DUFA. 16:2 and  $20:2\omega6$  were also present in low concentrations. Epipelagic concentration of  $18:2\omega6$  were highest in April (83 ng L $^{-1}$ ), consistent with the high phytoplankton production in April. Concentrations of  $18:2\omega6$  in November (42 ng L $^{-1}$ ) and October (35 ng L $^{-1}$ ) were about 50% that in April. Even so, mesopelagic concentrations in October (2.5-4.0 ng L $^{-1}$ ) were higher than in April, again indicative of higher abundance of surface derived material in the mesopelagic layer following Nicole.

Polyunsaturated fatty acids (PUFA). C<sub>16</sub> to C<sub>22</sub> even chained PUFA with 3-6 methylene-interrupted double bonds are synthesized de novo by phytoplankton, with the  $\omega$ 3 series being more predominant than the ω6 series in marine environments (Volkman et al., 1998). Phytoplankton classes differ in the relative abundances of the individual PUFA compounds synthesized (e.g., Rossi et al., 2006; Parrish, 2013), and thus PUFAs distributions in the euphotic zone reflect phytoplankton community composition. PUFAs are essential fatty acids and comprise a large percentage of animal storage lipids (Lewis, 1967; Linder et al., 2010). Zooplankton have been shown to bioaccumulate PUFAs from the diet at efficiencies of up to 95% (Bradshaw and Eglinton, 1993; Harvey et al., 1987), and during bioaccumulation PUFAs may be chain elongated and further desaturated (Monroig et al., 2013). Thus, animal tissues are enriched in  $20.5\omega 3$  and  $22.6\omega 3$  compounds relative to their phytoplankton diet (Levine and Sulkin, 1984; Sargent and Whittle, 1981; Tang et al., 2001). Because zooplankton contain copious quantities of PUFAs in their tissues, zooplankton biomass is an important secondary source of PUFAs in particulate material, presumably contributed to the detritus during animal predation, "sloppy feeding" (Frost, 1972; Vinogradov et al., 1977). In addition to de novo synthesis by phytoplankton, some microheterotrophs (Pereira et al., 2003) and piezophilic bacteria clades in the deep water column can biosynthesize 20:5ω3 and 22:6ω3 PUFAs (Fang et al., 2003), although their contribution to the total PUFA pool in the deep water column currently is not known.

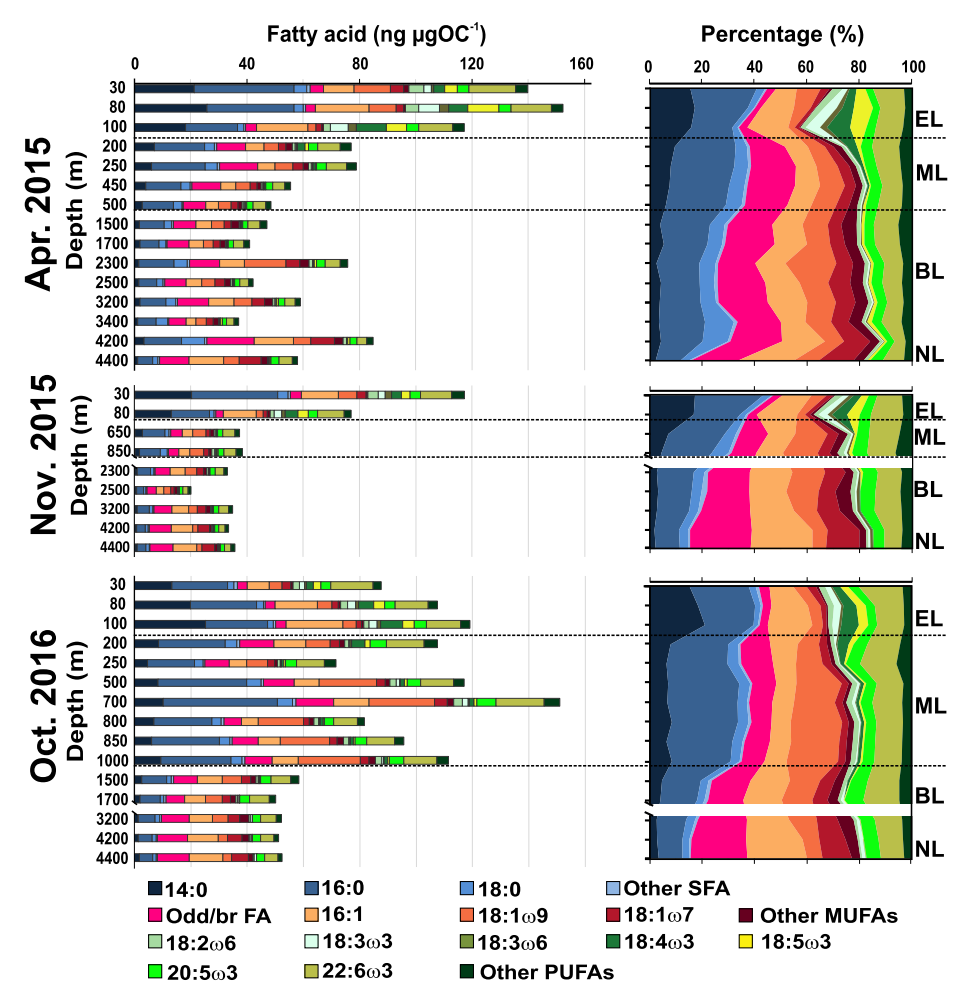


Fig. 8. OC-normalized concentration of fatty acids in the suspended particulate matter (bars, ng µgOC-1), as well as the percentage contribution of each fatty acid compound (%, gaps in the plot indicate > 1000 m between samples. EL, ML, BL and NL: Epipelagic, Mesopelagic, Bathypelagic and Nepheloid layers, respectively.

PUFAs comprised between 30 and 35% of TFA in the epipelagic layer. The PUFA contribution to TFA rapidly decreased with depth to  $\sim 15{\text -}20\%$  of TFA with the bathypelagic layer. Absolute and OC-normalized PUFA concentrations in the epipelagic layer in April (932 ng  $L^{-1}$ , 45 ng  $\mu g O C^{-1}$ ) were twice that in November (473 ng  $L^{-1}$ , 29 ng  $\mu g O C^{-1}$ ) and October (495 ng  $L^{-1}$ , 32 ng  $\mu g O C^{-1}$ ), reflecting the higher primary productivity in April. OC normalized concentrations in the lower mesopelagic layer in April and November, were about 30% of the concentrations observed in the epipelagic layer. However, OC-normalized PUFA concentrations in the mesopelagic layer in October were about 70% that in the epipelagic layer, again indicative of the high abundance of fresh, labile OC in the suspended particle pool in the mesopelagic layer following Hurricane Nicole.

The most abundant PUFAs in the suspended particles were  $20.5\omega 3$  and  $22.6\omega 3$ , which together comprised between 40 and 78% of the total PUFA (Table 3, Fig. 8).  $C_{18}$  PUFAs ( $18.3\omega 3$ , and  $18.3\omega 6$ ,  $18.4\omega 3$ ,  $18.5\omega 3$ , and  $18.6\omega 3$ ) were abundant in the upper water column, comprising 54% of the total PUFAs in the epipelagic layer in April, 43% in November and 40% in October (Fig. 8, Table 3). The contribution of  $C_{18}$  PUFAs decreased rapidly with depth to only 5–15% of the total PUFAs in the bathypelagic and nepheloid layers, and reflected the shift from phytoplankton- to animal-sourced PUFAs with increasing depth. The  $20.5\omega 3/22.6\omega 3$  ratio also increased with depth, from 0.30 to 0.34 in the epipelagic layer to  $\sim 0.60$  in the bathypelagic and nepheloid layers. This depth trend indicates either lower ecosystem retention of  $22.6\omega 3$  and/or possibly a higher  $20.5\omega 3/22.6\omega 3$  production ratio by heterotrophes and/or piezophilic bacteria in the deep water column.

Within the nepheloid layer, PUFA concentrations ranged from

 $4.4\,\mathrm{ng}~\mathrm{L}^{-1}$  in November to  $6.5\,\mathrm{ng}~\mathrm{L}^{-1}$  in October. As observed for MUFA, absolute PUFA concentrations were about 10% higher in the nepheloid layer while OC-normalized concentrations were similar (Table 3), indicating no enrichment in lability of the OC within the nepheloid layer.

*Odd chain and branched fatty acids (odd/br FA).* Odd chain and *iso*- and *anteiso*- branched fatty acids (odd/br FA) are abundant in bacteria (Cho and Salton, 1966; De Carvalho and Caramujo, 2012; Kaneda, 1991). The major odd/br FA compounds in the suspended particles were *n*15:0, *i*15:0, 17:0, and 17:1, which collectively comprised between 62 and 67% of the odd/br FA in the epipelagic layer and 40–50% in the bathypelagic and nepheloid layers.

The odd/br FA contribution to TFA increased significantly with depth, from  $\sim\!3\%$  of the TFA in the epipelagic layer to  $\sim\!10\text{--}15\%$  within the mesopelagic layer, to  $\sim\!20\%$  in the bathypelagic and nepheloid layers. In the epipelagic layer, odd/br FA concentrations were highest in April (78 ng L $^{-1}$ , 4 ng µgOC $^{-1}$ ) and about 30% lower in November (56 ng L $^{-1}$ , 3.4 ng µgOC $^{-1}$ ) and October (60 ng L $^{-1}$ , 3.9 ng µgOC $^{-1}$ ). Within the bathypelagic layers, concentrations were similar in April (6–7 ng L $^{-1}$ , 8.5–11.5 ng µgOC $^{-1}$ ) and October (6.0–8.5 ng L $^{-1}$ , 8.1–10.7 ng µgOC $^{-1}$ ) and about 50% lower in November (3.3–4.4 ng L $^{-1}$ , 4.5–7.6 ng µgOC $^{-1}$ ). The trends indicate a higher bacterial contribution to the suspended POC in the deep water column after high productivity conditions in April and October than in the low productivity conditions in November, suggesting bacterial activity is modulated by lability of the particulate organic carbon pool.

The average chain length of the odd/br FA in the suspended particles increased with depth (Fig. 9, Table 3). The contribution of the

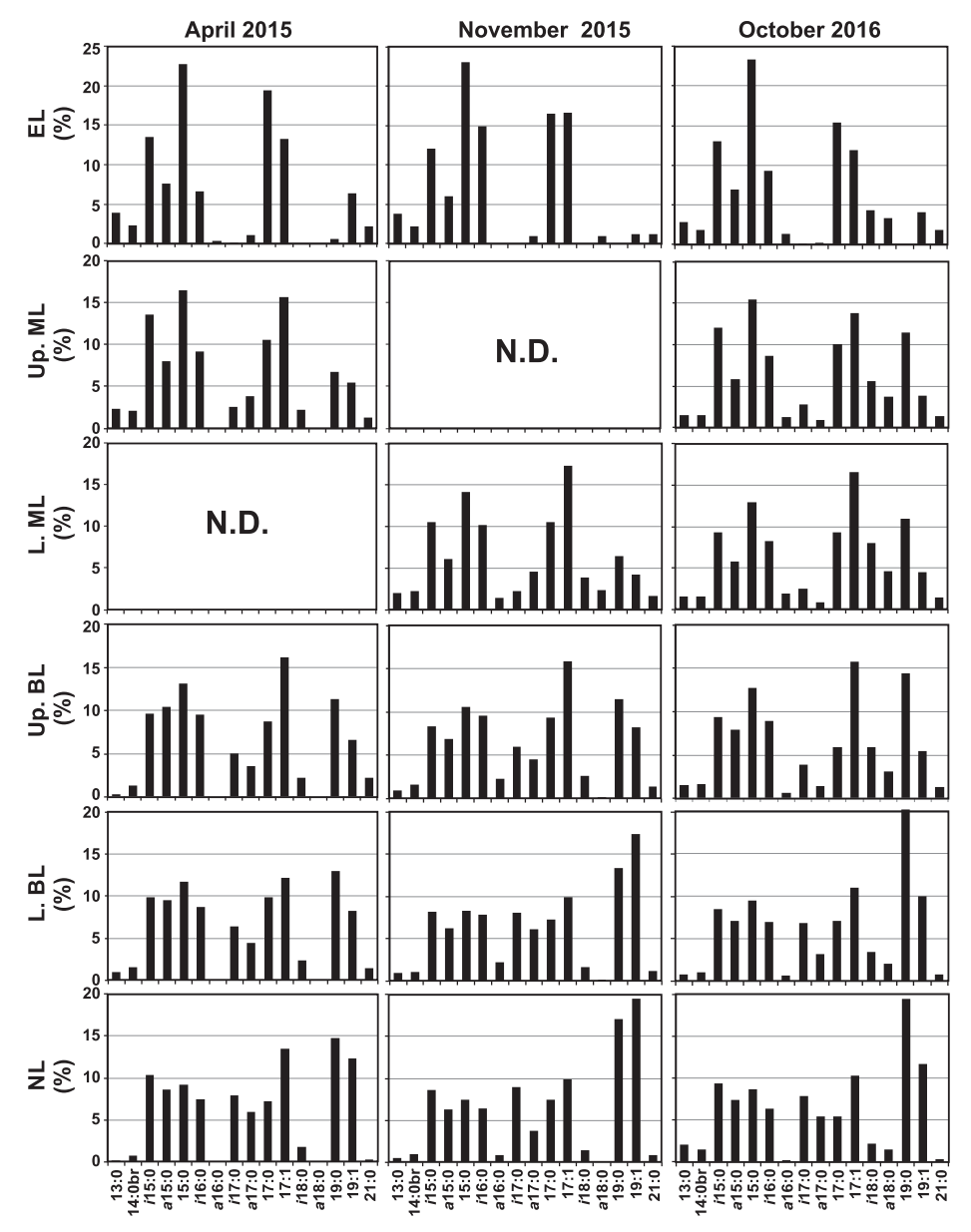


Fig. 9. Relative percentage of individual odd/br FA compounds (% odd/br FA) in the suspended particles collected in April and November 2015 and October 2016 at the epipelagic (EL), upper mesopelagic (Up. ML), lower mesopelagic (L. ML), upper bathypelagic (Up. BL), lower bathypelagic (L. BL) and nepheloid (NL) layers.

short-chain  $C_{13-15}$  compounds decreased from 46% of the total odd/br FA in the epipelagic layer to only 19–24% of the total in the nepheloid layer. Conversely, the contribution of the  $C_{19-21}$  compounds increased from 2.5 to 9% of the total odd/br FA in the epipelagic layer to 27–37% in the nepheloid layer. This trend of increasing chain length with depth, summarized by the ratio of  $\Sigma C_{13-15}/\Sigma C_{19-21}$  odd/br FA (Table 3), suggests a depth zonation of bacterial community structure.

Small compositional differences in odd/br FA were also observed in the three sampling periods that indicated differences in microbial communities (Fig. 9). For example, n19:0 and 19:1 were more abundant within the epipelagic layer in April while a16:0, i18:0 and a18:0 were more abundant in October. At bathypelagic depths,  $C_{19}$  and  $C_{21}$  compounds comprised a lower percentage of odd/br FA in April relative to November or October, whereas 13:0, br14:0, i18:0 and a18:0 compounds comprised a larger percentage of the total in October (post hurricane) relative to April or November.

Within the nepheloid layer, total odd/br FA concentration was 30% higher in October (7.9 ng  $L^{-1}$ ) than in April (6.1 ng  $L^{-1}$ ) or November (6.0 ng  $L^{-1}$ ). Compositionally,  $C_{19}$  and  $C_{21}$  compounds comprised a

greater percentage of the total odd/br FA in the nepheloid layer. The compositional differences observed in the nepheloid layer among the three sampling periods were similar to those observed in the bath-ypelagic layer, in particular the enrichment in 13:0, br14:0, i18:0 in the nepheloid layer in October (Fig. 9).

#### 3.2.3. Fatty alcohols

Fatty alcohols (FAL) are synthesized *de novo* by diverse phytoplankton, zooplankton and microbial sources (Sargent, 1976; Volkman et al., 1980b) and also produced by the hydrolysis of wax and chlorin esters (Cranwell, 1982; Sargent, 1976). Short-chain n-C<sub>12</sub>-C<sub>14</sub> FAL have microbial, plant or animal sources (Berge et al., 1995; Robinson et al., 1984a; Sargent, 1976). Even-chained n-C<sub>16</sub>-C<sub>24</sub> FAL are major components of zooplankton wax esters, with C<sub>16</sub> and C<sub>18</sub> compounds being the most prevalent (Harvey et al., 1987; Robinson et al., 1984b; Sargent and Falk-Petersen, 1988).

Unlike TFA, concentrations of FAL were highest at 30 m depth and did not exhibit any subsurface peak at the depth of the chlorophyll maximum (Fig. 6). FAL concentrations in the euphotic zone in October

were less than half those observed in April, while concentrations in the 100-250 m depth range were similar. The FAL contribution to TEL in the epipelagic layer also differed from that of the FA. FAL contribution to TEL increased from 0.9% in April to 1.4% in November, and the lowest FAL contribution was observed following Hurricane Nicole (0.7% of TEL in October). In the lower mesopelagic layer, FAL concentrations in October were about twice those in April and about three times those in November, consistent with the FA enrichment observed in the mesopelagic layer in October following Hurricane Nicole passage. At bathypelagic depths, FAL concentrations were similar in April and October, and about 50% lower in November, although FAL concentrations were more similar among sampling periods in the deep bathypelagic layer. FAL contributions to TEL increased with depth. from 4.6 to 5.6% of TEL in the mesopelagic layer and to 7.5-12.0% of TEL in the bathypelagic and nepheloid layers. Similarly, OC-normalized FAL concentrations increased with depth, from 0.9 to 1.8 ng  $\mu$ gOC<sup>-1</sup> in the epipelagic layer to  $5.5-7.1\,\mathrm{ng}~\mu\mathrm{gOC}^{-1}$  in the lower bathypelagic layer (Fig. 10).

Saturated long-chain  $C_{16-24}$  FAL were the most abundant FAL compounds, comprising between 50 and 93% of the total FAL. While  $C_{20}$ – $C_{24}$  FAL are often considered indicators of higher plant contributions (Eglinton and Hamilton, 1967; Ficken et al., 1998), the concentration profiles observed here indicate a significant marine source (s). A clear depth trend was observed in FAL composition (Fig. 10). In general, 20:0 and 22:0 FAL contributed a higher percentage of the total FAL in the upper water column, especially in April and October post-hurricane, 16:0 FAL tended to comprise a higher percentage within the mesopelagic and upper bathypelagic layers, and 18:0 FAL exhibited no consistent depth trend.

Monounsaturated, even chained  $C_{16}$ – $C_{22}$  FALs were also present. These are components of zooplankton wax esters (Lee et al., 2006; Sargent and Lee, 1975) but also have been found in some diatoms (e.g.,  $C_{16:1}$  and  $C_{18:1}$  FAL, Berge et al., 1995) suggesting minor phytoplankton sources. The major monounsaturated FALs were  $C_{16:1}$  and  $C_{18:1}$ . The highest contribution of monounsaturated FALs was observed in the lower bathypelagic and nepheloid layers in October, where they comprised 20–25% of the total FAL. In contrast, in November the highest contribution of  $C_{16:1}$  and  $C_{18:1}$  was observed in the epipelagic layer (23% of the total FAL).  $C_{20:1}$  and  $C_{22:1}$  FAL were also present in low (< 1 ng L<sup>-1</sup>) concentrations in the epipelagic layer. Absolute concentrations of  $C_{20:1}$  and  $C_{22:1}$  decreased with depth by two orders of magnitude in the mesopelagic layer and their relative contribution to total FAL also decreased sharply with depth in all sampling periods.

Odd chained fatty alcohols are found in bacteria (Mudge et al., 2008; Parkes and Taylor, 1983), although trace amounts have also been observed in animals. 15:0 FAL was the main odd chained FAL present, comprising 0.2–4.6% of the total FAL. The maximum percent contribution of odd chain compounds was observed in the mesopelagic layer in all months.

FAL compositional differences were observed among the three sampling periods. 18:0 FAL was most abundant within the epipelagic layer in April (62% of the total FAL) and least abundant in the deep water column (< 30% of total FAL). The opposite was observed in November, where 18:0 FAL was least abundant in the epipelagic layer (34% of total FAL) and most abundant in the lower bathypelagic and nepheloid layers (73–77% of total FAL). 16:0 FAL and 20:0 FAL were the main secondary FAL compounds in April (10% and 13% of total FAL, respectively), 14:0 FAL, 16:1 FAL and 18:1 FAL were the main secondary compounds in November (19%, 13% and 11% of total FAL, respectively), and 22:0 FAL and 16:0 FAL were the main secondary compounds in October following Hurricane Nicole. Monounsaturated FAL were abundant within the deep water column in April and October, but were only minor components of the total FAL in the deep water column in November.

#### 3.2.4. Sterol, stanols and steroidal ketones

Sterols, and their stanol and steroidal ketone degradation products, were the second most abundant lipid class in the suspended particles in the epipelagic layer and the third most abundant class in the mesopelagic and bathypelagic layers (Table 4). The most abundant sterols in the suspended particles were  $C_{28}\Delta^{5,22}$ ,  $C_{27}\Delta^{5,22}$ ,  $C_{27}\Delta^{5}$  (cholesterol),  $C_{29}\Delta^{5}$ , and  $C_{29}\Delta^{5,22}$ , and the most abundant stanols were  $C_{27}\Delta^{22}$ ,  $C_{28}\Delta^{22}$ ,  $C_{27}\Delta^{0}$ , and  $C_{29}\Delta^{0}$ . The sterols  $norC_{27}\Delta^{5,22}$ ,  $C_{27}\Delta^{5,22}$ ,  $C_{28}\Delta^{5,22}$ ,  $C_{28}\Delta^{5,22}$ , and  $C_{29}\Delta^{0}$ . The sterols  $norC_{27}\Delta^{5,22}$ ,  $C_{27}\Delta^{5,22}$ ,  $C_{28}\Delta^{5,22}$ ,  $C_{28}\Delta^{5,22}$ , and  $C_{30}\Delta^{22}$  are major sterols in phytoplankton, with different relative distributions in the different phytoplankton classes (Volkman, 1986). Cholesterol,  $C_{27}\Delta^{5}$ , is the predominant sterol in animals and is a transformation product of dietary sterols (e.g., Harvey et al., 1989; Teshima, 1971).  $C_{27}\Delta^{5}$  is also highly enriched in fecal material (Neal et al., 1986; Prahl et al., 1984; Wakeham and Canuel, 1986).

Total absolute and OC-normalized concentrations of sterols + stanols (STER) generally tracked those of TEL and FA, with maximum concentrations in the epipelagic layer and a rapid decrease with depth (Figs. 6 and 11). In April, STER showed a strong subsurface concentration peak at the depth of the chlorophyll maximum (~125 ng  $L^{-1}$ ), and then declined sharply to  $< 10 \text{ ng L}^{-1}$  by 200 m depth. STER concentrations continued to decrease with depth to  $\sim 2 \text{ ng L}^{-1}$  within the lower mesopelagic and bathypelagic layers. In November, STER concentrations within the mixed layer and upper bathypelagic layer were only about half those observed in April, consistent with the low productivity in November, although concentrations within the lower bathypelagic layer were similar. In October following Hurricane Nicole, STER concentrations again showed a strong subsurface peak at the depth of the chlorophyll maximum. Concentrations within the mesopelagic layer were almost double those observed in April, consistent with the increases observed for TFA and FAL. In particular OC-normalized concentrations of cholesterol and phytosterols ( $C_{nor27}\Delta^{5,22}$ ,  $C_{27}\Delta^{5,22}$ ,  $C_{28}\Delta^{5,22}$ , Table 2) and their corresponding stanols were significantly higher in the mesopelagic layer following Hurricane Nicole in October (Fig. 11), indicating enrichment in animal- and phytoplanktonsourced OC and early degradation products in the mesopelagic layer following Hurricane Nicole.

Stanols comprised 15–18% of the total STER in the epipelagic layer and between 20 and 28% deeper in the water column (Table 4). The major stanols were the  $\Delta^{22}$  and  $\Delta^0$  stanols of the corresponding  $\Delta^{5,22}$  and  $\Delta^5$  sterols. OC-normalized stanol concentrations were highest in the upper mesopelagic layer in April and October post-hurricane (0.9 ng  $\mu gOC^{-1}$  and 1.2 ng  $\mu gOC^{-1}$ , respectively), and lowest in the bathypelagic layer in November (0.4–0.5 ng  $\mu gOC^{-1}$ ).

The within class sterol and stanol composition is shown in Fig. 12.  $C_{27}\Delta^{5,22}$  and  $C_{28}\Delta^{5,22}$  were the most abundant compounds and comprised 25-30% and 12-15% of the total, respectively, in the epipelagic layer. Sterol composition clearly evolved with increasing depth. As the percentage of phytosterol compounds decreased below the euphotic zone, the percentage of the animal-sourced  $C_{27}\Delta^5$  increased by ~40–50%. Additionally, there was shift with depth in the phytosterol  $C_{27}\Delta^{5,22}$  to  $C_{28}\Delta^{5,22}$  ratio, from 0.4 to 0.7 in the epipelagic layer to 0.8-1.3 within the mesopelagic layer, and then a decrease to 0.7-0.9 within the bathypelagic and nepheloid layers. Additionally, the percentage of  $C_{29}\Delta^5$  increased with depth, from 8 to 13% in the epipelagic and mesopelagic layers to 16-17% in the bathypelagic and nepheloid layers. Stanol composition also exhibited clear depth trends, with percentages of  $C_{27}\Delta^0$  and  $C_{29}\Delta^0$  increasing from 30 to 40% of the total stanols in the epipelagic layer to 50-55% of the total in the bathypelagic and nepheloid layers. The percentage of  $C_{27}\Delta^0$  also was higher in the mesopelagic layer, corresponding to the increased percentage of  $C_{27}\Delta^5$ . The ratio of  $\Delta^0$  to  $\Delta^{22}$  stanols also increased with depth, from 0.7 to 1.0 in the epipelagic layer to 1.7-3.0 in the bathypelagic and nepheloid layers.

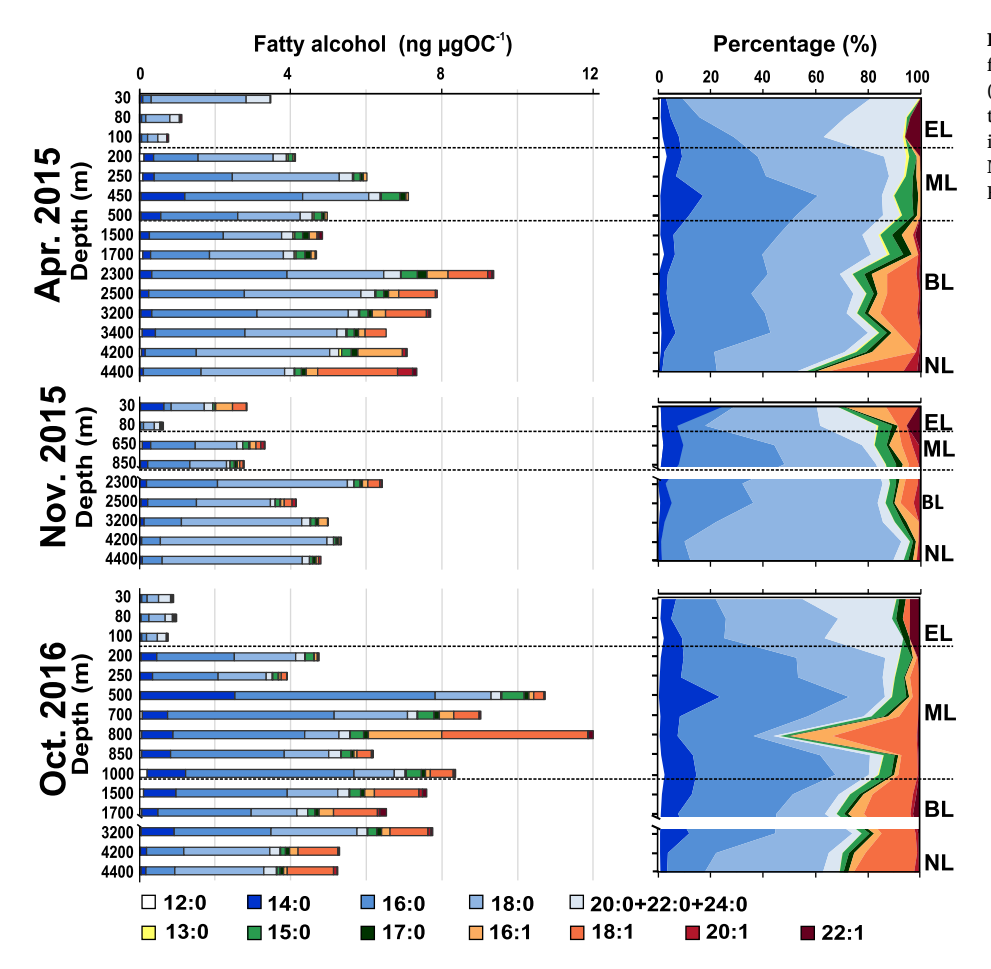


Fig. 10. OC-normalized concentration of selected fatty alcohols in the suspended particulate matter (bars, ng  $\mu$ gOC $^{-1}$ ), as well as the percentage contribution of each fatty alcohol compound (%, gaps in the plot indicate > 1000 m between samples. EL, ML, BL and NL: Epipelagic, Mesopelagic, Bathypelagic and Nepheloid layers, respectively.

Despite pigment evidence of significant differences in phytoplankton community composition (Fig. 3), the within class sterol and stanol composition was similar among the three sampling periods (Fig. 12).

The main differences were a small enrichment in  $C_{27}\Delta^{5,22}$  in April and in  $C_{29}$  sterols in November, and a higher relative abundance of the animal-sourced  $C_{27}\Delta^5$  (cholesterol) in October (20% of total sterols) as compared to April (12% of sterols). Stanol composition mirrored the small changes observed in the composition of the corresponding sterols. As observed in the corresponding sterols, the percentage of  $C_{27}\Delta^{22}$  was slightly higher in April,  $C_{29}\Delta^0$  slightly higher in November, and  $C_{27}\Delta^0$  higher following Nicole in October.

Stanol/sterol ratios have been commonly used as an index of early OM degradation (e.g., Wakeham and Lee, 1989). In general, stanol/ sterol ratios were low in the epipelagic layer and increased in the mesopelagic layer, consistent with bacterial transformation of primary  $\Delta^5$ sterols (Hudson et al., 2001; Stewart et al., 2007; Volkman, 2003). Difference among sampling periods were also observed in the deepwater column. Stanol/sterol ratios decreased between the bathypelagic and nepheloid layers in April, no decrease was observed in November, and stanol/sterol ratios increased in October with the exception of  $C_{27}\Delta^{22}/C_{27}\Delta^{5,22}$ . A particularly large increase between the bathypelagic (0.35) and nepheloid (0.71) layers was observed for the  $C_{28}\Delta^{22}$ /  $C_{28}\Delta^{5,22}$  ratio. Additionally, differences were observed in the  $C_{28}\Delta^0/$  $C_{28}\Delta^5$  and  $C_{29}\Delta^0/C_{28}\Delta^5$  ratios between the mesopelagic and bathypelagic layers among the three sampling periods, with ratios being highest in April (0.5-0.9), lower in November (0.3-0.6), and lowest in October (0.2–0.3).

Steroidal ketones (SK) were minor components of the suspended particles, comprising 0.05–0.22% of TEL (0.03–0.18 ng  $\mu$ gOC $^{-1}$ ). SK are intermediates in the degradation of sterols to sterenes (Gagosian

and Smith, 1979), although some studies indicate that they are also synthesized by some dinoflagellates (Robinson et al., 1984b). The major steroidal ketone was  $5\alpha$ -cholestan-3-one, a degradation product of cholesterol, which accounted for 34–100% of the total SK. SK concentrations were highest in the epipelagic layer, and decreased by an order of magnitude in the mesopelagic layer. OC-normalized concentrations in the epipelagic layer were similar in all sampling periods (0.09–0.11 ng  $\mu$ gOC $^{-1}$ ). OC-normalized concentrations remained high within the mesopelagic layer in April and October following Hurricane Nicole (0.11–0.14 ng  $\mu$ gOC $^{-1}$ ), but were about 50% lower in November.

# 3.2.5. Other lipid classes

Akenones. Long-chain C37-C39 methyl ketones (alkenones) are synthesized by the cosmopolitan coccolithophores Emiliana huxleyi and Gephyrocapsa oceanica (Conte et al., 1994; Volkman et al., 1980a). Alkenones were present in low concentrations, comprising between 0 and 1.3% of TEL (Table 5). The C<sub>37:2</sub> alkenone was generally detectable throughout the water column, but longer chain alkenones were detectable only in the epipelagic layer due to the low concentrations. Alkenone concentration profiles showed large differences among sampling periods (Fig. 6f). In April, an extreme concentration peak (64 ng L<sup>-1</sup>) was observed at the deep chlorophyll maximum, coincident with the peak in Hex-fuco (Fig. 3) and CaCO3 (Fig. 4), indicating a large production peak in coccolithophorids, including Emiliana huxleyi. Surface concentrations in November and October were much lower  $(< 15 \text{ ng L}^{-1})$  and no subsurface maximum was apparent. Alkenone concentrations were very low in the deep water column, averaging  $\sim$  0.02 ng L $^{-1}$  below 1500 m. An exception was two alkenone-enriched samples at 1500 m and 1700 m following the hurricane in October, suggesting a higher amount of phytodetritus from earlier E. huxleyi

Table 4 Absolute (ng  $L^{-1}$ ) and OC-normalized (ng  $\mu$ gOC $^{-1}$ ) concentrations of fatty alcohols (FAL), sterols and steroidal ketones (SK) in the epipelagic layer (EL), mesopelagic layer (ML), upper and lower bathypelagic layers (Up. BL and L. BL, respectively) and the nepheloid layer (NL). The data are average concentrations within each layer. See Table 2 for compound abbreviations. Symbols "+" indicate concentrations < 0.01 ng  $L^{-1}$  or < 1%, and symbol "-" indicate not detected.

			Aj	pril 2015	;			Nov	vember 2	015			October 2016					
		EL	Up. ML	Up. BL	L. BL	NL	EL	L. ML	Up. BL	L. BL	NL	EL	Up. ML	L. ML	Up. BL	L. BL	NL	
Total fatty alcohol (ng	L-1)	32.5	11.6	4.74	4.40	4.30	28.1	4.32	3.83	2.97	3.39	14.2	15.1	11.2	7.27	3.62	3.50	
Total fatty alcohol (ng		1.79	5.56	6.70	7.11	7.33	1.74	3.04	5.28	5.17	4.80	0.90	6.46	8.90	7.06	6.53	5.2	
(%FAL):	12:0	1	1	1	1	0	1	2	1	0	0	1	1	1	1	1	1	
	14:0	4	10	4	4	1	13	7	3	2	1	5	13	10	9	7	2	
	16:0	13	37	36	31	21	9	38	30	14	11	17	46	45	38	26	14	
	18:0	54	38	35	39	30	37	34	50	73	77	38	27	15	18	36	45	
	20:0	15	2	2	2	2	7	2	1	2	2	2	1	1	2	2	4	
	22:0	9	1	1 2	1 1	1 1	5 3	1 1	1 1	1 1	1	20 7	2 1	1	1	1	2 1	
	24:0 11:0	-	3	_	1	_	3 +	1	_	1	1	1	+	1	1	1	_	
	13:0	1	1	1	1	+	+	+	+	+	+	+	+	+	+	+	+	
	15:0	+	4	4	3	2	4	4	3	2	2	1	5	4	3	3	1	
	17:0		1	3	2	2	1	2	1	1	2	3	1	1	2	2	2	
	16:1	_	1	4	8	4	8	4	2	3	1	_	1	6	5	4	2	
	18:1	_	_	6	8	29	8	4	5	_	_	1	2	13	17	16	23	
	20:1	_	_	1	1	5	_	1	2	+	1	_	_	+	1	1	2	
	22:1	3	+	1	+	1	3	+	+	-	_	4	+	1	2	1	+	
Total sterols & stanols		108	7.72	1.90	1.27	1.70	60.4	2.77	1.31	1.13	1.04	90.2	14.7	6.57	4.02	1.70	1.92	
Total sterol & stanols (	ng μgOC <sup>-1</sup> )	5.57	3.67	2.64	2.06	2.90	3.69	1.93	1.80	1.98	1.48	5.71	5.47	5.34	3.92	3.08	2.84	
(%Sterol):	$C_{26}\Delta^{5,22}$	3	2	2	2	3	3	3	2	2	3	3	3	3	3	4	4	
	$C_{\text{nor}27}\Delta^{5,22}$	7	5	4	4	4	5	5	5	4	6	7	5	5	6	4	5	
	$C_{27}\Delta^{5,22}$	12	20	14	12	12	15	16	13	10	10	16	18	18	15	12	11	
	$C_{27}\Delta^{5}$	12	30	30	23	29	16	29	26	20	22	19	31	30	25	22	23	
	$C_{28}\Delta^{5,22}$ $C_{28}\Delta^{5,24(28)}$	31	17	17	17	16	24	14	17	16	16	23	14	15	17	17	16	
	$C_{28}\Delta^{5,2}$ (28)	4	1	-	2	2	3	1	1	2	2	1	+	1	1	1	1	
	$egin{array}{l} {\sf C}_{28} \Delta^5 \ {\sf C}_{29} \Delta^{5,22} \end{array}$	4 7	3	5 7	6 6	7	2	4 6	6 6	8 6	7 7	5	5 6	5 6	6 6	8	7 6	
	$C_{29}\Delta^5$ $C_{29}\Delta^5$	9	6 8	14	16	5 15	8 12	9	6 15	16	14	5 9	8	9	12	6 16	15	
	$C_{30}\Delta^{5,24(28)}$	2	-	-	-	-	1	1	-	10	-	2	1	1	1	1	1	
	$4\alpha C_{30}\Delta^{22}$	3	4	5	6	3	3	4	4	5	4	3	3	2	3	2	2	
Total Stanol (ng L <sup>-1</sup> )	40304	12.9	1.71	0.41	0.32	0.33	8.49	0.60	0.25	0.23	0.22	13.1	2.74	1.17	0.73	0.29	0.33	
Total Stanol (ng µgOC	-1)	0.66	0.82	0.57	0.51	0.56	0.52	0.42	0.35	0.41	0.31	0.82	1.04	0.96	0.71	0.52	0.49	
(%Stanol):	$C_{26}\Delta^{22}$	6	5	7	4	8	9	7	5	5	6	5	4	5	4	5	6	
, ,	$C_{27}\Delta^{22}$	11	15	8	7	8	15	15	9	7	8	13	11	14	11	9	6	
	$C_{29}\Delta^{22}$	24	16	14	14	11	19	14	13	13	13	20	14	15	14	10	9	
	$C_{29}\Delta^{22}$	8	4	4	4	3	9	5	5	5	4	9	7	6	6	5	6	
	$C_{27}\Delta^0$	14	22	25	21	25	16	25	24	20	22	22	22	27	24	19	21	
	$C_{28}\Delta^0$	5	9	9	10	10	8	8	10	13	14	8	8	7	9	10	11	
	$C_{29}\Delta^0$	18	25	24	28	24	20	19	27	28	25	15	25	22	24	29	29	
	$4\alpha C_{30}\Delta^0$	13	4	8	13	11	4	7	9	10	8	7	8	4	8	12	12	
Ratios stanol/sterol:	$C_{27}\Delta^{22}/C_{27}\Delta^{5,22}$	0.13	0.21	0.16	0.20	0.16	0.15	0.26	0.17	0.17	0.21	0.13	0.14	0.16	0.17	0.16	0.11	
	$C_{28}\Delta^{22}/C_{28}\Delta^{5,22}$	0.11	0.27	0.22	0.28	0.16	0.13	0.29	0.18	0.22	0.22	0.15	0.23	0.21	0.17	0.12	0.12	
	$C_{29}\Delta^{22}/C_{29}\Delta^{5,22}$	0.17	0.18	0.17	0.23	0.14	0.18	0.27	0.18	0.21	0.17	0.28	0.28	0.20	0.21	0.20	0.21	
	$C_{27}\Delta^{0}/C_{27}\Delta^{5}$	0.16	0.21	0.23	0.31	0.20	0.17	0.27	0.21	0.25	0.26	0.19	0.17	0.20	0.21	0.17	0.19	
	$C_{28}\Delta^{0}/C_{28}\Delta^{5}$	0.18	0.75	0.52	0.58	0.32	0.57	0.56	0.41	0.41	0.50	0.27	0.39	0.29	0.30	0.26	0.31	
	$C_{29}\Delta^{0}/C_{29}\Delta^{5}$	0.29	0.89	0.50	0.62	0.36	0.27	0.65	0.42	0.44	0.47	0.28	0.69	0.51	0.44	0.36	0.39	
	$4\alpha C_{30}\Delta^0/4\alpha C_{30}\Delta^{22}$ $C_{27}\Delta^5$ /phytosterol	0.66 0.15	0.32 0.46	0.46 0.45	0.71 0.34	0.96 0.43	0.27 0.21	0.58 0.49	0.56 0.39	0.51 0.28	0.52	0.42 0.27	0.65 0.49	0.39 0.47	0.73 0.37	1.03 0.33	0.97	
TOTAL Steroidal keton		1.87	0.30	0.43	0.06	0.43	1.71	0.49	0.04	0.28	0.04	1.81	0.49	0.47	0.08	0.02	0.02	
TOTAL Steroidal keton		0.09	0.30	0.04	0.06	0.04	0.10	0.11	0.04	0.02	0.04	0.11	0.29	0.16	0.08	0.02	0.02	
(%SK):	ε (ng μgOC ) 5β cholestan-3-one	31	15	11	36	19	24	22	28	38	30	35	22	25	32	37	61	
(/volt).	5α cholestan-3-one	54	57	82	57	69	47	52	61	62	30 46	35 40	47	62	32 48	63	39	
	24-ethyl-5α-cholestan-3-one		28	7	7	12	30	26	11	-	23	25	30	13	21	_	-	
	2-1-cutyr-3u-cholestan-3-one	10	20	,	,	14	30	20	11	-	۷3	23	30	13	41	_	-	

production at these depths. OC-normalized alkenone concentrations in the epipelagic layer in April were a factor of four higher than observed in November or October (Table 5), reflecting the higher coccolithophore production in April.

The ratio of di-  $(C_{37:2})$  or tri-unsaturated  $(C_{37:3})$   $C_{37}$  alkenones  $(U_{37}^{K'})$  reflects growth temperature, and can be used to estimate surface water production temperature. The values of  $U_{37}^{K'}$  at 30 m were 0.73 in April, 0.91 in November and 0.94 in October. Applying the Bermuda surface water calibration of Conte et al. (2001b), these  $U_{37}^{K'}$  values correspond to growth temperatures of 21.2 °C in April, 25.4 °C in November and 26.4 °C in October. These estimates are consistent with the mixed layer

temperatures measured in situ during these seasons.

 $C_{30}$  alkan-1,15-diol ( $C_{30}$  diol).  $C_{30}$  diols have been commonly reported in marine and freshwater environments (e.g., Versteegh et al., 1997, 2000; Rampen et al., 2012; Pedrosa-Pàmies et al., 2015), but little is known about specific biological sources and distributions throughout the water column. Long-chain n-alkan-1,15-diols have been identified in the *Nannochloropsis* sp. (class Eustigmatophyceae) (Gelin et al., 1997; Versteegh et al., 1997; Volkman, 1986; Volkman et al., 1992), and in some members of the *Proboscia* diatom genus (Sinninghe Damsté et al., 2003).

C<sub>30</sub> alkan-1,15-diol (C<sub>30</sub> diol) was the only long-chain diol detected,

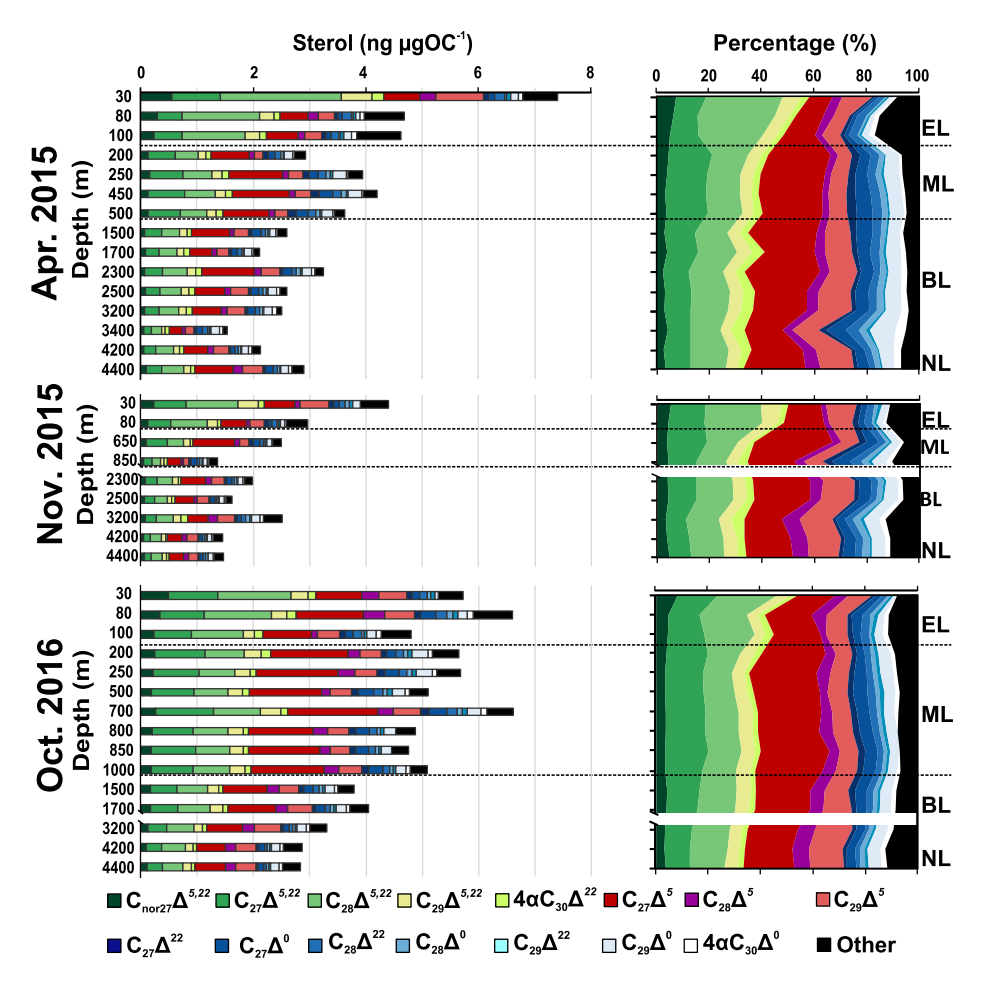


Fig. 11. OC-normalized concentration of selected sterols in the suspended particulate matter (bars, ng μgOC-1), as well as the percentage contribution of each compound (%, gaps in the plot indicate > 1000 m between samples. Fills with blue colors corresponds to stanol compounds. EL, ML, BL and NL: Epipelagic, Mesopelagic, Bathypelagic and Nepheloid layers, respectively. (For interpretation of the references to color in this figure legend, the reader is referred to the web version of this article.)

comprising between 0.02 and 1.33% of TEL.  $C_{30}$  diol concentrations were highest in the mixed layer in all periods (Fig. 6g). Concentrations were highest following Hurricane Nicole in October ( $\sim$ 14 ng L $^{-1}$  at 30 m depth) and remained high throughout the mesopelagic layer. An increase in  $C_{30}$  diol concentrations was observed in the 1500 m and 1700 m samples in October, as observed for alkenones, also suggesting phytoplankton-enriched material at these depths.  $C_{30}$  diol concentrations in the epipelagic and mesopelagic layers in April and November were similar and about 50% lower than following Nicole in October.  $C_{30}$  diol concentrations within bathypelagic waters were very low, averaging  $\sim$ 0.02 ng L $^{-1}$  in April and November. Concentrations in October were about 50% higher ( $\sim$ 0.03 ng L $^{-1}$ ), a reflection of the higher surface concentrations following Hurricane Nicole.

**Hopanoids**. Hopanoids (HOP), which include hopanoic acids, alcohols and ketones, are early degradation products of  $C_{35}$  bacteriohopanepolyols synthesized by bacteria, including some marine cyanobacteria such as *Synechococcus* (Ourisson et al., 1979; Rohmer et al., 1984). The major hopanoid compound in the samples was 22,29,30-trisnorhop-17(21)-ene (HOP-a), which accounted for  $\sim$ 75% of the total HOP.

HOP comprised 0.02–2.32% of TEL, and concentrations ranged from 0.2 to 2.8 ng  $L^{-1}$  (0.02 to 2.30 ng  $\mu g O C^{-1}$ ) (Table 5). Unlike other major lipid classes, HOP concentrations were low in the epipelagic layer (0.8–1.0 ng  $L^{-1}$ ) and highest in the mesopelagic layer (Fig. 6h, Table 5). Large differences were observed among sampling periods. In particular, HOP concentrations in the mesopelagic layer in October (~2.5 ng  $L^{-1}$ ) were more than twice those in April (~1.0 ng  $L^{-1}$ ), indicating higher bacterially-sourced OC following Hurricane Nicole. In contrast to LCK and  $C_{30}$  diol, no enrichment in HOP concentrations was observed at 1500 m or 1700 m in October.

Significant differences among sampling periods were observed in the bathypelagic layer. HOP concentrations in April (0.8 ng  $\rm L^{-1})$  were double than those observed in November (0.4 ng  $\rm L^{-1})$ . Within the nepheloid layer, HOP concentrations in April and October ( $\sim\!0.5$  ng  $\rm L^{-1})$  were also twice that in November (0.25 ng  $\rm L^{-1})$ .

Hydroxy fatty acids. β-hydroxy acids (β-OH) ranging from  $C_{10}$  to  $C_{20}$  are constituents of structural biopolymers of many microorganisms, including bacteria, yeasts, fungi and protozoa (e.g., Cardoso and Eglinton, 1983; De Leeuw et al., 1995). The source of (ω-1)-hydroxy acids (ω-OH) has long been the subject of conjecture (e.g., Boon et al., 1977; Fukushima et al., 1992) but is usually believed to be associated with bacteria (Cardoso and Eglinton, 1983; Skerratt et al., 1992).

 $C_{14}$  was the most abundant  $\beta$ -OH compound and comprised up to 47% of the total  $\beta$ -OH. This contribution is typical of that found in the cell wall lipopolysaccharide of gram-negative bacteria (Ratledge, 2008).  $\beta$ -OH concentrations ranged from 0.2 to 45 ng L<sup>-1</sup> (0.33 to 2.02 ng  $\mu$ gOC<sup>-1</sup>) and comprised 0.6–1.7% of TEL (Table 5). Concentration profiles of total  $\beta$ -OH and  $\omega$ -OH were very similar to FA profiles, including a strong concentration peak at the chlorophyll maximum in April and a weaker concentration peak in October (Fig. 6i). Additionally, concentrations in the mesopelagic layer in October were 2–3 times those in April and November. Bathypelagic concentrations were similar to trends observed for other lipid classes, with April concentrations about twice those in November. As observed for HOP, concentrations increased by ~20% between 4200 m and 4400 m in November and October, but decreased by ~20% in April.

The highest OC-normalized  $\beta$ -OH concentrations were observed in the epipelagic layer in April (1.7 ng  $\mu gOC^{-1}$ ) and October (1.4 ng  $\mu gOC^{-1}$ ) and lowest concentrations were observed in November (0.9 ng  $\mu gOC^{-1}$ ). In contrast to  $\beta$ -OH,  $\omega$ -OH concentrations in the epipelagic

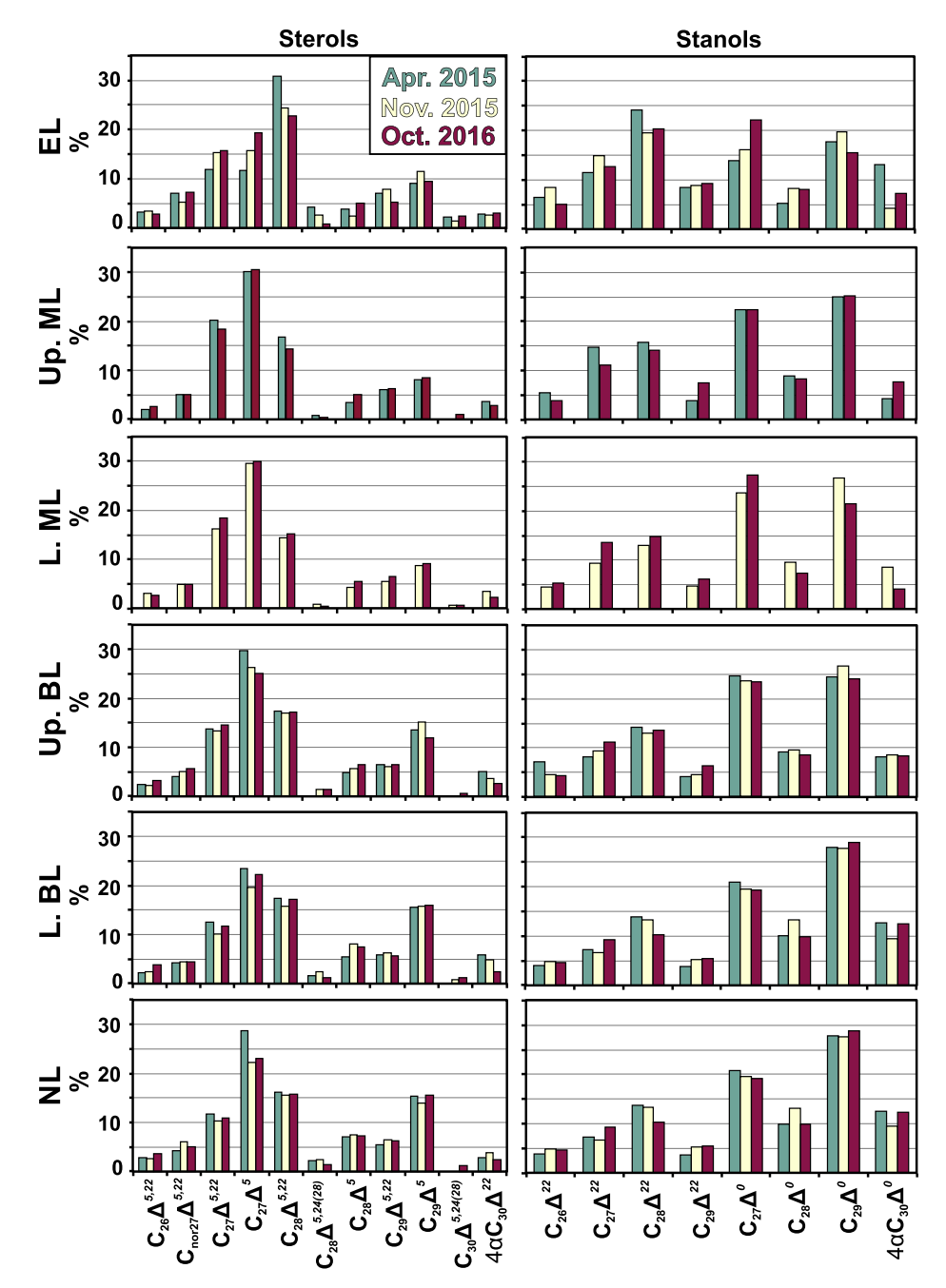


Fig. 12. Relative percentage of individual sterols and stanols (%) in the suspended particles collected in April and November 2015 and October 2016 at the epipelagic (EL), upper mesopelagic (Up. ML), lower mesopelagic (L. ML), upper bathypelagic (Up. BL), lower bathypelagic (L. BL) and nepheloid (NL) layers.

layer in April (40 ng  $L^{-1})$  were twice that observed in October (24 ng  $L^{-1}),\;$  although mesopelagic and bathypelagic concentrations in October were higher than in April. Within the nepheloid layer, both  $\beta$ -OH and  $\omega$ -OH absolute concentrations were highest in October (1.1 and 0.7 ng  $L^{-1},\;$  respectively), while OC-normalized  $\beta$ -OH concentrations were highest in April (0.8 ng  $\mu g O C^{-1}).$ 

1-O-alkylglycerols. The sources of 1-O-alkylglycerols are still largely unknown. 1-O-alkylglycerols (AG) have been found in diverse animal sources, including sharks, squid and the pteropods (Bordier et al., 1996; Kattner et al., 1998), and also have been identified in sulfate-reducing bacteria (Zeng, 1988), suggesting aerobic bacterial sources as well. This is the first study to report 1-O-alkylglycerols concentrations in suspended material. Previously these compounds have been reported in sediment trap material (Conte et al., 1998; Wakeham, 1982) and in surface sediments (Madureira, 1994).

1-O-alkylglycerols concentrations ranged from 0.6 to 39.4 ng L $^{-1}$  (0.7–2.9 ng  $\mu g O C^{-1}$ ) and comprised 0.8–3.2% of TEL (Table 5). Concentration profiles for AG were distinct from any other lipid class (Fig. 6j). Although concentrations within the epipelagic layer in April were high ( $\sim\!35$  ng L $^{-1}$ ), there was no subsurface concentration peak at the chlorophyll maximum. Conversely a subsurface concentration peak was observed in October at 100 m depth following Hurricane Nicole. The relatively high concentrations within the euphotic zone suggests that they are synthesized by organisms living within the epipelagic layer. The concentrations of 1-O-alkylglycerol in deep water exhibited a general covariation with that of cholesterol,  $18:1\omega 9$ , long-chained FAL and odd/br FA that suggests de novo synthesis and/or bioaccumulation in deep zooplankton and/or possibly additional bacterial sources. However, there was much lower enrichment in AG concentrations within the mesopelagic and bathypelagic layers in October following

Table 5
Absolute (ng  $L^{-1}$ ) and OC-normalized (ng  $\mu$ gOC<sup>-1</sup>) concentrations of long-chain alkenones (LCK),  $C_{30}$  alkyldiols, hopanoids (HOP), alkylglycerols,  $\beta$ - and (ω-1)-hydroxy fatty acids in the epipelagic layer (EL), mesopelagic layer (ML), upper and lower bathypelagic layers (Up. BL and L. BL, respectively) and the nepheloid layer (NL). The data are average concentrations within each layer. See Table 2 for compound abbreviations. Symbols "+" indicate concentrations < 0.01 ng  $L^{-1}$  or < 1%, and symbol "–" indicate not detected.

			A	pril 2015				Nov	vember 20	015				Octobe	r 2016		
		EL	Up. ML	Up. BL	L. BL	NL	EL	L. ML	Up. BL	L. BL	NL	EL	Up. ML	L. ML	Up. BL	L. BL	NL
Total alkenone (1	ng L <sup>-1</sup> )	34.6	0.30	0.02	0.02	0.02	11.1	0.04	0.02	-	_	4.58	0.06	0.07	0.07	0.02	0.02
Total alkenone (1	ng μgOC <sup>-1</sup> )	1.58	0.12	0.02	0.04	0.03	0.68	0.03	0.03	-	-	0.28	0.02	0.07	0.07	0.04	0.03
(% LCK):	37:3 Me	16	24	33	30	29	5	38	27	-	-	5	16	25	25	29	32
	37:2 Me	36	61	67	70	71	49	62	73	-	-	35	84	75	75	71	68
	38:3 Et	4	3	-	-	-	1	-	-	-	-	5	-	-	-	-	-
	38:3 Me	6	4	-	-	-	1	-	-	-	-	12	-	-	-	-	-
	38:2 Et	20	5	-	-	-	24	-	-	-	-	21	-	-	-	-	-
	38:2 Me	12	2	-	-	-	16	-	-	-	-	14	-	-	-	-	-
	38:3 Et	1	1	-	-	-	+	-	-	-	-	3	-	-	-	-	-
$C_{30}$ diol (ng L <sup>-1</sup>	)	3.34	0.05	0.02	0.02	0.02	3.94	0.05	0.02	0.02	0.02	7.44	0.44	0.09	0.11	0.03	0.03
C <sub>30</sub> diol (ng μgO		0.20	0.03	0.02	0.03	0.03	0.25	0.04	0.03	0.04	0.02	0.47	0.16	0.07	0.11	0.05	0.05
TOTAL hopanoid	ls (ng L <sup>-1</sup> )	0.95	2.19	1.11	0.82	0.52	0.76	0.92	0.55	0.39	0.26	0.81	2.61	1.32	1.32	0.64	0.53
TOTA hopanoids	, ,	0.05	1.08	1.53	1.33	0.89	0.05	0.65	0.76	0.68	0.37	0.05	1.07	1.29	1.29	1.15	0.78
(%HOP):	HOP-a	_	58	60	60	57	_	62	58	54	49	70	52	61	61	60	52
	НОР-Ъ	_	7	8	8	2	_	5	4	3	_	_	6	5	5	3	3
	HOP-c	17	4	3	2	2	_	4	3	3	_	_	5	3	3	2	3
	HOP-d	26	6	4	4	5	43	6	7	6	6	30	11	11	11	8	7
	НОР-е	-	5	5	7	12	-	6	8	17	21	-	12	7	7	14	21
Total β-hydroxy	acid (ng L <sup>-1</sup> )	34.1	2.55	0.53	0.57	0.46	14.4	1.00	0.32	0.28	0.34	45.7	7.08	3.25	1.82	0.89	1.07
	acid (ng µgOC <sup>-1</sup> )	1.71	1.15	0.74	0.93	0.79	0.88	0.71	0.43	0.49	0.48	1.41	1.02	1.09	0.89	0.58	0.51
(%β-OH):	10:0	2	3	2	9	_	2	1	2	2	2	1	1	0	2	2	4
. 1	12:0	10	14	11	1	7	8	4	5	9	4	9	7	3	3	2	1
	14:0	32	29	27	21	31	44	34	26	27	32	38	39	37	13	11	10
	18:0	4	6	7	6	6	5	7	9	10	12	4	5	1	3	7	5
	11:0	1	3	2	4	-	1	+	_	-	_	+	-	-	_	_	-
	13:0	1	3	4	1	-	3	5	8	1	-	2	5	8	7	6	3
	15:0	22	23	22	25	15	27	23	32	33	35	25	25	32	52	47	49
	17:0	19	5	16	24	31	7	8	16	19	16	15	12	13	16	17	22
	19:0	9	14	8	8	11	4	17	2	-	-	5	7	7	5	8	6
Total ω-hydroxy	acid (ng L <sup>-1</sup> )	40.2	2.44	0.64	0.59	0.48	19.0	0.48	0.24	0.38	0.39	23.8	4.48	1.94	0.91	0.57	0.73
Total ω-hydroxy	acid (ng μgOC <sup>-1</sup> )	1.97	0.98	0.88	1.03	0.81	1.16	0.33	0.33	0.67	0.55	1.55	1.65	1.59	0.89	1.03	1.08
Total 1-O-alkylgl	ycerols (ng L <sup>-1</sup> )	34.8	3.59	1.19	1.07	1.21	15.6	1.81	0.76	0.87	1.04	27.3	5.05	2.45	1.43	0.66	1.01
, , ,	ycerols (ng µgOC <sup>-1</sup> )	1.82	1.67	1.65	1.70	2.06	0.95	1.29	1.05	1.51	1.47	1.81	1.98	2.01	1.40	1.21	1.50

Hurricane Nicole in comparison to other lipid classes. Within the nepheloid layer, both absolute and OC-normalized AG concentrations were highest in April (1.2 ng L $^{-1}$ , 2.1 ng  $\mu g O C^{-1}$ ) and similar in November and October (1.0 ng L $^{-1}$  and 1.5 ng  $\mu g O C^{-1}$ , respectively).

#### 3.3. Compositional variations with depth

# 3.3.1. Organic matter constituents

We estimated the relative contributions of OM sources by summing the absolute and OC-normalized concentrations of key lipid biomarkers into three groups: Phytoplankton and labile OC (PHYTO/labile), zooplankton-derived OC (ZOO) and bacterial-derived OC (BACT):

- (1) PHYTO/labile =  $C_{18}$  PUFAs + 20:5 $\omega$ 3 PUFA + 22:6 $\omega$ 3 PUFA + phytosterols + alkenones
- (2) ZOO =  $18:1\omega9 + 20:1\omega9 + 22:1\omega9 + 22:1\omega11 +$  cholesterol + MUFALs
- (3) BACT = Odd/br FA +  $18:1\omega7$  + odd FALs + HOP

A significant positive correlation was observed between absolute concentrations of PHYTO/labile and ZOO constituents throughout the water column (r > 0.90, p < 0.0001) (Fig. 13a), indicating the tight association between phytoplankton/labile OC and zooplankton OC throughout the water column. Absolute concentrations of BACT constituents are also positively correlated with PHYTO/labile and ZOO constituents (Fig. 13b and c). Different trends within and below the

euphotic zone reflect the relative dominance of primary production and zooplankton-associated secondary production in the upper water column

Depth profiles of OC-normalized concentrations of PHYTO/labile, ZOO and BACT differed among the three sampling periods (Fig. 14). In the post bloom conditions of April 2015, a strong maximum in PHYTO/ labile was observed at the deep chlorophyll maximum (70 ng  $\mu$ gOC<sup>-1</sup>). PHYTO/labile concentrations decreased rapidly with depth in the upper mesopelagic and then remained  $\sim$  constant (15–20 ng  $\mu$ gOC<sup>-1</sup>) deeper in the water column. In contrast, ZOO and BACT concentrations were higher near the surface, decreased to a minimum at 100 m depth and then increased to maximum concentrations in the mesopelagic and bathypelagic layers. In the low productivity period of November 2015, OC-normalized PHYTO/labile contributions did not show any enrichment at the chlorophyll maximum and were 60% lower (39 ng µgOC<sup>-1</sup>) than in April. Similarly, both ZOO and BACT concentrations in the epipelagic layer were also lower. Within the deep water column, ZOO and BACT concentrations in November were ~60% of those observed in April. Major differences in the depth profiles of all three constituents were observed in October 2016 following Hurricane Nicole. PHYTO/ labile concentrations were high throughout the epipelagic layer, and remain elevated within the mesopelagic. Additionally, ZOO concentrations increase from  $\sim 10 \text{ ng } \mu\text{gOC}^{-1}$  in the epipelagic layer to  $\sim$  30–40 ng µgOC $^{-1}$  in the mesopelagic layer. BACT concentrations also doubled, and indicated higher bacterial OM in the mesopelagic layer following Hurricane Nicole.

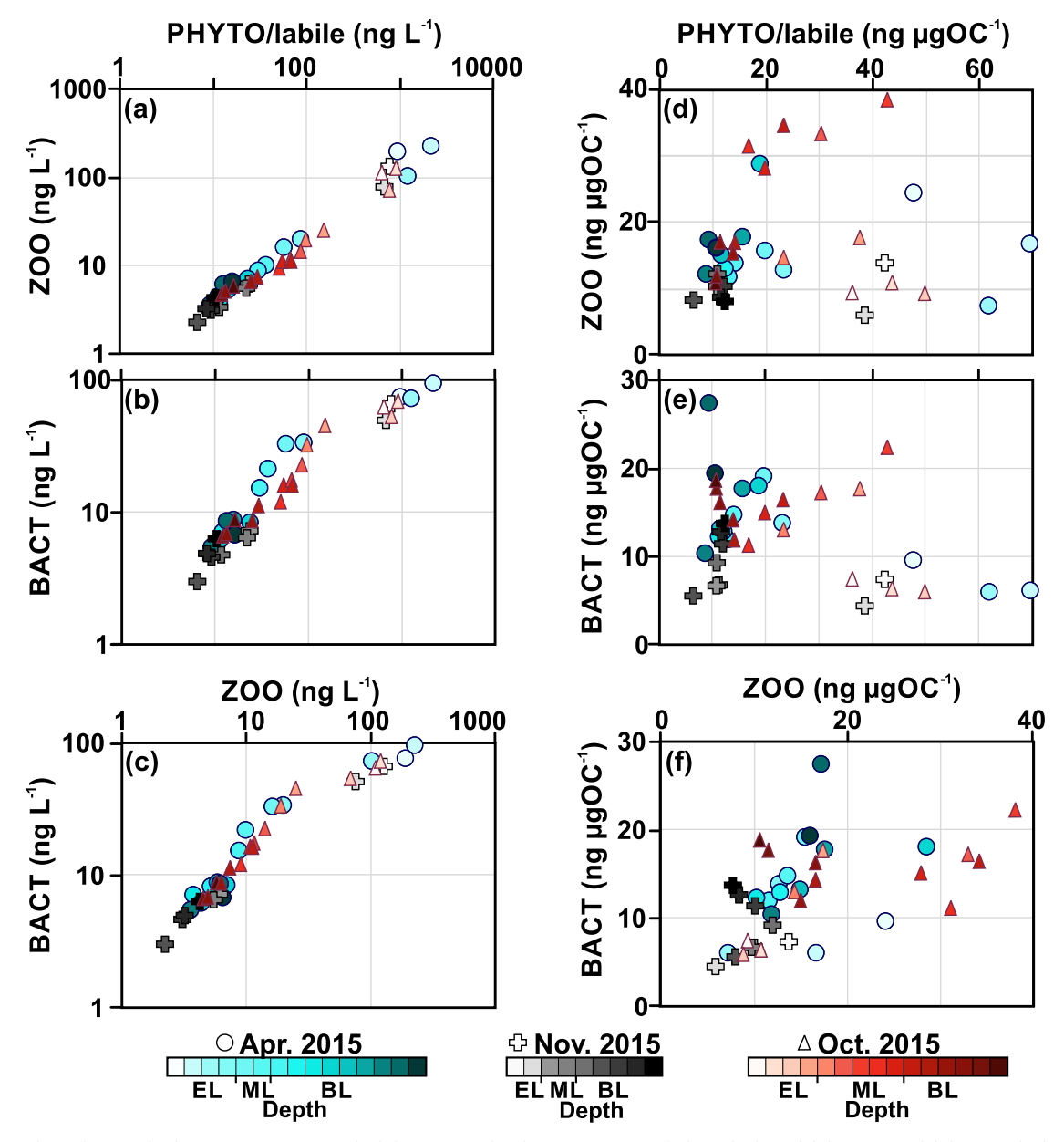


Fig. 13. Scatterplots of (a–c) absolute concentrations and (d–f) OC-normalized concentrations of phytoplankton/labile (PHYTO/labile), zooplankton (ZOO) and bacteria (BACT) OM constituents of the suspended particles collected in April 2015 (blue/green color scale), November 2015 (white/black color scale) and October 2016 (red color scale). The light to dark color gradient in each month represents the sampled depth in the epipelagic (EL), mesopelagic (ML), bathypelagic (BL) and nepheloid layers (NL). (For interpretation of the references to color in this figure legend, the reader is referred to the web version of this article.)

#### 3.3.2. Principal component analysis (PCA)

Principal component analysis (PCA) was performed to identify the dominant factors responsible for the lipid compositional variability. The first three principal components (PC1, PC2 and PC3) accounted for 62.7% of the total variation within the data set.

Factor loadings of individual lipid compounds are shown in Fig. 15. PC1 (26.4% of the variance) showed strong positive loadings for compounds associated with phytoplankton-derived OC (phytosterols, LCK,  $C_{30}$  diol, PUFAs, 14:0 and 16:0 SFA, 14:1 and 16:1 MUFA),  $\beta$ - and  $\omega$ -OH acids and indicators of labile organic material such as  $C_{20}$  and  $C_{22}$  PUFAs. Negative loadings were observed for hopanoids, fatty alcohols (except  $C_{20}$  and  $C_{22}$ ),  $C_{16:0}$  and  $C_{18:0}$  SFA, MUFA and odd/br FA. Thus, PC1 can be considered to represent a phytoplankton/labile OC source end member.

PC2 (22.0% of the total variance) showed strong positive loadings for compounds associated with animal sources, such as  $C_{16}$ - $C_{24}$  SFA,  $18:1\omega9$ ,  $20:1\omega9$ ,  $22:1\omega9$  MUFA, cholesterol ( $C_{27}\Delta^5$ ), and  $C_{20}$  and  $C_{22}$ 

PUFAS. The sterol  $C_{27}\Delta^{5,22}$ , stanols, odd/br FA,  $C_{12}$ - $C_{16}$  FAL,  $C_{15}$  FAL, HOP, AG, SK, and  $\beta$ - and  $\omega$ -OH acids also had positive loadings on PC2. The most negative loadings were found for the odd/br FAs  $C_{17:0}$  and  $C_{19:1}$ ,  $C_{16}$  and  $C_{18}$  PUFAs,  $C_{18}$  FAL and alkenones. Thus, PC2 encompasses mainly zooplankton-derived sources, early degradation products and some bacterial sources (possibly associated with zooplankton OM).

PC3 accounted for 14.2% of the total variance. The strongest loadings on PC3 were for 18:1 $\omega$ 7, odd/br FA, 22:1 $\omega$ 11 and 22:1 $\omega$ 9 MUFAs, 18:0 SFA, odd C<sub>13</sub>-C<sub>17</sub> FAL, HOP, and AG. The most negative loadings were for PUFAs, 14:1 MUFA, sterols,  $\Delta^{22}$  stanols, LCK, and C<sub>30</sub> diol. Interestingly, loading of hydroxy acids were lower on PC3 than for either PC1 or PC2. Thus, PC3 is mainly indicative of bacterial sources and more refractory, degraded OM materials.

Depth profiles of sample factor scores show the evolution in OC composition with increasing depth and also indicate compositional difference among sampling periods (Fig. 16). All epipelagic samples

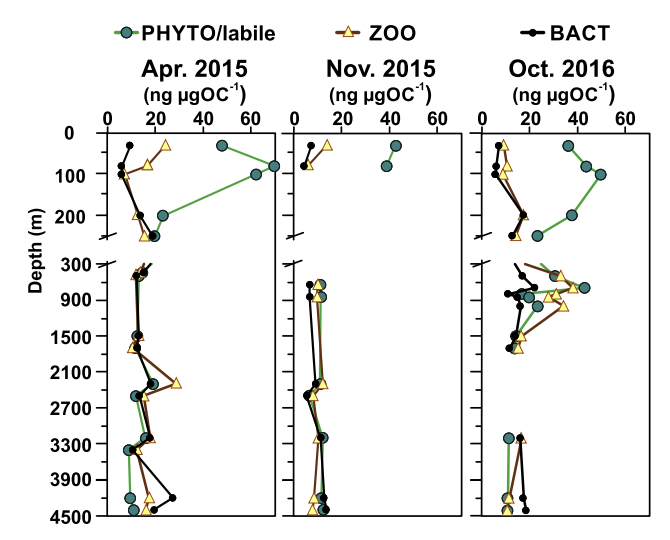


**Fig. 14.** OC-normalized concentrations of fresh/labile phytoplankton (PHYTO/labile, green;  $C_{18}$  and  $20:5\omega 3$  and  $22:6\omega 3$  PUFAs, phytosterols and long-chain alkenones), zooplankton (ZOO, yellow;  $18:1\omega 9$  MUFA, cholesterol,  $20:1\omega 9$  and  $22:1\omega 9$ ,  $22:1\omega 11$  MUFAs, and MUFAL) and bacterial (BACT, black; odd/br FA,  $18:1\omega 7$  MUFA, odd FAL and HOP) sources of the suspended particles collected in April and November 2015 and October 2016. (For interpretation of the references to color in this figure legend, the reader is referred to the web version of this article.)

have positive PC1 scores, reflecting the highest contribution of phytoplankton-derived OC in surface waters. Highest scores are observed in April 2015 and lowest scores in November 2015, reflecting the seasonal differences in production. High scores in October are consistent with other evidence for increased production stimulated by the passage of Hurricane Nicole.

PC2 scores within the epipelagic layer are negative or near zero or negative, reflecting the predominance of phytoplankton-derived OC in the euphotic zone relative to zooplankton-derived OC. Within the mesopelagic layer, PC2 scores become strongly positive in April and in October following Nicole, reflecting the rapid transition from phytoplankton- to zooplankton-sourced OC within the upper mesopelagic layer and also the high contribution of zooplankton OM in these two periods. In contrast, PC2 scores in November are much lower, consistent with a more refractory composition. Within the bathypelagic and nepheloid layers PC2 scores become strongly negative, especially at 4200 m and 4400 m depths.

PC3 scores are generally negative within the epipelagic layer except in April at 30 m within the euphotic zone. PC3 scores remain negative throughout the mesopelagic layer except in April at 200 m and 250 m, which suggest significant microbial sources are associated with OC degradation within the upper mesopelagic layer. PC3 scores became strongly positive within the bathypelagic and nepheloid layers in April and in Oct following Hurricane Nicole, indicating an increase in microbe-sourced OC. In contrast, PC3 scores were negative or near zero in the deep water column in November, suggesting a more refractory OC composition of deep suspended POC during the low productivity period.

#### 4. Discussion

This is the first study that documents vertical profiles of suspended lipid concentration and composition throughout the water column in the northwest Atlantic, from the surface to the nepheloid layer. The particulate lipid profiles of the three contrasting time periods provide new insights on seasonal and non-seasonal processes that influence the production, distribution and degradation of organic matter within the ocean's interior.

Tables 6a,b compares our data with previous studies of suspended

lipids in oligotrophic regions. The scarcity of data underscores the existing knowledge gap on the molecular composition of suspended POC in the water column. Lipid concentrations in surface waters reported here are comparable to concentrations reported in the central North Pacific (Loh et al., 2008; Wakeham, 1995), but are ~30% higher than reported in the equatorial Pacific (Sheridan et al. 2002) and ~40% higher than those reported in April in the western Mediterranean near the Strait of Gibraltar (Gérin and Goutx, 1994). FA concentrations reported in the Eastern Tropical North Pacific (Close et al., 2014) are lower but the this study only reported fatty acids contained within glycolipids and phospholipids. Lipids concentrations reported in the eastern Atlantic (Gašparović et al., 2016, 2014) and southwest Atlantic (Nemirovskava and Kravchishina, 2016) are significantly higher than in other studies; comparisons are problematic due to differences in analytical methods used in these studies (Iatroscan TLC-FID and IR spectrometry, respectively) and emphasizes a need for method calibration between different lipid analytical methods and standardized data reporting.

# 4.1. Epipelagic suspended lipid composition and plankton community structure

Phytoplankton-derived lipids in suspended particles within the epipelagic layer clearly reflected phytoplankton abundance and the vertical structure of the phytoplankton community. Higher absolute and OC-normalized concentrations of phytoplankton-derived lipids and diagnostic indicators (PHYTO/labile and PC1 factor scores) in April and October than in November mirrored the higher phytoplankton pigment concentrations (Fig. 3). Depth profiles of PHYTO/labile and PC1 also closely tracked depth profiles of Chl a. An exception was the high absolute and OC-normalized concentration of phytoplankton-derived lipids, in particular  $16:1\omega7$  and  $C_{29}\Delta^5$ , relative to Chl a in the shallow nutrient-depleted mixed layer in November. This may be due to enhanced lipid biosynthesis by phytoplankton under nutrient limitation, as documented in other studies (Frka et al., 2011; Shifrin and Chisholm, 2008; Smith et al., 1997).

Suspended lipid compositional signatures reflected differences in the phytoplankton community composition. In April high concentrations of 16:1ω7 MUFA, 18:4ω3 and 18:5ω3 PUFAs, phytosterols, and alkenones in the chlorophyll maximum indicate a diverse phytoplankton community comprised of haptophytes, pelagophytes, dictyochophytes, chlorophytes, prasinophytes, dinoflagellates and diatoms (Jeffrey et al., 1997). Concentrations of the sterols  $C_{28}\Delta^{5,24(28)}$  (abundant in many diatoms) and  $4\alpha C_{30}\Delta^{22}$  (abundant in dinoflagellates) were relatively low in comparison to more productive regions (e.g., Tolosa et al., 2008), consistent with BATS pigment data which indicates that diatoms and dinoflagellates are generally minor components of the phytoplankton community (DuRand et al., 2001; Lomas et al., 2013; Madin et al., 2001; Olson et al., 1990). Concentrations of C<sub>30</sub> diol, a biomarker of Eustigmatophytes (Nannochloropsis sp.), were consistently higher within the mixed layer than within the deep chlorophyll maximum in all periods, suggesting a preference of Eustigmatophytes for high light conditions. This finding agrees with culture studies of Nannochloropsis sp., showing that as light intensity increases, levels of cellular Chl a decrease but levels of lipid and carbohydrates increase (Sukenik et al., 1989; Wolf et al., 2018).

Phytoplankton lipid composition differed between October and April, indicating that the phytoplankton species that were stimulated by the short-lived upwelling induced by Hurricane Nicole were not the same as those growing under typical post spring bloom conditions. In particular, there was only a minimal increase in alkenone and  $C_{28}\Delta^{5,22}$  concentrations following Hurricane Nicole, indicating relatively little stimulation of coccolithophore production as compared to other phytoplankton classes. In contrast, there was a large increase in  $C_{30}$  diol concentration, indicating the nutrient upwelling induced by Hurricane Nicole particularly stimulated Eustigmatophyte production. One

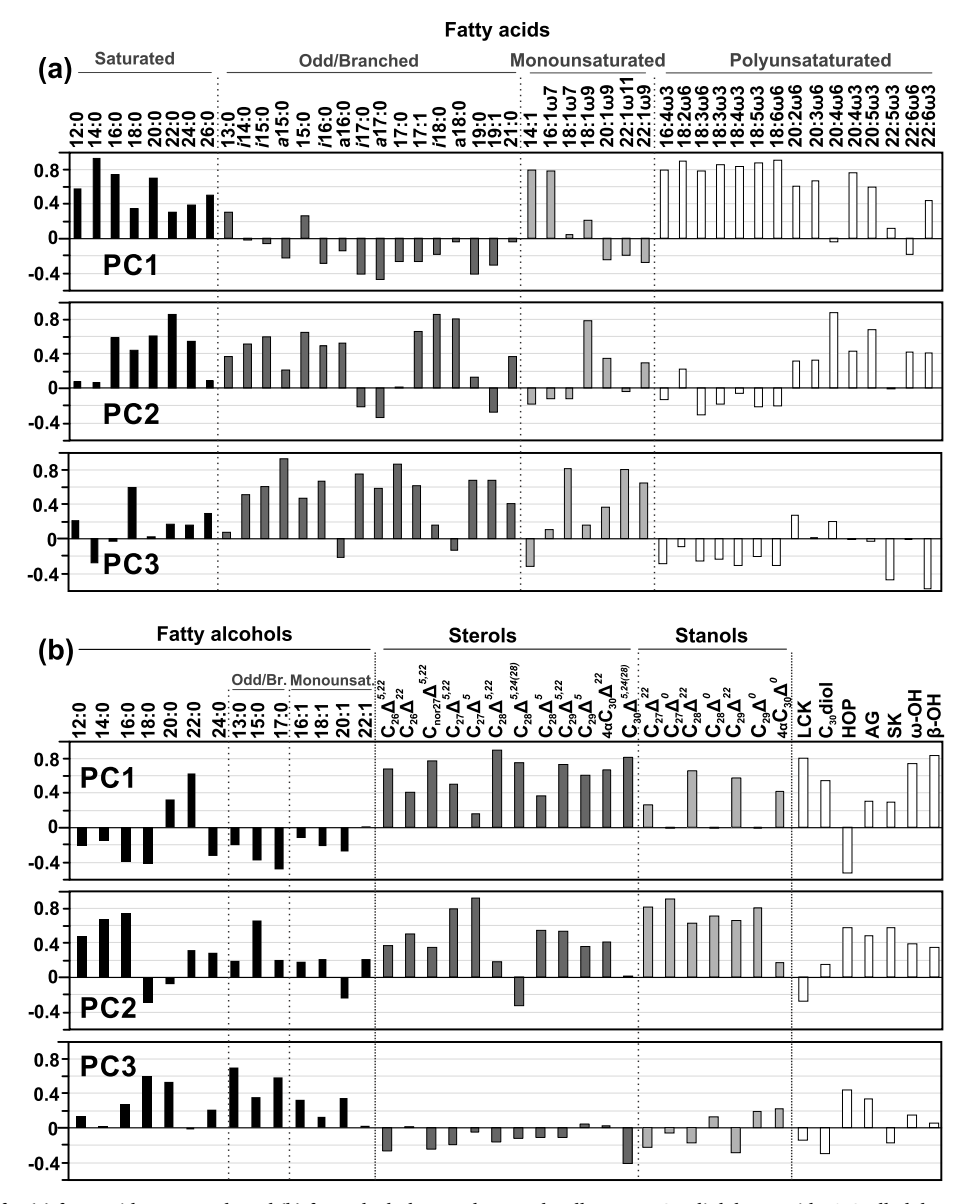


Fig. 15. Factor loadings for (a) fatty acid compounds and (b) fatty alcohols, sterols, stanols, alkenones, C<sub>30</sub> diol, hopanoids, 1-O-alkylglycerols, steroidal ketones, and hydroxy acids for the principal components (PC1, PC2 and PC3) considering each suspended particulate matter sample (See abbreviations in Table 2).

possible explanation for the lower community contribution of Eustigmatophytes to production in April is their preference for higher growth temperatures (Rampen et al., 2012; Versteegh et al., 1997, 2000).

Depth profiles of  $\delta^{13}$ C and C/N reflected the relative abundance of primary versus reworked OM within the epipelagic layer. A minimum in  $\delta^{13}$ C and the low C/N ratios at the chlorophyll maximum, a pattern also observed in the Sargasso Sea by Druffel et al. (2003), suggest a high contribution of lipid- and protein-rich phytoplankton to the OM. The more depleted  $\delta^{13}$ C values in the surface in April relative to November, may also reflect isotopic fractionation associated with OM recycling (e.g., Close et al., 2014; Druffel et al., 2003, 1998; Hwang et al., 2009; Jeffrey et al., 1983). This implies a greater loss of labile <sup>12</sup>C-enriched compounds (e.g., carbohydrates and proteins) in the residual particulate OM in April due to more intensive OM recycling during higher productivity conditions. This idea is supported by the observation that δ<sup>13</sup>C is most depleted during the high productive periods (post-hurricane and late-spring conditions), when there are relatively low C/N ratios (5.0-6.2, Fig. 4e) and high concentrations of phytoplankton-derived pigments and lipids (e.g., alkenones, PUFAs, phytosterols).

Correlations in absolute and OC-normalized concentrations of phytoplankton-derived lipids with zooplankton- and bacterially-derived lipids within the epipelagic layer indicate that zooplankton and bacterial OM closely track that of the phytoplankton (Fig. 15). Zooplankton-sourced lipids within suspended particles include living microzooplankton biomass (e.g., Brett et al., 2009; Kattner et al., 2007), detrital particles of mesozooplankton tissues produced during "sloppy feeding" (Frost, 1972; Vinogradov, 1968) and fecal particles of reworked dietary OM. While fecal material can be a significant source of SFA, MUFA, cholesterol, stanols and a minor source of bacterial lipids, it is extremely depleted in PUFAs due to high PUFA bioassimilation efficiencies in animals (Bradshaw and Eglinton, 1993; Harvey et al., 1987)

Changes in the FAL composition (e.g., relative ratios of  $C_{18}$ - $C_{24}$  saturated FAL and the relative abundance of MUFAL) indicated differences in wax ester composition of the zooplankton community among the three periods. Higher relative contributions of 20:1 and 22:1 FAL were observed in the epipelagic layer in April and October, and higher relative contributions of 14:0 FAL and MUFAL were observed in November. The differences in these FAL, which are primarily derived

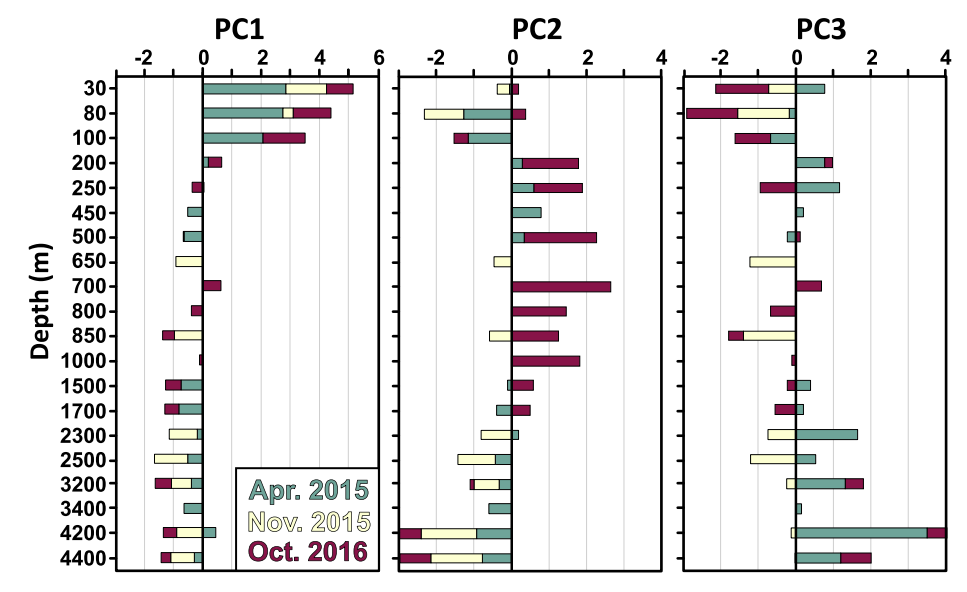


Fig. 16. Factor scores of each analyzed sample for each principal component (PC1, PC2 and PC3).

from zooplankton wax esters, may possibly reflect the greater abundance of herbivorous zooplankton during periods of high phytoplankton productivity, as herbivorous and carnivorous copepods show differences in their wax ester composition (Lee et al., 2006; Ratnayake and Ackman, 1979; Sargent and Falk-Petersen, 1981). Further research is needed to more quantitatively assess the relationship between the fatty alcohol composition and zooplankton trophic level.

The suspended lipid composition also indicated differences in the relative abundances of zooplankton and bacterial communities among the sampling periods. The  $18:1\omega9/18:1\omega7$  ratio, an indicator of relative contribution of zooplankton versus bacterial carbon, was highest in April and lowest in November, consistent with relative contribution of zooplankton OM in the suspended particles (Fig. 14). The trend suggests transition to a more microbially-dominated food web in low productivity conditions (Giovannoni and Vergin, 2012). Differences in bacterial community structure among the three sampling periods, presumably associated with OM compositional changes, are indicated by compositional differences in odd/br FA, stanols,  $\beta$ -hydroxy acids and HOP.

#### 4.2. Remineralization and particle cycling within the mesopelagic layer

The rapid decrease in concentrations of total extractable lipids and most lipid classes below the euphotic zone evidences the intense OM remineralization and particle cycling within upper mesopelagic waters. For example, fatty acid and sterol absolute concentrations in April decreased about 95% between the chlorophyll maximum and 200 m (Fig. 6, Tables 3–5). Similar rates of lipid losses have been observed in the oligotrophic North Atlantic (Conte, 1990), eastern tropical North Pacific (Close et al., 2014), and Mediterranean Sea (Tolosa et al., 2003).

The decrease in particulate lipid concentration was accompanied by a rapid alteration in suspended lipid composition below the euphotic zone that indicated a transition from phytoplankton-dominated OM in the euphotic zone to increasingly zooplankton- and bacterially-dominated OM in the upper mesopelagic layer. OC-normalized concentrations of lipids primarily associated with phytoplankton decreased more rapidly than those associated with zooplankton and bacteria. For example, in April, OC-normalized concentrations of phytoplankton-derived lipids decreased by 25% between the chlorophyll maximum and 200 m, whereas those of zooplankton-derived lipids (e.g., cholesterol,  $18:1\omega9$ , long-chain FAL, MUFAL and long-chain FAL) declined on average by only 5%. The transition in OM composition below the euphotic zone is also clearly observed in the PCA factor scores (Fig. 16). OC-normalized concentrations of long-chain  $C_{20}$ - $C_{22}$  PUFAs, abundant

in living and fresh detrital zooplankton tissue but depleted in fecal materials, persisted with depth in all sampling periods, indicating that fecal material was not the exclusive source of the zooplankton-derived OM in the mesopelagic layer. The positive increase in  $\delta^{13}\text{C}$  of POC with depth below the chlorophyll maximum is also consistent with the transition to more recycled OM with increasing depth, as heterotrophic biomass becomes increasingly  $^{13}\text{C}$ -enriched as a result of isotopic fractionation during metabolism (DeNiro and Epstein, 1978) and as a result of  $^{13}\text{C}$ -enrichment in the residual suspended pool due to preferential reactivity of  $^{12}\text{C}$  bonds during remineralization (Sun et al., 2004).

Zooplankton- and bacteria-derived lipid concentrations covaried over this depth transition (Figs. 14 and 15). This may reflect ingrowth of bacteria associated with zooplankton activity (Cnudde et al., 2013), which contributes to the OM substrate available for microbial degradation (Dang and Lovell, 2016; Gowing and Silver, 1983; Grossart et al., 2003; Karl et al., 1988), as well as colonization of zooplankton detritus by free living bacteria (Jing et al., 2012).

The intensity of the OM remineralization and transformation within the mesopelagic layer is particularly noticeable in the increases with depth in relative abundances of bacteria-derived compounds such as odd/br FA,  $18:1\omega7$ , FAL  $C_{15}$ - $C_{17}$  and in absolute HOP concentrations (Figs. 6 and 8–10, Tables 3–5). An interesting observation is the increase in concentrations of the major hopanoid compound Hop-a within the oxygen minimum zone, suggesting a greater dominance of bacterial OM at this depth (Fig. 6h, Table 5). This is consistent with studies that suggest a connection between bacterial metabolism of hopanoid producers and N cycling under low-O<sub>2</sub> conditions (Kharbush et al., 2016, 2013).

A depth trend was also observed in the relative abundances and within-class composition of bacteria lipids, evidencing a depth evolution in microbial community structure. The relative contributions of HOP-c, HOP-d, short-chained odd/br FA, and even short-chained  $\beta$ -OH decreased from the euphotic zone into the mesopelagic layer (Tables 4 and 5), suggesting that these compounds are predominantly associated with fresh labile material and/or phytoplankton-associated bacterial populations (e.g., Tholosan et al., 1999; Grossart and Gust, 2009). Vertical stratification of free-living bacterial and archaeal groups between the euphotic and mesopelagic layers in the open ocean is well documented in the Sargasso Sea (Carlson et al., 2009; Gordon and Giovannoni, 1996), the North Pacific Subtropical Gyre (DeLong et al., 2006), and the northeast Pacific (Gordon and Giovannoni, 1996) and the Mediterranean Sea (Moeseneder et al., 2001) and may be controlled

Table 6a Data compilation of total extractable lipids concentrations (ng  $L^{-1}$ ) in suspended material published for open ocean areas.

	Tota	Total lipids (ng L <sup>-1</sup> )			Total lipid	$ls (ng L^{-1})$		Total lipids (ng L <sup>-1</sup> )						
Area	5	Sargasso Sea	ı		Equatoria	al Pacific			E Tropical S Atlantic	NE Atlantic	SW Atlantic			
Lat Long	31.50N 64.10W Apr 2015	31.50N 64.10W Nov 2015	31.50N 64.10W Oct 2016	5–12N 140W Aug–Sep 1992	0–5N 140W Aug–Sep 1992	0–5S 140W Aug–Sep 1992	5–12S 140W Aug–Sep 1992	26-44N Nov 2008	11N 8S Nov 2008	49.0N 16.5W Jun 2013	0N 30W Feb–March 2012	0N 30W May 2012		
Method	GC-MS	GC-MS	GC-MS	GC-MS	GC-MS	GC-MS	GC-MS	Iatroscan TLC-FID	Iatroscan TLC- FID	Iatroscan TLC- FID	IR spectroscopy	IR spectro-		
Reference	1	1	1	2	2	2	2	3	3	4	5	scopy 5		
Depth range (1	n)			<u> </u>										
0-30	2729	2287	1734	573	1913	1513	973	7100 ± 2100	7500 ± 1000	18120 ± 4906	8000-42000	3000-21000		
30–50	-	-	-	684	1595	1181	-	10800	-	1113	-	-		
50-80	4957	1611	2382	-	-	-	-	$5600 \pm 800$	$8500 \pm 800$	-				
80–100	2606	-	1965	535	414		607	5900	-	4280	-	-		
100–150	-	-	-	145	-	308		6400	-	-	-	-		
150-200	375	-	432	-	-	-	-	-	-	449	-	-		
200–250	243	-	295	87	96	183	130	-	-	5220	-	-		
300–350		-	-	-	-	-	-	_	_	-	_	_		
350-400	167	-	-	-	-	-	-	-	-	4930	-	_		
400–450	167	-	050	48		87	82	-	-	-	_	-		
450–500 500–550	122	-	253	-	-	-	-	_	-	_	_	-		
550-600	_	-		-	-	-	_	_	-	- 4420	_	-		
600-700		- 80	- 194	- 43	-	-	- 43	_	-	4420	_	-		
700–800	-	-	164	43 34	-	-	43 29	- 8100	- 5100	7320	_	-		
800-900	_	- 74	164 157	34 -	_	_	29 -	0100	5100	/ 320	_	-		
900–1000	_	/ <del>4</del> -	179	_	_	-	_	_	_	- 7190	_	_		
1000-1000	62	_	87	_	_	_	_	_	_	5630	_	_		
1500-2000	52	_	73	_	_	_	_	_	_	10310	_	_		
2000–2000	62 ± 20	- 32 ± 8	/3	_	_	_	_	_	_	4590 ± 57	_	_		
3000-4000	$62 \pm 20$ 57 ± 10	32 ± 8 35	43	_	-	-	_	-	-	4590 ± 57 3105 ± 191	_	_		
4000–4000	55 ± 9	$33 \pm 5$	43 ± 8	_	_	_	_	3500	_	5315 ± 1563	_	_		
4000-3000	33 ± 9	33 ± 3	49 ± 6	-	_	-	_	3300	-	3313 ± 1303	-	_		

References: (1) This study, (2) Sheridan et al. (2002), (3) Gašparović et al. (2014), (4) Gašparović et al. (2016), and (5) Nemirovskaya and Kravchishina (2016).

by gradients of nutrient and substrate lability, as suggested by Robinson et al. (2010) and references therein.

The depth profiles of zooplankton and bacterial lipids in the upper mesopelagic layer differed between the two productive sample periods. OC-normalized concentrations of ZOO and BACT, respectively, increased ~40%- and ~60% between the chlorophyll maximum and 200 m depths and then decreased by 20% by 500 m, paralleling the rapid decrease in PHYTO/labile concentrations (Fig. 14). This reflected the rapid remineralization of phytoplankton-derived products and secondary inputs by zooplankton and bacterial production in the late spring conditions. In contrast, in October following the passage of Hurricane Nicole, OC-normalized concentrations of PHYTO/labile, ZOO and BACT, as well as stanols,  $C_{15\text{--}17}$   $\beta\text{-OH}$  and 1-O-alkylglycerols, were ~30% higher between 100 and 500 m than observed in April (Figs. 14–16, Tables 4 and 5). Additionally, the  $\delta^{13}C$  of the POC was more depleted than in April (Fig. 4d). This suggests a higher efficiency of export of fresh phytodetritus following the passage of Hurricane Nicole, and also a greater stimulation of zooplankton and bacterial communities in the mesopelagic layer by the increase in labile OM (see Section 4.5).

The strong correlations observed among phytoplankton, zooplankton and microbial lipids in the euphotic and mesopelagic layers indicate close coupling between primary and secondary production. This agrees with previous studies showing linkages between phytoplankton concentration in surface waters and zooplankton and bacterial production (e.g., Azaml et al., 1983; Li et al., 1993; De Kluijver et al., 2010; Gilbert et al., 2012). Our results clearly show that this coupling persists into the mesopelagic. Even so, there were differences in this phytoplankton-bacteria coupling between April and October. For example, the slopes of the regression of absolute concentrations of BACT with PHYTO/labile differed between April and October (Fig. 13b). Additionally, there was a correlation between OC-normalized concentrations of PHYTO/labile and BACT in October, but not in April (Fig. 13e). One explanation for these differences could be lower bacterial production in the surface layer in October due to rapid cooling of the mixed layer, as suggested by studies showing the reduction of bacterial production after entrainment of cold subsurface water into the mixed layer (Kim, 2017). A second could be differences in phytoplankton physiology and phytoplankton exudation of carbon-rich substances, which in turn would affect phytoplankton-bacterial coupling due to differences in the carbon substrate available to bacteria (De Kluijver et al., 2010).

# 4.3. Suspended lipid composition within the bathypelagic layer

### 4.3.1. Depth trends

The zooplankton dominance of suspended particle OM in the upper bathypelagic transitioned to a stronger bacterial dominance in the lower bathypelagic in all sampling periods (Fig. 14). Significant zooplankton input into the suspended particle pool in the upper bathypelagic layer was indicated by the high relative abundances of cholesterol,  $18:1\omega 9,\ n\text{-}C_{16}\text{-}C_{18}$  and  $n\text{-}C_{16:1}\text{-}C_{18:1}$  fatty alcohols (Figs. 8, 10-12, Tables 3 and 4). The zooplankton-derived lipids can be contributed by "sloppy feeding" of predators on zooplankton prey (Frost,

Table 6b Data compilation of total fatty acids concentrations (ng  $L^{-1}$ ) in suspended material published for open ocean areas.

				$FA (ng L^{-1})$	)			FA (r	$\log L^{-1}$ )	$FA (ng L^{-1})$	$FA (ng L^{-1})$		
Area				Sargasso Sea	a			N Centr	al Pacific	Mediterranean Sea	E Tropic	al N Pacific	
Lat Long	31.50N 64.10W	31.50N 64.10W	31.50N 64.10W	38N 64W	38N 66W	38N 6W	31.50N 63.30W	31N 159W	28N 155W	6N 2W	9N 90W	12N 105W	
DATE	Apr 2015	Nov 2015	Oct 2016	Aug 1982	Oct 1982	Oct 1982*	Jun 2000	Jul 1999	Jul/Aug 1983	Apr 1991	Dec-Jan 2009	Dec-Jan 2009	
Method	GC-MS	GC-MS	GC-MS	GC-MS	GC-MS	GC-MS	GC-MS	GC-MS	GC-MS	GC-MS	GC-MS	GC-MS	
Reference	1	1	1	6	6	6	7	7	8	9	10	10	
Depth range (m)													
0-30	2186	1904	1392	_	_	814	853	_	_	1170	_	49	
30-50	_	-	-	1276	1243	-	_	1254	1720	580	303	-	
50-80	4179	1355	1963	_	_	_	_	_	_	_	_	199	
80-100	2171	_	1616	_	979	462	_	_	_	1165	_	113	
100-150	_	_	-	_	141	166	_	_	570	510	_	81	
150-200	237	_	346	_	_	_	_	_	_	_	24	_	
200-250	173	_	228	176	89	87	_	_	130	_	_	_	
300-350	_	_	_	107	_	88	_	_	_	_	17	46	
350-400	_	_	-	_	_		_	_	_	_	37	_	
400-450	103	_	-	81	89	69	_	_	340	_	_	_	
450-500	80	_	200	_	_	_	_	_	_	_	_	_	
500-550	_	_	-	90	83	90	_	_	_	_	_	13	
550-600	_	_	_	77	_	65	_	_	_	_	11	_	
600-700	_	57	152	89	_	_	_	_	120	_	_	_	
700-800	_	_	131	_	_	_	_	_	_	_	10	_	
800-900	_	53	116	_	_	_	53	20	_	_	_	_	
900-1000	_	_	144	_	_	_	_	_	_	_	_	_	
1000-1500	39	-	63	-	-	-	29		110	_	-	-	
1500-2000	31	-	51	-	-	-	_	11	_	_	-	-	
2000-3000	$40 \pm 16$	$20 \pm 7$	-	-	-	-	_	-	-	_	-	-	
3000-4000	$344 \pm 10$	20	30	-	-	-	_	_	_	_	-	-	
4000-5000	$37 \pm 4$	$23 \pm 4$	$32 \pm 6$	_	_	_	_	_	_	_	_	_	

References: (1) This study, (6) Conte (1990), (7) Loh et al. (2008), (8) Wakeham et al. (1995), (9) Close et al. (2014), and (10) Gerin and Goux (1994).

1972; Møller, 2007; Vinogradov et al., 1977) and/or by living microzooplankton biomass. The bacterial contribution was more dominant in the lower bathypelagic layer, as indicated by the higher OC-normalized concentrations of odd/br FA,  $\Delta^0$  stanols, hopanoids and hydroxy acids (Tables 3–5). The bacterial dominance in the bathypelagic particle pool observed here is consistent with studies in the North Atlantic showing that bacterial reprocessing plays the major role in remineralization of detrital OM in the deep ocean (Kaiser and Benner, 2008). The heterotrophic microbial community in the bathypelagic layers is poorly characterized although new metagenomic tools are revealing that deep sea microbial communities have a diverse phylogenetic composition and metabolic capability (Arístegui et al., 2009; Bergauer et al., 2017; Herndld and Reinthaler, 2013; Nagata et al., 2010).

Depth profiles of suspended lipids indicated significant compositional heterogeneity of the bathypelagic suspended particle OM (Figs. 5 and 6, Tables 3–5). This compositional heterogeneity is imperceptible from bulk properties. For example, in April the suspended OM at 2300 m, 3200 m and 4200 m depth was enriched in FA, FAL and AG. Suspended lipids at 2300 m were also enriched in cholesterol and other zooplankton lipids, as well as depleted in  $\delta^{13} C$ , indicating more zooplankton lipid-rich OM. Suspended lipids at 4200 m showed greater enrichment of bacterial biomarkers. Bathypelagic suspended particles appeared to have a more homogeneous composition in November and October. The depth heterogeneity observed here may reflect temporally and compositionally variable OM export to the deep ocean during spring bloom conditions, which in turn, would result in more variable POC pool and heterotrophic reprocessing.

Depth trends were observed in several lipid classes although, given the current dearth of lipid information on deep sea organisms, reasons for these trends are unclear. For example, there was a substantial increase with depth in the stanol/sterol ratios of  $C_{29}$  and  $C_{30}$  compounds  $(C_{29}\Delta^0/C_{29}\Delta^5$  and  $4\alpha C_{30}\Delta^0/4\alpha C_{30}\Delta^{22}$ , respectively) but not of  $C_{27}$   $(C_{27}\Delta^0/C_{27}\Delta^5)$  and  $C_{28}$   $(C_{28}\Delta^0/C_{28}\Delta^5)$  compounds (Table 4). There also was an increasing contribution of  $C_{29}\Delta^5$  with depth (Fig. 12). One explanation is that this reflects an increasing relative sterol contribution from *de novo* production by deep ocean prokaryotes, as studies have shown that some cyanobacteria synthesize  $C_{29}\Delta^5$  (Paoletti et al., 1976; Volkman, 2003, 1986). The increase in the  $\Delta^0/\Delta^{22}$  ratio, which is mainly due to the increase in  $C_{27}\Delta^0$  and  $C_{29}\Delta^0$ , may reflect an increasing contribution of zooplankton fecal material and/or bacterially-reworked OM with depth, as  $\Delta^0$  stanols are easily hydrogenated by bacteria and abundant in fecal material (Harvey et al., 1987).

Within class distributions of fatty acids and fatty alcohols also showed significant trends with depth indicating a continuing turnover of suspended particles throughout the deep ocean. (Figs. 8 and 10). The relative abundance of 14:0 and 16:0 fatty acids decreased with depth, while the 16:1 fatty acid increased. Similarly, the relative abundance of  $C_{14^-16}$  fatty alcohols decreased with depth, while the  $C_{18}$  fatty alcohol increased. Similar trends in suspended particle FAL composition have been suggested in mesopelagic waters in the equatorial Pacific Ocean (Sheridan et al., 2002). The increase in FA and FAL chain-length may reflect a biochemical adjustment in deep ocean organisms to maintain membrane fluidity as pressure increases and temperature decreases (Pond et al., 2014; Siliakus et al., 2017).

Depth trends in bacterial lipid composition through the bathypelagic layer suggest a depth zonation in bacterial community structure from upper-ocean to the deep sea. For instance, there was a clear increase in the chain length of bacterial odd/br FA with depth (Fig. 9). Odd/br FA are important bacterial membrane components (e.g., Cho and Salton, 1966; Kaneda, 1991; Russell and Sandercock, 1980), so the

<sup>\*</sup> New warm-core ring.

increase in chain length with depth may similarly reflect a biochemical adjustment to maintain membrane fluidity. This is consistent with studies that have shown that piezophilic bacteria have evolved unique metabolic capabilities and molecular architectures which allow them to thrive under cold high-pressure conditions (DeLong et al., 2006; Lauro et al., 2007; Lauro and Bartlett, 2008).

#### 4.3.2. Seasonal and non-seasonal variability

The results clearly show that seasonal and non-seasonal variability in the upper ocean extends into the deep sea. Concentrations of zoo-plankton-derived lipids in the bathypelagic layer covaried with overlying upper ocean productivity, being relatively high in April and October and low in November (Fig. 14). Additionally, in the bathypelagic layer, higher relative contributions of 16:1 and 18:1 MUFAL, constituents of wax esters, were observed in April and October, which suggest higher contributions from omnivorous zooplankton feeding on phytodetritus (Lee et al., 2006; Ratnayake and Ackman, 1979; Sargent and Falk-Petersen, 1981). In contrast, 16:1 and 18:1 MUFAL were highest in the epipelagic layer in November, when phytodetrital contributions would be minimal.

Concentrations of bacterial-derived lipids were higher during April and October following Hurricane Nicole, and covaried with the concentrations of zooplankton-derived lipids (Fig. 14). PC3 scores also were strongly positive within the bathypelagic and nepheloid layers, indicating an increase in microbe-sourced OC in deep waters when surface productivity is high. An interesting observation is that the relative contribution of bacterial versus zooplankton lipids in deep waters was slightly higher in November during low productivity conditions, which suggests a greater relative reduction in microzooplankton biomass and/or zooplankton activity when suspended POC is more refractory. Previous studies have indicated a link between the deep phytodetritus flux and zooplankton and bacterial biomass (Azaml et al., 1983; Conte et al., 1995; Pozzato et al., 2013; Rice et al., 1986; Schnack-Schiel and Isla, 2005). Our observations provide further evidence that zooplankton processing of OM and bacterial remineralization are coupled and closely tied to the lability of the POC pool. This is supported by studies that have shown increased bacterial activity in deep waters during periods of high POC export flux (Bergauer et al., 2017; Hansell and Ducklow, 2003; Kaiser and Benner, 2008; Koppelmann et al., 2005; Nagata et al., 2010; Reinthaler et al., 2006).

In contrast to the FA and FAL lipid classes, sterol and stanol composition showed a high degree of similarity throughout the deep ocean in all study periods (Fig. 12), which suggests that sterols and stanol biomarkers are of limited utility to assess OM variability in the deep ocean. This stability in the sterol composition may be a reflection of the stability/proportionality/persistence of the deep eukaryotic membrane lipid composition (Dufourc, 2008).

### 4.4. Lipid composition of the deep nepheloid layer

Nepheloid layers are formed by the balance between particle settling and resuspension processes and act as a interface between pelagic and benthic particle cycling (Ransom et al., 1998). Previous studies have observed a weak nepheloid layer in the Sargasso Sea (e.g., (Gardner et al., 2017; Ohnemus and Lam, 2015) but this is the first to characterize its molecular organic composition and temporal variability.

The nepheloid layer had higher concentrations of POC and lipids in comparison with the overlying water column (Fig. 5, Tables 3–5). The enrichment in zooplanktonic and bacterial biomarkers (e.g., MUFA 18:1 $\omega$ 7, odd/br FA, SFAL and MUFAL, cholesterol  $C_{29}\Delta^5$ , stanols  $\Delta^0$  and 1-O-alkylglycerols; Fig. 12, Tables 3–5) indicates the accumulation of zooplankton and bacterial biomass and bacterial alteration products. These observations are consistent with other studies that found zooplankton-derived OM and phytodetritus in deep ocean nepheloid layers (e.g., Conte et al., 1995; Huvenne et al., 2011; Kiriakoulakis et al.,

2011; Walsh et al., 1988; Wilson, 2016). The relatively high concentrations of sterols, labile PUFAs such as  $20:5\omega 3$  and  $22:6\omega 3$ , and the depletion of compounds that are usually abundant in sediments (e.g., hopanoids and  $> C_{22}$  saturated acids) shows that the nepheloid layer in this region contains relatively undegraded material and is not composed exclusively of resuspended sediments.

Compositional differences among the three sampling periods indicate seasonal and non-seasonal variability. Lower C/N ratios and higher absolute concentrations of labile compounds (e.g., PUFAs  $20.5\omega3$  and  $22.6\omega3$ , phytosterols) were observed in April and October relative to November, suggesting increased deposition of phytodetritus and labile OM during periods of higher surface productivity. This is consistent with observations of increased deep flux of labile OM during the spring bloom and following transient phytoplankton blooms (Conte et al., 2003, 2001a). The deposition of fresh phytoplankton detritus on the seafloor following the phytoplankton blooms is well-documented for the deep temperate eastern North Atlantic (Billett et al., 1983; Gooday, 2002; Lampitt, 1985; Rice et al., 1986) and eastern Pacific (Smith et al., 1996, 2017), but has not been previously documented for the Sargasso Sea.

Despite similarities, compositional differences were apparent between the two productive periods. The April nepheloid layer had higher relative concentrations of phytosterols, MUFA, MUFAL and was more depleted in  $\delta^{13}$ C than the October nepheloid layer, which had higher relative concentrations of PUFAs and bacterially-derived lipids (e.g. odd/br FA and stanols). This evidence is consistent with higher bacterial OM, and by extension suggests increased bacterial activity in the nepheloid layer in response to a pulse of labile OM to depth following Hurricane Nicole (see Section 4.5).

The input and nutritional quality of OM deposited on the seafloor is a key determinant in sustaining benthic communities (e.g., Tyler, 2003). Compositional differences in the nepheloid layer observed here provide strong evidence of temporal variability in OM input and nutritional quality, even in the oligotrophic Sargasso Sea, and underscore the close coupling between the water column and deep benthic ecosystem.

# 4.5. Influence of Hurricane Nicole on particle cycling in the upper water column

The wind stress and heat flux generated by passage of Hurricane Nicole on October 2016 resulted in strong near-inertial currents > 300 m depth, a decrease in sea surface temperature, a deepening of the mixed layer by at least 30 m and transient upwelling of deep nutrient-rich waters induced by Ekman pumping (Figs. 2–4). The upper ocean physical responses following hurricane passage are well-studied (Brink, 1989; Price, 1981; Price et al., 2008). The surface cooling and near inertial currents generated by hurricane passage dissipate on a time scale of  $\sim 5$  to 20 days (Dickey et al., 1998; Price et al., 2008), which is consistent with our observations (Figs. 2a and 5).

Our results clearly show that upper-ocean physical responses to hurricane passage and the transient phytoplankton blooms that develop can greatly increase the delivery of labile carbon to the deep ocean. Pigment profiles and the high absolute and OC-normalized concentrations of phytoplankton-sourced lipids, the PHYTO/labile index and PC1 factor scores measured in the epipelagic layer 12 days later evidence the magnitude of this hurricane-induced bloom (Figs. 4e-h, 5d, 14 and 16). Black and Dickey (2008) showed that the passage of Hurricane Fabian (2003) over the Bermuda Time Series Site triggered a phytoplankton bloom, visible in SeaWIFS satellite images. Similarly, other satellite observations of hurricane-induced phytoplankton blooms have been observed in the Sargasso Sea (Babin et al., 2004; Merritt-Takeuchi et al., 2013; Shropshire et al., 2016) as well as in the Gulf of Mexico (Gierach and Subrahmanyam, 2008; Shi and Wang, 2011, 2007; Walker et al., 2005). These studies found that the increased surface Chl a concentrations after a hurricane can persist for ~2 to 3 weeks, which

agrees with the high concentrations of phyto-derived lipids observed in the epipelagic layer twelve days after Nicole's passage.

Unique to this study is the evidence for the large export of this labile bloom-derived OM into the deep ocean. The comparison of the FA concentrations of this study with FA concentrations observed in the Sargasso Sea in other studies underscore the extreme lipid enrichment in the suspended particle pool within the mesopelagic and upper bathypelagic layers following Hurricane Nicole (Fig. 7). Both absolute and OC-normalized concentrations of particulate TEL and individual phytoplankton-derived lipids were significantly higher down to depths of at least 1700 m than concentrations observed in April 2015 following the spring bloom (Fig. 6). This deep phyto/labile OM penetration is particularly noteworthy in the relatively high concentrations of 18:4 $\omega$ 3 and 18:5 $\omega$ 3 PUFAs and of alkenone and C30 diol in the deep mesopelagic and upper bathypelagic layer (Fig. 8, Table 3–5), and suggests an enhanced export efficiency of the bloom products following Hurricane Nicole

The export of labile material subsequently stimulated heterotrophic communities within the mesopelagic and upper bathypelagic layers. The large increases in concentrations of the zooplankton lipids  $18{:}1\omega 9$ , cholesterol and long-chain FAL in the mesopelagic and upper bathypelagic depths provide strong evidence for stimulation of zooplankton grazing by the increased supply of labile OM (Figs. 14 and 16). In addition, the increases in concentrations of odd/br FA, HOP and hydroxy acids compounds in the mesopelagic and bathypelagic depths indicate stimulation of bacterial production by the influx of labile OM. Baltar et al. (2016) has hypothesized that episodic flux events, such as observed after Nicole, may trigger rapid increases in generally rare members of the bacterial community that are adapted for such situations, enhancing heterotrophic and autotrophic carbon uptake rates and ultimately affecting carbon cycling in the deep ocean. Our results lend support to this hypothesis.

#### 5. Conclusions

This study evidences a rapid transition in particulate organic matter composition accompanies the intense organic carbon remineralization in the upper mesopelagic layer. The suspended particulate lipid composition clearly shows a rapid loss with depth in phytoplankton-derived material below the euphotic zone and an increase in materials from zooplankton and bacterial production. The coupling between remineralization of phytoplankton-derived products and secondary production by heterotrophic consumers within the upper mesopelagic zone controls the vertical attenuation and nutritional quality of the carbon flux, yet the carbon cycle dynamics that control mesopelagic remineralization remain poorly understood.

Depth profiles of suspended lipids reveal a depth evolution in deepsea zooplankton and bacterial communities within the deep ocean as well as heterogeneity in particulate organic composition. Despite the fact that the bathypelagic ocean is the largest ecosystem on Earth, we still have a very limited knowledge of deep ocean ecosystems and their contributions to carbon cycling. Collaborative studies that combine biochemical, molecular and metagenomic approaches could provide new insights and greatly improve our understanding of how deep ocean ecosystems are organized and the key factors that control their functioning.

The composition of the particulate organic carbon pool, from the surface to the deep seafloor, is tightly coupled to upper ocean productivity and the processes that control the efficiency of the export flux. Temporal changes in the deep nepheloid layer composition further indicate the connectivity between benthic and upper ocean ecosystems. The results of this study underscore the sensitivity of the ocean carbon cycle and deep-sea ecosystems to variability in climate forcing.

This study has clearly demonstrated that extreme weather events can have a major impact on the particle cycle in the oligotrophic ocean, both by inducing transient blooms and by increasing the export flux of labile OM to the deep ocean. This in turn stimulates carbon recycling and remineralization by deep zooplankton and microbial communities. There remain several key questions concerning how storm physical dynamics affect the efficiency of surface export, and how differences in surface and mesopelagic ecosystem structure of autotrophic and heterotrophic communities may affect the carbon remineralization. Despite these unknowns, results presented here indicate that hurricanes have a significant influence on the biological pump, and suggest that storm-driven physical forcing may significantly influence regional and global carbon budgets on annual to decadal time-scales.

#### Acknowledgments

This work and the OFP time-series were supported by the National Science Foundation Chemical Oceanography Program grant OCE 1536644. The Bermuda Atlantic Time Series and Hydrostation S time series are supported by NSF grants OCE 1258836 and OCE 1633125, respectively. We acknowledge the contribution of REU Emily Maness with lipid analyses, and the contributions of BATS technicians with CTD and pigment analyses. We sincerely thank the officers and crew of R/V Atlantic Explorer (Bermuda Institute of Ocean Sciences) for their expert assistance on the cruises.

#### References

- Abramson, L., Lee, C., Liu, Z., Wakeham, S.G., Szlosek, J., 2010. Exchange between suspended and sinking particles in the northwest Mediterranean as inferred from the organic composition of in situ pump and sediment trap samples. Limnol. Oceanogr. 55, 725–739. https://doi.org/10.4319/lo.2009.55.2.0725.
- Arístegui, J., Gasol, J.M., Duarte, C.M., Herndld, G.J., 2009. Microbial oceanography of the dark ocean's pelagic realm. Limnol. Oceanogr. 54, 1501–1529. https://doi.org/ 10.4319/lo.2009.54.5.1501.
- Azaml, F., Fenche, T., Field, J.G., Gra, J.S., Meyer-Rei, L.A., Thingstad, F., 1983. The ecological role of water-column microbes in the sea. Mar. Ecol. Prog. Ser. 10, 257–263. https://doi.org/10.3354/meps010257.
- Babin, S.M., Carton, J.A., Dickey, T.D., Wiggert, J.D., 2004. Satellite evidence of hurricane-induced phytoplankton blooms in an oceanic desert. J. Geophys. Res 109. https://doi.org/10.1029/2003JC001938.
- Baltar, F., Lundin, D., Palovaara, J., Lekunberri, I., Reinthaler, T., Herndld, G.J., Pinhassi, J., 2016. Prokaryotic responses to ammonium and organic carbon reveal alternative CO<sub>2</sub> fixation pathways and importance of alkaline phosphatase in the mesopelagic North Atlantic. Front. Microbiol. 7, 1670. https://doi.org/10.3389/fmicb.2016.
- Benitez-Nelson, C.R., Bidigare, R.R., Dickey, T.D., Landry, M.R., Leonard, C.L., Brown, S. L., Nencioli, F., Rii, Y.M., Maiti, K., Becker, J.W., Bibby, T.S., Black, W., Cai, W.-J., Carlson, C.A., Chen, F., Kuwahara, V.S., Mahaffey, C., McAndrew, P.M., Quay, P.D., Rappe, M.S., Selph, K.E., Simmons, M.P., Yang, E.J., 2007. Mesoscale eddies drive increased silica export in the subtropical Pacific ocean. Science (80-.). 316, 1017–1021. https://doi.org/10.1126/science.1136221.
- Bergauer, K., Fernandez-Guerra, A., Garcia, J.A.L., Sprenger, R.R., Stepanauskas, R., Pachiadaki, M.G., Jensen, O.N., Herndld, G.J., 2017. Organic matter processing by microbial communities throughout the Atlantic water column as revealed by metaproteomics. Proc. Natl. Acad. Sci. USA 115, E400–E408. https://doi.org/10.1073/ pnas.1708779115.
- Berge, J.-P., Gouygou, J.-P., Dubacqt, J.-P., Durand, P., 1995. Reassessment of lipid composition of the diatom, *Skeletonema costatum*. Phytochemistry 39, 1017–1021. https://doi.org/10.1016/0031-9422(94)00156-N.
- Bidigare, R.R., 1991. Analysis of algal chlorophylls and carotenoids, in: Hurd, D., Spencer, D. (Eds.), Marine Particles: Analysis and Characterization. American Geophysical Union, Washington DC, pp. 119–123. https://doi.org/10.1029/GM063p0119.
- Billett, D.S.M., Lampitt, R.S., Rice, A.L., Mantoura, R.F.C., 1983. Seasonal sedimentation of phytoplankton to the deep-sea benthos. Nature 302, 520–522. https://doi.org/10. 1038/302520a0.
- Bishop, J.K.B., Fong, M.B., Wood, T.J., 2016. Robotic observations of high wintertime carbon export in California coastal waters. Biogeosciences 13, 3109–3129. https:// doi.org/10.5194/bg-13-3109-2016.
- Black, W.J., Dickey, T.D., 2008. Observations and analyses of upper ocean responses to tropical storms and hurricanes in the vicinity of Bermuda. J. Geophys. Res. Ocean. 113
- Boon, J.J., de Leeuw, J.W., Hoek, G.J., Vosjan, J.H., 1977. Significance and taxonomic value of iso and anteiso monoenoic fatty acids and branded beta-hydroxy acids in *Desulfovibrio desulfuricans*. J. Bacteriol. 129, 1183–1191.
- Bordier, C.G., Sellier, N., Foucault, A.P., Le Goffic, F., 1996. Purification and characterization of deep sea shark *Centrophorus squamosus* liver oil 1-O-aklylglycerol ether lipids. Lipids 31, 521–528. https://doi.org/10.1007/BF02522646.
- Boyd, P.W., Sherry, N.D., Berges, J.A., Bishop, J.K.B., Calvert, S.E., Charette, M.A., Giovannoni, S.J., Goldblatt, R., Harrison, P.J., Moran, S.B., Roy, S., Soon, M., Strom, S., Thibault, D., Vergin, K.L., Whitney, F.A., Wong, C.S., 1999. Transformations of

- biogenic particulates from the pelagic to the deep ocean realm. Deep Sea Res Part II Top. Stud. Oceanogr. 46, 2761–2792. https://doi.org/10.1016/S0967-0645(99) 00083-1.
- Bradshaw, S.A., Eglinton, G., 1993. Marine invertebrate feeding and the sedimentary lipid record. In: Engel, M.H., A., M.S. (Eds.), Organic Geochemistry, Topics in Geobiology. Springer, Boston, MA, pp. 225–235. https://doi.org/10.1007/978-1-4615-2890-6\_10.
- Brett, M.T., Müller-Navarra, D.C., Persson, J., 2009. Crustacean zooplankton fatty acid composition. In: Kain, M., Brett, M., M., A. (Eds.), Lipids in Aquatic Ecosystems. Springer, New York, NY, pp. 115–146. https://doi.org/10.1007/978-0-387-89366-2\_6.
- Brink, K.H., 1989. Observations of the response of thermocline currents to a hurricane. J. Phys. Oceanogr. 19, 1017–1022. https://doi.org/10.1175/1520-0485(1989) 019 < 1017:00TROT > 2.0.CO:2.
- Buesseler, K.O., Lamborg, C., Cai, P., Escoube, R., Johnson, R., Pike, S., Masque, P., Mcgillicuddy, D., Verdeny, E., 2008. Particle fluxes associated with mesoscale eddies in the Sargasso Sea. Deep Sea Res Part II Top. Stud. Oceanogr. 55, 1426–1444. https://doi.org/10.1016/j.dsr2.2008.02.007.
- Cardoso, J.N., Eglinton, G., 1983. The use of hydroxyacids as geochemical indicators.

  Geochim. Cosmochim. Acta 47, 723–730. https://doi.org/10.1016/0016-7037(83)
- Carlson, C.A., Morris, R., Parsons, R., Treusch, A.H., Giovannoni, S.J., Vergin, K., 2009. Seasonal dynamics of SAR11 populations in the euphotic and mesopelagic zones of the northwestern Sargasso Sea. ISME J. 3, 283–295. https://doi.org/10.1038/ismej. 2008.117.
- Cavagna, A.-J., Dehairs, F., Bouillon, S., Woule-Ebongué, V., Planchon, F., Delille, B., Bouloubassi, I., 2013. Water column distribution and carbon isotopic signal of cholesterol, brassicasterol and particulate organic carbon in the Atlantic sector of the Southern Ocean. Biogeosciences 10, 2787–2801. https://doi.org/10.5194/bg-10-2787-2013.
- Cavan, E.L., Trimmer, M., Shelley, F., Sanders, R., 2017. Remineralization of particulate organic carbon in an ocean oxygen minimum zone. Nat. Commun. 8. https://doi.org/ 10.1038/ncomms14847.
- Chen, K.-S., Hung, C.-C., Gong, G.-C., Chou, W.-C., Chung, C.-C., Shih, Y.-Y., Wang, C.-C., 2013. Enhanced POC export in the oligotrophic northwest Pacific Ocean after extreme weather events. Geophys. Res. Lett. 40, 5728–5734. https://doi.org/10.1002/ 2013GL058300.
- Cho, K.Y., Salton, M.R.J., 1966. Fatty acid composition of bacterial membrane and wall lipids. Biochim. Biophys. Acta - Lipids Lipid Metab. 116, 73–79. https://doi.org/10. 1016/0005-2760(66)90093-2.
- Christie, W.W., 1982. Lipid Analysis: Isolation, Separation, Identification, and Structural Analysis of Lipids. Pergamon Press.
- Close, H.G., Wakeham, S.G., Pearson, A., 2014. Lipid and <sup>13</sup>C signatures of submicron and suspended particulate organic matter in the Eastern Tropical North Pacific: implications for the contribution of Bacteria. Deep. Res. Part I 85, 15–34. https://doi. org/10.1016/j.dsr.2013.11.005.
- Cnudde, C., Sanchez Clavano, C., Moens, T., Willems, A., De Troch, M., 2013. Structural and functional patterns of active bacterial communities during aging of harpacticoid copepod fecal pellets. Aquat. Microb. Ecol. 71, 25–42. https://doi.org/10.3354/ame01663.
- Conte, M.H., 1990. The Biogeochemistry of Particulate Lipids in Warm-core Gulf Stream Rings Systems. PhD Thesis. Columbia University, NY.
- Conte, M.H., Dickey, T.D., Weber, J.C., Johnson, R.J., Knap, A.H., 2003. Transient physical forcing of pulsed export of bioreactive material to the deep Sargasso Sea. Deep Sea Res. Part I Oceanogr. Res. Pap. 50, 1157–1187. https://doi.org/10.1016/S0967-0637(03)00141-9
- Conte, M.H., Eglinton, G., S., M.L.A., 1995. Origin and fate of organic biomarker compounds in the water column and sediments of the eastern North Atlantic. Philos. Trans. R. Soc. London. Ser. B Biol. Sci. 348, 169–178. https://doi.org/10.1098/rstb.1995.0059
- Conte, M.H., Ralph, N., Ross, E.H., 2001a. Seasonal and interannual variability in deep ocean particle fluxes at the Oceanic Flux Program (OFP)/Bermuda Atlantic Time Series (BATS) site in the western Sargasso Sea near Bermuda. Deep Sea Res Part II Top. Stud. Oceanogr. 48, 1471–1505. https://doi.org/10.1016/S0967-0645(00) 00150-8
- Conte, M.H., Volkman, J.K., Eglinton, G., 1994. Lipid biomarkers of the Haptophyta. In: Green, J.C., Leadbetter, B.S.C. (Eds.), The Haptophyte Algae. Clarendon Press, Oxford, pp. 351–377.
- Conte, M.H., Weber, J., 2014. Particle flux in the deep Sargasso Sea: the 35-year Oceanic Flux Program time series. Oceanography 27, 142–147. https://doi.org/10.5670/ oceanog.2014.17.
- Conte, M.H., Weber, J.C., King, L.L., Wakeham, S.G., 2001b. The alkenone temperature signal in western North Atlantic surface waters. Geochim. Cosmochim. Acta 65, 4275–4287. https://doi.org/10.1016/S0016-7037(01)00718-9.
- Conte, M.H., Weber, J.C., Ralph, N., 1998. Episodic particle flux in the deep Sargasso Sea. Deep Sea Res. Part I Oceanogr. Res. Pap. 45, 1819–1841. https://doi.org/10.1016/ S0967-0637(98)00046-6.
- Cranwell, P.A., 1982. Lipids of aquatic sediments and sedimenting particulates. Prog. Lipid Res. 21, 271–308. https://doi.org/10.1016/0163-7827(82)90012-1.
- Dalsgaard, J., St John, M., Kattner, G., Müller-Navarra, D., Hagen, W., 2003. Fatty acid trophic markers in the pelagic marine environment. Adv. Mar. Biol. 46, 225–340.
- Dang, H., Lovell, C.R., 2016. Microbial surface colonization and biofilm development in marine environments. Microbiol. Mol. Biol. Rev. 80, 91–138. https://doi.org/10. 1128/MMBR.00037-15.
- De Carvalho, C.C.C.R., Caramujo, M.J., 2012. Lipids of prokaryotic origin at the base of marine food webs. Mar. Drugs 10, 2698–2714.
- De Kluijver, A., Soetaert, K., Schulz, K.G., Riebesell, U., Bellerby, R.G.J., Middelburg, J.J.,

- 2010. Phytoplankton-bacteria coupling under elevated CO2 levels: a stable isotope labelling study. Biogeosciences 7, 3783–3797. https://doi.org/10.5194/bg-7-3783-
- De Leeuw, J.W., Irene, W., Rijpstra, C., Nienhuis, P.H., 1995. Free and bound fatty acids and hydroxy fatty acids in the living and decomposing eelgrass *Zostera marina* L. Org. Geochem. 23, 721–728. https://doi.org/10.1016/0146-6380(95)00062-J.
- DeLong, E.F., Preston, C.M., Mincer, T., Rich, V., Hallam, S.J., Frigaard, N.-U., Martinez, A., Sullivan, M.B., Edwards, R., Brito, B.R., Chisholm, S.W., Karl, D.M., 2006.
  Community genomics among stratified microbial assemblages in the ocean's interior.
  Science (80-.). 311, 496–503. https://doi.org/10.1126/science.1120250.
- DeNiro, M.J., Epstein, S., 1978. Influence of diet on the distribution of carbon isotopes in animals. Geochim. Cosmochim. Acta 42, 495–506. https://doi.org/10.1016/0016-7037(78)90199-0.
- Deuser, W.G., 1986. Seasonal and interannual variations in deep-water particle fluxes in the Sargasso Sea and their relation to surface hydrography. Deep Sea Res Part A. Oceanogr. Res. Pap. 33, 225–246. https://doi.org/10.1016/0198-0149(86)90120-2.
- Dickey, T., Frye, D., McNeil, J., Manov, D., Nelson, N., Sigurdson, D., Jannasch, H., Siegel, D., Michaels, T., Johnson, R., Dickey, T., Frye, D., McNeil, J., Manov, D., Nelson, N., Sigurdson, D., Jannasch, H., Siegel, D., Michaels, T., Johnson, R., 1998. Upper-Ocean temperature response to Hurricane Felix as measured by the Bermuda Testbed Mooring. Mon. Weather Rev. 126, 1195–1201. https://doi.org/10.1175/1520-0493(1998) 126 < 1195:UOTRTH > 2.0.CO;2.
- Dickey, T., Zedler, S., Yu, X., Doney, S.C., Frye, D., Jannasch, H., Manov, D., Sigurdson, D., McNeil, J.D., Dobeck, L., Gilboy, T., Bravo, C., Siegel, D.A., Nelson, N., 2001. Physical and biogeochemical variability from hours to years at the Bermuda Testbed Mooring site: June 1994–March 1998. Deep Sea Res Part II Top. Stud. Oceanogr. 48, 2105–2140. https://doi.org/10.1016/S0967-0645(00)00173-9.
- Domingues, R., Goni, G., Bringas, F., Lee, S.-K., Kim, H.-S., Halliwell, G., Dong, J., Morell, J., Pomales, L., 2015. Upper ocean response to Hurricane Gonzalo (2014): Salinity effects revealed by targeted and sustained underwater glider observations. Geophys. Res. Lett. 42, 7131–7138. https://doi.org/10.1002/2015GL065378.
- Dong, H.-P., Wang, D.-Z., Dai, M., Hong, H.-S., 2010. Characterization of particulate organic matter in the water column of the South China Sea using a shotgun proteomic approach. Limnol. Oceanogr. 55, 1565–1578. https://doi.org/10.4319/LO.2010.55. 4 1565
- Druffel, E.R.M., Bauer, J.E., Griffin, S., Hwang, J., 2003. Penetration of anthropogenic carbon into organic particles of the deep ocean. Geophys. Res. Lett. 30. https://doi.org/10.1029/2003GI.017423.
- Druffel, E.R.M., Griffin, S., Bauer, J.E., Wolgast, D.M., Wang, X.-C., 1998. Distribution of particulate organic carbon and radiocarbon in the water column from the upper slope to the abyssal NE Pacific Ocean. Deep Sea Res Part II Top. Stud. Oceanogr. 45, 667–687. https://doi.org/10.1016/S0967-0645(98)00002-2.
- Dufourc, E.J., 2008. Sterols and membrane dynamics. J. Chem. Biol. 1, 63–77. https://doi.org/10.1007/s12154-008-0010-6.
- DuRand, M.D., Olson, R.J., Chisholm, S.W., 2001. Phytoplankton population dynamics at the Bermuda Atlantic Time-series station in the Sargasso Sea. Deep Sea Res Part II Top. Stud. Oceanogr. 48, 1983–2003. https://doi.org/10.1016/S0967-0645(00) 00166-1
- Eglinton, G., Hamilton, R.J., 1967. Leaf Epicuticular Waxes. Science (80-.). 156, 1322–1335. https://doi.org/10.1126/science.156.3780.1322.
- Engleman, E.E., Jackson, L.L., Norton, D.R., 1985. Determination of carbonate carbon in geological materials by coulometric titration. Chem. Geol. 53, 125–128. https://doi. org/10.1016/0009-2541(85)90025-7
- Fang, J., Chan, O., Kato, C., Sato, T., Peeples, T., Nigggemeyer, K., 2003. Phospholipid FA of piezophilic bacteria from the deep sea. Lipids 38, 885–887. https://doi.org/10. 1007/s11745-003-1140-7.
- Ficken, K.J., Barber, K.E., Eglinton, G., 1998. Lipid biomarker,  $\delta^{13}C$  and plant macrofossil stratigraphy of a Scottish montane peat bog over the last two millennia. Org. Geochem. 28, 217–237.
- Folch, J., Lees, M., Sloane-Stanley, G.H., 1957. A simple method for the isolation and purification of total lipides from animal tissues. J. Biol. Chem. 226, 497–509.
- Frka, S., Gašparović, B., Marić, D., Godrijan, J., Djakovac, T., Vojvodić, V., Dautović, J., Kozarac, Z., 2011. Phytoplankton driven distribution of dissolved and particulate lipids in a semi-enclosed temperate sea (Mediterranean): spring to summer situation. Estuar. Coast. Shelf Sci. 93, 290–304. https://doi.org/10.1016/J.ECSS.2011.04.017.
- Fröb, F., Olsen, A., Våge, K., Moore, G.W.K., Yashayaev, I., Jeansson, E., Rajasakaren, B., 2016. Irminger Sea deep convection injects oxygen and anthropogenic carbon to the ocean interior. Nat. Commun. 7, 13244. https://doi.org/10.1038/ncomms13244.
- Frost, B.W., 1972. Effects of size and concentration of food particles on the feeding behavior of the marine planktonic copepod *Calanus pacificus*. Limnol. Oceanogr. 17, 805–815.
- Fukushima, K., Uzaki, M., Sakata, S., 1992. Geochemistry of hydroxy acids in sediments—II. Estuarine and coastal marine environments. Org. Geochem. 18, 923–932. https://doi.org/10.1016/0146-6380(92)90059-7.
- Gagosian, R.B., Smith, S.O., 1979. Steroids ketones in surface sediments from the southwest African shelf. Nature 277, 287–289. https://doi.org/10.1038/277287a0.
- Gardner, W.D., Tucholke, B.E., Richardson, M.J., Biscaye, P.E., 2017. Benthic storms, nepheloid layers, and linkage with upper ocean dynamics in the western North Atlantic. Mar. Geol. 385, 304–327. https://doi.org/10.1016/j.margeo.2016.12.012.
- Gašparović, B., Frka, S., Koch, B.P., Zhu, Z.Y., Bracher, A., Lechtenfeld, O.J., Neogi, S.B., Lara, R.J., Kattner, G., 2014. Factors influencing particulate lipid production in the East Atlantic Ocean. Deep Sea Res. Part I Oceanogr. Res. Pap. 89, 56–67. https://doi. org/10.1016/J.DSR.2014.04.005.
- Gašparović, B., Penezić, A., Frka, S., Kazazić, S., Lampitt, R.S., Holguin, F.O., Sudasinghe, N., Schaub, T., 2018. Particulate sulfur-containing lipids: Production and cycling from the epipelagic to the abyssopelagic zone. Deep Sea Res Part I Oceanogr. Res.

- Pap. 134, 12-22. https://doi.org/10.1016/J.DSR.2018.03.007.
- Gašparović, B., Penezić, A., Lampitt, R.S., Sudasinghe, N., Schaub, T., 2017. Depth-related cycling of suspended nitrogen-containing lipids in the northeast Atlantic. Org. Geochem. 113, 55–66. https://doi.org/10.1016/J.ORGGEOCHEM.2017.07.008.
- Gašparović, B., Penezić, A., Lampitt, R.S., Sudasinghe, N., Schaub, T., 2016. Free fatty acids, tri-, di- and monoacylglycerol production and depth-related cycling in the Northeast Atlantic. Mar. Chem. 186, 101–109. https://doi.org/10.1016/J. MARCHEM.2016.09.002.
- Gelin, F., Boogers, I., Noordeloos, A.A.M., Damste, J.S.S., Riegman, R., De Leeuw, J.W., 1997. Resistant biomacromolecules in marine microalgae of the classes Eustigmatophyceae and Chlorophyceae: geochemical implications. Org. Geochem. 26, 659–675. https://doi.org/10.1016/S0146-6380(97)00035-1.
- Gérin, C., Goutx, M., 1994. Iatroscan-measured particulate and dissolved lipids in the Almeria-Oran frontal system (Almofront-1, May 1991). J. Mar. Syst. 5, 343–360. https://doi.org/10.1016/0924-7963(94)90055-8.
- Gierach, M.M., Subrahmanyam, B., 2008. Biophysical responses of the upper ocean to major Gulf of Mexico hurricanes in 2005. J. Geophys. Res. 113, C04029. https://doi. org/10.1029/2007JC004419.
- Gilbert, J.A., Steele, J.A., Caporaso, J.G., Steinbrück, L., Reeder, J., Temperton, B., Huse, S., McHardy, A.C., Knight, R., Joint, I., Somerfield, P., Fuhrman, J.A., Field, D., 2012. Defining seasonal marine microbial community dynamics. ISME J. 6, 298–308. https://doi.org/10.1038/ismej.2011.107.
- Giovannoni, S.J., Vergin, K.L., 2012. Seasonality in ocean microbial communities. Science (80-.). 335, 671–676. https://doi.org/10.1126/science.1198078.
- Goni, G., Todd, R., Jayne, S., Halliwell, G., Glenn, S., Dong, J., Curry, R., Domingues, R., Bringas, F., Centurioni, L., DiMarco, S., Miles, T., Morell, J., Pomales, L., Kim, H.-S., Robbins, P., Gawarkiewicz, G., Wilkin, J., Heiderich, J., Baltes, B., Cione, J., Seroka, G., Knee, K., Sanabia, E., 2017. Autonomous and lagrangian ocean observations for Atlantic tropical cyclone studies and forecasts. Oceanography 30, 92–103. https://doi.org/10.5670/oceanog.2017.227.
- Gooday, A.J., 2002. Biological responses to seasonally varying fluxes of organic matter to the ocean floor: a review. J. Oceanogr. 58, 305–332. https://doi.org/10.1023/ A:1015865826379.
- Gordon, D.A., Giovannoni, S.J., 1996. Detection of stratified microbial populations related to *Chlorobium* and *Fibrobacter* species in the Atlantic and Pacific Oceans. Appl. Environ. Microbiol. 62, 1171–1177.
- Gowing, M.M., Silver, M.W., 1983. Origins and microenvironments of bacteria mediating fecal pellet decomposition in the sea. Mar. Biol. 73, 7–16. https://doi.org/10.1007/ BF00396280.
- Grossart, H.-P., Kiørboe, T., Tang, K., Ploug, H., 2003. Bacterial colonization of particles: growth and interactions. Appl. Environ. Microbiol. 69, 3500–3509. https://doi.org/ 10.1128/AEM.69.6.3500-3509.2003.
- Grossart, H., Gust, G., 2009. Hydrostatic pressure affects physiology and community structure of marine bacteria during settling to 4000 m: an experimental approach. Mar. Ecol. Prog. Ser. 390, 97–104. https://doi.org/10.3354/meps08201.
- Mar. Ecol. Prog. Ser. 390, 97–104. https://doi.org/10.3354/meps08201.
  Guan, S., Zhao, W., Huthnance, J., Tian, J., Wang, J., 2014. Observed upper ocean response to typhoon Megi (2010) in the Northern South China Sea. J. Geophys. Res. Ocean. 119, 3134–3157. https://doi.org/10.1002/2013JC009661.
- Gundersen, K., Orcutt, K.M., Purdie, D.A., Michaels, A.F., Knap, A.H., 2001. Particulate organic carbon mass distribution at the Bermuda Atlantic Time-series Study (BATS) site. Deep. Res. II 48, 1697–1718. https://doi.org/10.1016/S0967-0645(00)00156-9.
- Gust, G., Michaels, A.F., Johnson, R., Deuser, W.G., Bowles, W., 1994. Mooring line motions and sediment trap hydromechanics: in situ intercomparison of three common deployment designs. Deep Sea Res Part I Oceanogr. Res. Pap. 41, 831–857. https://doi.org/10.1016/0967-0637(94)90079-5.
- Hannides, C.C.S., Popp, B.N., Choy, C.A., Drazen, J.C., 2013. Midwater zooplankton and suspended particle dynamics in the North Pacific Subtropical Gyre: a stable isotope perspective. Limnol. Oceanogr. 58, 1931–1946. https://doi.org/10.4319/lo.2013.58. 6.1931
- Hansell, D.A., Ducklow, H.W., 2003. Bacterioplankton distribution and production in the bathypelagic ocean: directly coupled to particulate organic carbon export? Limnol. Oceanogr. 48, 150–156. https://doi.org/10.4319/lo.2003.48.1.0150.
- Harvey, H.R., Eglinton, G., O'Hara, S.C.M., Corner, E.D.S., 1987. Biotransformation and assimilation of dietary lipids by *Calanus* feeding on a dinoflagellate. Geochim. Cosmochim. Acta 51, 3031–3040. https://doi.org/10.1016/0016-7037(87)90376-0.
- Harvey, H.R., O'Hara, S.C.M., Eglinton, G., Corner, E.D.S., 1989. The comparative fate of dinosterol and cholesterol in copepod feeding: Implications for a conservative molecular biomarker in the marine water column. Org. Geochem. 14, 635–641. https:// doi.org/10.1016/0146-6380(89)90042-9.
- Henson, S.A., Sanders, R., Madsen, E., 2012. Global patterns in efficiency of particulate organic carbon export and transfer to the deep ocean. Global Biogeochem. Cycles 26. https://doi.org/10.1029/2011GB004099.
- Herndld, G.J., Reinthaler, T., 2013. Microbial control of the dark end of the biological pump. Nat. Geosci. 6, 718–724. https://doi.org/10.1038/ngeo1921.
- Hodson, H., 2013. Underwater robot gliders are the eyes of the storm. New Sci. 219, 19. https://doi.org/10.1016/S0262-4079(13)62281-2.
- Hudson, E.D., Parrish, C.C., Helleur, R.J., 2001. Biogeochemistry of sterols in plankton, settling particles and recent sediments in a cold ocean ecosystem (Trinity Bay, Newfoundland). Mar. Chem. 76, 253–270. https://doi.org/10.1016/S0304-4203(01) 00066-4.
- Huffman, E.W.D., 1977. Performance of a new automatic carbon dioxide coulometer. Microchem. J. 22, 567–573. https://doi.org/10.1016/0026-265X(77)90128-X.
- Hung, C.-C., Gong, G.-C., Chung, W.-C., Kuo, W.-T., Lin, F.-C., 2009. Enhancement of particulate organic carbon export flux induced by atmospheric forcing in the

- subtropical oligotrophic northwest Pacific Ocean. Mar. Chem. 113, 19–24. https://doi.org/10.1016/j.marchem.2008.11.004.
- Huvenne, V.A.I., Tyler, P.A., Masson, D.G., Fisher, E.H., Hauton, C., Hühnerbach, V., Le Bas, T.P., Wolff, G.A., 2011. A picture on the wall: innovative mapping reveals coldwater coral refuge in submarine canyon. PLoS One 6, e28755.
- Hwang, J., Montlucon, D., Eglinton, T.I., 2009. Molecular and isotopic constraints on the sources of suspended particulate organic carbon on the northwestern Atlantic margin. Deep Sea Res Part I Oceanogr. Res. Pap. 56, 1284–1297. https://doi.org/10.1016/j. dsr.2009.01.012.
- Ittekkot, V., 1993. The abiotically driven biological pump in the ocean and short-term fluctuations in atmospheric CO<sub>2</sub> contents. Glob. Planet. Change 8, 17–25. https://doi. org/10.1016/0921-8181(93)90060-2.
- Jacob, S.D., Shay, L.K., Mariano, A.J., Black, P.G., Jacob, S.D., Shay, L.K., Mariano, A.J., Black, P.G., 2000. The 3D oceanic mixed layer response to Hurricane Gilbert. J. Phys. Oceanogr. 30, 1407–1429. https://doi.org/10.1175/1520-0485(2000) 030 < 1407:TOMLRT > 2.0.CO;2.
- Jeffrey, A.W.A., Pflaum, R.C., Brooks, J.M., Sackett, W.M., 1983. Vertical trends in particulate organic carbon <sup>13</sup>C: <sup>12</sup>C ratios in the upper water column. Deep Sea Res Part A. Oceanogr. Res. Pap. 30, 971–983. https://doi.org/10.1016/0198-0149(83) 90052-3.
- Jeffrey, S.W., Mantoura, R.F.C., Wright, S.W., 1997. Phytoplankton Pigments in Oceanography. Monographs on Oceanographic Methods, Paris.
- Jing, H., Shek, L., Yung, W., Jin, X., Liu, H., 2012. Dynamics of bacterial community composition during degradation of copepod fecal pellets. J. Plankton Res. 34, 700–710. https://doi.org/10.1093/plankt/fbs043.
- Kaiser, K., Benner, R., 2008. Major bacterial contribution to the ocean reservoir of detrital organic carbon and nitrogen. Limnol. Oceanogr. 53, 99–112. https://doi.org/10. 4319/lo.2008.53.1.0099.
- Kaneda, T., 1991. Iso- and anteiso-fatty acids in bacteria: biosynthesis, function, and taxonomic significance. Microbiol. Rev. 55, 288–302.
- Karl, D.M., Knauer, G.A., Martin, J.H., 1988. Downward flux of particulate organic matter in the ocean: a particle decomposition paradox. Nature 332, 438–441. https://doi. org/10.1038/332438a0.
- Kattner, G., Hagen, W., Graeve, M., Albers, C., 1998. Exceptional lipids and fatty acids in the pteropod *Clione limacina* (Gastropoda) from both polar oceans. Mar. Chem. 61, 219–228. https://doi.org/10.1016/S0304-4203(98)00013-9.
- Kattner, G., Hagen, W., Lee, R.F., Campbell, R., Deibel, D., Falk-Petersen, S., Graeve, M., Hansen, B.W., Hirche, H.J., Jónasdóttir, S.H., Madsen, M.L., Mayzaud, P., Müller-Navarra, D., Nichols, P.D., Paffenhöfer, G.-A., Pond, D., Saito, H., Stübing, D., Virtue, P., 2007. Perspectives on marine zooplankton lipids. Can. J. Fish. Aquat. Sci. 64, 1628–1639. https://doi.org/10.1139/f07-122.
- Kharbush, J.J., Kejriwal, K., Aluwihare, L.I., 2016. Distribution and abundance of hopanoid producers in low-oxygen environments of the eastern Pacific Ocean. Microb. Ecol. 71, 401–408. https://doi.org/10.1007/s00248-015-0671-y.
- Kharbush, J.J., Ugalde, J.A., Hogle, S.L., Allen, E.E., Aluwihare, L.I., 2013. Composite bacterial hopanoids and their microbial producers across oxygen gradients in the water column of the California Current. Appl. Environ. Microbiol. 79, 7491–7501. https://doi.org/10.1128/AEM.02367-13.
- Kim, H., 2017. Microbial Interactions in Coupled Climate-Biogeochemical Systems. PhD Thesis. Columbia University.
- Kiriakoulakis, K., Blackbird, S., Ingels, J., Vanreusel, A., Wolff, G.A., 2011. Organic geochemistry of submarine canyons: the Portuguese Margin. Deep Sea Res Part II Top. Stud. Oceanogr. 58, 2477–2488. https://doi.org/10.1016/j.dsr2.2011.04.010.
- Knap, A.H., Michaels, A.F., Steinberg, D.K., Bahr, F., Bates, N.R., Bell, S., Countway, P.,
  Close, A.R., Doyle, A.P., Dow, R.L., Howse, F.A., Gundersen, K., Johnson, R.J., Kelly,
  R., Little, R., Orcutt, K., Parsons, R., Rathburn, C., Sanderson, M., Stone, S., 1997.
  BATS Methods Manual, Version 4. U.S. JGOFS Planning Office, Woods Hole, MA, US.
- Koppelmann, R., Zimmermann-Timm, H., Weikert, H., 2005. Bacterial and zooplankton distribution in deep waters of the Arabian Sea. Deep. Res. I 52, 2184–2192. https:// doi.org/10.1016/j.dsr.2005.06.012.
- Krause, J.W., Nelson, D.M., Lomas, M.W., 2010. Production, dissolution, accumulation, and potential export of biogenic silica in a Sargasso Sea mode-water eddy. Limnol. Oceanogr. 55, 569–579. https://doi.org/10.4319/lo.2010.55.2.0569.
- Lampitt, R.S., 1985. Evidence for the seasonal deposition of detritus to the deep-sea floor and its subsequent resuspension. Deep Sea Res. Part A. Oceanogr. Res. Pap. 32, 885–897. https://doi.org/10.1016/0198-0149(85)90034-2.
- Lauro, F.M., Bartlett, D.H., 2008. Prokaryotic lifestyles in deep sea habitats. Extremophiles 12, 15–25. https://doi.org/10.1007/s00792-006-0059-5.
- Lauro, F.M., Chastain, R.A., Blankenship, L.E., Yayanos, A.A., Bartlett, D.H., 2007. The unique 16S rRNA genes of piezophiles reflect both phylogeny and adaptation. Appl. Environ. Microbiol. 73, 838–845. https://doi.org/10.1128/AEM.01726-06.
- Lee, C., Wakeham, S.G., Arnosti, C., 2004. Particulate organic matter in the sea: the composition conundrum. Ambio 33, 565–575. https://doi.org/10.1639/0044-7447(2004) 033[0565:POMITS]2.0.CO;2.
- Lee, C., Wakeham, S.G., Hedges, J.I., 1988. The measurement of oceanic particle flux are "swimmers" a problem? Oceanography 1, 34–36. https://doi.org/10.2307/43924419.
- Lee, R., Hagen, W., Kattner, G., 2006. Lipid storage in marine zooplankton. Mar. Ecol. Prog. Ser. 307, 273–306. https://doi.org/10.3354/meps307273.
- Levine, D.M., Sulkin, S.D., 1984. Nutritional significance of long-chain polyunsaturated fatty acids to the zoeal development of the brachyuran crab, *Eurypanopeus depressus* (Smith). J. Exp. Mar. Bio. Ecol. 81, 211–223. https://doi.org/10.1016/0022-0981(84)90141-2.
- Levy, M., Bopp, L., Karleskind, P., Resplandy, L., Ethe, C., Pinsard, F., 2013. Physical

- pathways for carbon transfers between the surface mixed layer and the ocean interior. Global Biogeochem. Cycles 27, 1001–1012. https://doi.org/10.1002/gbc. 20092.
- Lewis, M.R., Hebert, D., Harrison, W.G., Platt, T., Oakey, N.S., 1986. Vertical nitrate fluxes in the oligotrophic ocean. Science 234, 870–873. https://doi.org/10.1126/ science 234, 4778, 870
- Lewis, R.W., 1967. Fatty acid composition of some marine animals from various depths. J. Fish. Res. Board Canada 24, 1101–1115. https://doi.org/10.1139/f67-093. Li, W.K.W., Irwin, B.D., Dickie, P.M., 1993. Dark fixation of <sup>14</sup>C: variations related to
- Li, W.K.W., Irwin, B.D., Dickie, P.M., 1993. Dark fixation of <sup>14</sup>C: variations related to biomass and productivity of phytoplankton and bacteria. Limnol. Oceanogr. 38, 483–494. https://doi.org/10.4319/lo.1993.38.3.0483.
- Linder, M., Belhaj, N., Sautot, P., Arab Tehrany, E., 2010. From krill to whale: an overview of marine fatty acids and lipid compositions. Oléagineux, Corps Gras, Lipides 17, 194–204. https://doi.org/10.1051/ocl.2010.0328.
- Loh, A.N., Canuel, E.A., Bauer, J.E., 2008. Potential source and diagenetic signatures of oceanic dissolved and particulate organic matter as distinguished by lipid biomarker distributions. Mar. Chem. 112, 189–202. https://doi.org/10.1016/j.marchem.2008.
- Lomas, M.W., Bates, N.R., Johnson, R.J., Knap, A.H., Steinberg, D.K., Carlson, C.A., 2013. Two decades and counting: 24-years of sustained open ocean biogeochemical measurements in the Sargasso Sea. Deep Sea Res Part II Top. Stud. Oceanogr. 93, 16–32. https://doi.org/10.1016/J.DSR2.2013.01.008.
- Lomas, M.W., Lipschultz, F., 2006. Forming the primary nitrite maximum: nitrifiers or phytoplankton? Limnol. Oceanogr. 51, 2453–2467. https://doi.org/10.4319/lo. 2006.51.5.2453.
- Madin, L.P., Horgan, E.F., Steinberg, D.K., 2001. Zooplankton at the Bermuda Atlantic Time-series Study (BATS) station: diel, seasonal and interannual variation in biomass, 1994–1998. Deep Sea Res. Part II Top. Stud. Oceanogr. 48, 2063–2082. https://doi. org/10.1016/S0967-0645(00)00171-5.
- Madureira, L.A.S., 1994. Lipids in recent sediments of the eastern north Atlantic. Ph.D thesis. University of Bristol.
- Marañón, E., Behrenfeld, M.J., González, N., Mouriño, B., Zubkov, M.V., 2003. High variability of primary production in oligotrophic waters of the Atlantic Ocean: uncoupling from phytoplankton biomass and size structure. Mar. Ecol. Prog. Ser. 257, 1–11. https://doi.org/10.3354/meps257001.
- Martiny, A.C., Vrugt, J.A., Lomas, M.W., 2014. Concentrations and ratios of particulate organic carbon, nitrogen, and phosphorus in the global ocean. Sci. data 1, 140048.
- McGillicuddy, D.J., Robinson, A.R., Siegel, D.A., Jannasch, H.W., Johnson, R., Dickey, T.D., McNeil, J., Michaels, A.F., Knap, A.H., 1998. Influence of mesoscale eddies on new production in the Sargasso Sea. Nature 394, 263–266. https://doi.org/10.1038/28367.
- McKee, T.K., Francis, E.A., Hogg, N.G., 1981. A compilation of moored current-meter data from three topographic experiments: the Bermuda microstructure array, the Island Trapped Waves array and the Gibbs Fracture zone array. Volume 27.
- McNeil, J.D., Jannasch, H.W., Dickey, T., McGillicuddy, D., Brzezinski, M., Sakamoto, C.M., 1999. New chemical, bio-optical and physical observations of upper ocean response to the passage of a mesoscale eddy off Bermuda. J. Geophys. Res. Ocean. 104, 15537–15548. https://doi.org/10.1029/1999JC900137.
- Merritt-Takeuchi, A.M., Chiao, S., Merritt-Takeuchi, A.M., Chiao, S., 2013. Case studies of tropical cyclones and phytoplankton blooms over Atlantic and Pacific regions. Earth Interact. 17, 1–19. https://doi.org/10.1175/2013El000517.1.
- Meyers, P.A., 1997. Organic geochemical proxies of paleoceanographic, paleolimnologic, and paleoclimatic processes. Org. Geochem. 27, 213–250. https://doi.org/10.1016/ S0146-6380(97)00049-1.
- Michaels, A.F., Knap, A.H., 1996. Overview of the U.S. JGOFS Bermuda Atlantic timeseries Study and the Hydrostation S program. Deep Sea Res. Part II Top. Stud. Oceanogr. 43, 157–198. https://doi.org/10.1016/0967-0645(96)000004-5.
- Moeseneder, M.M., Winter, C., Herndld, G.J., 2001. Horizontal and vertical complexity of attached and free-living bacteria of the eastern Mediterranean Sea, determined by 16S rDNA and 16S rRNA fingerprints. Limnol. Ocean. 46, 95–107.
- Møller, E.F., 2007. Production of dissolved organic carbon by sloppy feeding in the copepods Acartia tonsa, Centropages typicus, and Temora longicornis. Limnol. Oceanogr. 52, 79–84. https://doi.org/10.4319/lo.2007.52.1.0079.
- Monroig, Ó., Tocher, D.R., Navarro, J.C., 2013. Biosynthesis of polyunsaturated fatty acids in marine invertebrates: recent advances in molecular mechanisms. Mar. Drugs 11, 3998–4018. https://doi.org/10.3390/md11103998.
- Mudge, S.M., Belanger, S.E., Nielsen, A.M., 2008. Fatty Alcohols: Anthropogenic and Natural Occurrence in the Environment. Royal Society of Chemistry.
- Nagata, T., Tamburini, C., Arístegui, J., Baltar, F., Bochdansky, A.B., Fonda-Umani, S., Fukuda, H., Gogou, A., Hansman, R.L., Herndld, G.J., Panagiotopoulos, C., Reinthaler, T., Sohrin, R., Verdugo, P., Yamada, N., Yamashita, Y., Yokokawa, T., Bartlett, D.H., 2010. Emerging concepts on microbial processes in the bathypelagic ocean ecology, biogeochemistry, and genomics. Deep Sea Res Part II Top. Stud. Oceanogr. 57, 1519–1536. https://doi.org/10.1016/J.DSR2.2010.02.019.
- Neal, A.C., Prahl, F.G., Eglinton, G., O'Hara, S.C.M., Corner, E.D.S., 1986. Lipid changes during a planktonic feeding sequence involving unicellular algae, Elminius Nauplii and Adult Calanus. J. Mar. Biol. Assoc. United Kingdom 66, 1. https://doi.org/10. 1017/S0025315400039606.
- Nemirovskaya, I.A., Kravchishina, M.D., 2016. Variability of suspended particulate matter concentrations and organic compounds in frontal zones of the Atlantic and Southern oceans. Oceanology 56, 55–64. https://doi.org/10.1134/ S0001437016010124.
- Ohnemus, D.C., Lam, P.J., 2015. Cycling of lithogenic marine particles in the US

- GEOTRACES North Atlantic transect. Deep Sea Res Part II Top. Stud. Oceanogr. 116, 283–302. https://doi.org/10.1016/J.DSR2.2014.11.019.
- Olson, R.J., Chisholm, S.W., Zettler, E.R., Armbrust, E.V., 1990. Pigments, size, and distributions of *Synechococcus* in the North Atlantic and Pacific Oceans. Limnol. Oceanogr. 35, 45–58. https://doi.org/10.4319/lo.1990.35.1.0045.
- Oschlies, A., 2002. Can eddies make ocean deserts bloom? Global Biogeochem. Cycles 16https://doi.org/10.1029/2001GB001830. 53-1-53-11.
- Ourisson, G., Albrecht, P., Rohmer, M., 1979. The hopanoids: palaeochemistry and biochemistry of a group of natural products. Pure Appl. Chem. https://doi.org/10.1351/pac197951040709.
- Paoletti, C., Pushparaj, B., Florenzano, G., Capella, P., Lercker, G., 1976. Unsaponifiable matter of green and blue-green algal lipids as a factor of biochemical differentiation of their biomasses: I. Total unsaponifiable and hydrocarbon fraction. Lipids 11, 258–265. https://doi.org/10.1007/BF02544051.
- Parkes, R.J., Taylor, J., 1983. The relationship between fatty acid distributions and bacterial respiratory types in contemporary marine sediments. Estuar. Coast. Shelf Sci. 16, 173–189. https://doi.org/10.1016/0272-7714(83)90139-7.
- Parrish, C.C., 2013. Lipids in marine ecosystems. ISRN Oceanogr. 2013, 1–16. https://doi. org/10.5402/2013/604045.
- Pedrosa-Pàmies, R., Parinos, C., Sanchez-Vidal, A., Gogou, A., Calafat, A., Canals, M., Bouloubassi, I., Lampadariou, N., 2015. Composition and sources of sedimentary organic matter in the deep eastern Mediterranean Sea. Biogeosciences 12, 7379–7402. https://doi.org/10.5194/bg-12-7379-2015.
- Pedrosa-Pàmies, R., Sanchez-Vidal, A., Canals, M., Lampadariou, N., Velaoras, D., Gogou, A., Parinos, C., Calafat, A., 2016. Enhanced carbon export to the abyssal depths driven by atmosphere dynamics. Geophys. Res. Lett. 43, 8626–8636. https://doi.org/10.1002/2016GI.069781
- Pereira, S.L., Leonard, A.E., Mukerji, P., 2003. Recent advances in the study of fatty acid desaturases from animals and lower eukaryotes. Prostaglandins Leukot. Essent. Fat. Acids 68, 97–106. https://doi.org/10.1016/S0952-3278(02)00259-4.
- Phillips, H.E., Joyce, T.M., 2007. Bermuda's tale of two time series: Hydrostation S and BATS. J. Phys. Oceanogr. 37, 554–571. https://doi.org/10.1175/JPO2997.1.
- Pond, D.W., Tarling, G.A., Mayor, D.J., 2014. Hydrostatic Ppessure and temperature effects on the membranes of a seasonally migrating marine copepod. PLoS One 9, e111043. https://doi.org/10.1371/journal.pone.0111043.
- Pozzato, L., Oevelen, D. Van, Moodley, L., Soetaert, K., Middelburg, J.J., 2013. Sink or link? The bacterial role in benthic carbon cycling in the Arabian Sea's oxygen minimum zone. Biogeosciences 10, 6879–6891. https://doi.org/10.5194/bg-10-6879-2013.
- Prahl, F.G., Eglinton, G., Corner, E.D.S., O'Hara, S.C.M., Forsberg, T.E.V., 1984. Changes in plant lipids during passage through the gut of Calanus. J. Mar. Biol. Assoc. United Kingdom 64, 317. https://doi.org/10.1017/S0025315400030022.
- Price, J.F., 1981. Upper ocean response to a hurricane. J. Phys. Oceanogr. 11, 153–175. https://doi.org/10.1175/1520-0485(1981) 011 < 0153:UORTAH > 2.0.CO;2.
- Price, J.F., Morzel, J., Niiler, P.P., 2008. Warming of SST in the cool wake of a moving hurricane. J. Geophys. Res. Ocean. 113, 1–19. https://doi.org/10.1029/ 2007JC004393.
- Rampen, S.W., Willmott, V., Kim, J.-H., Uliana, E., Mollenhauer, G., Schefuß, E., Sinninghe Damsté, J.S., Schouten, S., 2012. Long chain 1,13- and 1,15-diols as a potential proxy for palaeotemperature reconstruction. Geochim. Cosmochim. Acta 84, 201–216. https://doi.org/10.1016/j.gca.2012.01.024.
- Ransom, B., Shea, K.F., Burkett, P.J., Bennett, R.H., Baerwald, R., 1998. Comparison of pelagic and nepheloid layer marine snow: implications for carbon cycling. Mar. Geol. 150, 39–50. https://doi.org/10.1016/S0025-3227(98)00052-8.
- Ratledge, C., 2008. Microbial Lipids, in: Biotechnology. Wiley-VCH Verlag GmbH, pp. 133–197. https://doi.org/10.1002/9783527620890.ch4.
- Ratnayake, W.N., Ackman, R.G., 1979. Fatty alcohols in capelin, herring and mackerel oils and muscle lipids: I. Fatty alcohol details linking dietary copepod fat with certain fish depot fats. Lipids 14, 795–803.
- Reinthaler, T., van Aken, H., Veth, C., Arístegui, J., Robinson, C., Williams, P.J.le B., Lebaron, P., Herndld, G.J., 2006. Prokaryotic respiration and production in the mesoand bathypelagic realm of the eastern and western North Atlantic basin. Limnol. Oceanogr. 51, 1262–1273. https://doi.org/10.4319/lo.2006.51.3.1262.
- Rice, A.L., Billett, D.S.M., Fry, J., John, A.W.G., Lampitt, R.S., Mantoura, R.F.C., Morris, R.J., 1986. Seasonal deposition of phytodetritus to the deep-sea floor. Proc. R. Soc. Edinburgh. Sect. B. Biol. Sci. 88, 265–279. https://doi.org/10.1017/S0269727000004590.
- Robinson, C., Steinberg, D.K., Anderson, T.R., Arístegui, J., Carlson, C.A., Frost, J.R., Ghiglione, J.-F., Hernández-León, S., Jackson, G.A., Koppelmann, R., Quéguiner, B., Ragueneau, O., Rassoulzadegan, F., Robison, B.H., Tamburini, C., Tanaka, T., Wishner, K.F., Zhang, J., 2010. Mesopelagic zone ecology and biogeochemistry a synthesis. Deep Sea Res Part II Top. Stud. Oceanogr. 57, 1504–1518. https://doi.org/10.1016/j.dsr2.2010.02.018.
- Robinson, N., Cranwell, P.A., Finlay, B.J., Eglinton, G., 1984a. Lipids of aquatic organisms as potential contributors to lacustrine sediments. Org. Geochem. 6, 143–152. https://doi.org/10.1016/0146-6380(84)90035-4.
- Robinson, N., Eglinton, G., Brassell, S.C., Cranwell, P.A., 1984b. Dinoflagellate origin for sedimentary  $4\alpha$ -methylsteroids and  $5\alpha(H)$ -stanols. Nature 308, 439–442. https://doi.org/10.1038/308439a0.
- Rohmer, M., Bouvier-Nave, P., Ourisson, G., 1984. Distribution of hopanoid triterpenes in prokaryotes. Microbiology 130, 1137–1150. https://doi.org/10.1099/00221287-130-5-1137.
- Rossi, S., Sabatés, A., Latasa, M., Reyes, E., 2006. Lipid biomarkers and trophic linkages

- between phytoplankton, zooplankton and anchovy (*Engraulis encrasicolus*) larvae in the NW Mediterranean. J. Plankton Res. 28, 551–562. https://doi.org/10.1093/plankt/fbi140.
- Russell, N.J., Sandercock, S.P., 1980. The regulation of bacterial membrane fluidity by modification of phospholipid fatty acyl chain length, in: Membrane Fluidity. Humana Press, Totowa, NJ, pp. 181–190. https://doi.org/10.1007/978-1-4612-6120-9\_14.
- Sanders, R.J., Henson, S.A., Martin, A.P., Anderson, T.R., Bernardello, R., Enderlein, P., Fielding, S., Giering, S.L.C., Hartmann, M., Iversen, M., 2016. Controls over ocean mesopelagic interior carbon storage (COMICS): fieldwork, synthesis, and modeling efforts. Front. Mar. Sci. 3, 136.
- Sargent, J.R., 1976. The Structure, Function and Metabolism of Lipids in Marine Organisms. In: Malins, D.C., Sargent, J.R. (Eds.), Biochemical and Biophysical Perspectives in Marine Biology. Academic Press, London, pp. 149–212.
- Sargent, J.R., Falk-Petersen, S., 1988. The lipid biochemistry of calanoid copepods. Hydrobiologia 167, 101–114. https://doi.org/10.1007/BF00026297.
- Sargent, J.R., Falk-Petersen, S., 1981. Ecological investigations on the zooplankton community in balsfjorden, northern Norway: lipids and fatty acids in *Meganyctiphanes* norvegica, *Thysanoessa raschi* and *T. inermis* during mid-winter. Mar. Biol. 62, 131–137. https://doi.org/10.1007/BF00388175.
- Sargent, J.R., Lee, R.F., 1975. Biosynthesis of lipds in zooplankton from Saanich Inlet, British Columbia. Canada. Mar. Biol. 31, 15–23. https://doi.org/10.1007/ BF00390643.
- Sargent, J.R., Whittle, K.J., 1981. Lipids and Hydrocarbons in the Marine Food Web. Anal. Mar. Ecosyst. Longhurst.
- Schnack-Schiel, S.B., Isla, E., 2005. The role of zooplankton in the pelagic-benthic coupling of the Southern Ocean. Sci. Mar. 69, 39-55.
- Sheridan, C.C., Lee, C., Wakeham, S.G., Bishop, J.K.B., 2002. Suspended particle organic composition and cycling in surface and midwaters of the equatorial Pacific Ocean. Deep Sea Res. Part I Oceanogr. Res. Pap. 49, 1983–2008. https://doi.org/10.1016/ S0967-0637(02)00118-8.
- Shi, W., Wang, M., 2011. Satellite observations of asymmetrical physical and biological responses to Hurricane Earl. Geophys. Res. Lett. 38, 1–5. https://doi.org/10.1029/ 2010GL046574
- Shi, W., Wang, M., 2007. Observations of a Hurricane Katrina-induced phytoplankton bloom in the Gulf of Mexico. Geophys. Res. Lett. 34, 1–7. https://doi.org/10.1029/ 2007GI.029724.
- Shifrin, N.S., Chisholm, S.W., 2008. Phytoplankton lipids: interspecific differences and effects of nitrate, silicate and light-dark cycles. J. Phycol. 17, 374–384. https://doi. org/10.1111/j.1529-8817.1981.tb00865.x.
- Shih, Y.-Y., Hung, C.-C., Gong, G.-C., Chung, W.-C., Wang, Y.-H., Lee, I.-H., Chen, K.-S., Ho, C.-Y., 2015. Enhanced particulate organic carbon export at eddy edges in the oligotrophic western north pacific ocean. PLoS One 10, e0131538. https://doi.org/ 10.1371/journal.pone.0131538
- Shropshire, T., Li, Y., He, R., 2016. Storm impact on sea surface temperature and chlorophyll a in the Gulf of Mexico and Sargasso Sea based on daily cloud-free satellite data reconstructions. Geophys. Res. Lett. 43, 12199–12207. https://doi.org/ 10.1002/2016GL071178.
- Siegel, D.A., McGillicuddy, D.J., Fields, E.A., 1999. Mesoscale eddies, satellite altimetry, and new production in the Sargasso Sea. J. Geophys. Res. 104, 13359. https://doi. org/10.1029/1999JC900051.
- Siliakus, M.F., van der Oost, J., Kengen, S.W.M., 2017. Adaptations of archaeal and bacterial membranes to variations in temperature, pH and pressure. Extremophiles 21, 651–670. https://doi.org/10.1007/s00792-017-0939-x.
- Sinninghe Damsté, J.S., Rampen, S., Irene, W., Rijpstra, C., Abbas, B., Muyzer, G., Schouten, S., 2003. A diatomaceous origin for long-chain diols and mid-chain hydroxy methyl alkanoates widely occurring in quaternary marine sediments: indicators for high-nutrient conditions. Geochim. Cosmochim. Acta 67, 1339–1348. https://doi.org/10.1016/S0016-7037(02)01225-5.
- Skerratt, J.H., Nichols, P.D., Bowman, J.P., Sly, L.I., 1992. Occurrence and significance of long-chain (ω-1)-hydroxy fatty acids in methane-utilizing bacteria. Org. Geochem. 18, 189–194. https://doi.org/10.1016/0146-6380(92)90129-L.
- Smith, C.R., Hoover, D.J., Doan, S.E., Pope, R.H., Demaster, D.J., Dobbs, F.C., Altabet, M.A., 1996. Phytodetritus at the abyssal seafloor across 10° of latitude in the central equatorial Pacific. Deep Sea Res. Part II Top. Stud. Oceanogr. 43, 1309–1338. https://doi.org/10.1016/0967-0645(96)00015-X.
- Smith, K., Sherman, A., McGill, P., Henthorn, R., Ferreira, J., Huffard, C., 2017. Evolution of monitoring an abyssal time-series station in the northeast Pacific over 28 years. Oceanography 30, 72–81. https://doi.org/10.5670/oceanog.2017.425.
- Smith, K.L., Ruhl, H.A., Bett, B.J., Billett, D.S.M., Lampitt, R.S., Kaufmann, R.S., 2009. Climate, carbon cycling, and deep-ocean ecosystems. Proc. Natl. Acad. Sci. USA 106, 19211–19218. https://doi.org/10.1073/pnas.0908322106.
- Smith, K.L., Ruhl, H.A., Kahru, M., Huffard, C.L., Sherman, A.D., 2013. Deep ocean communities impacted by changing climate over 24 y in the abyssal northeast Pacific Ocean. Proc. Natl. Acad. Sci. USA 110, 19838–19841. https://doi.org/10.1073/pnas. 1315447110.
- Smith, R., Gosselin, M., Kattner, G., Legendre, L., Pesant, S., 1997. Biosynthesis of macromolecular and lipid classes by phytoplankton in the Northeast Water Polynya. Mar. Ecol. Prog. Ser. 147, 231–242. https://doi.org/10.3354/meps147231.
- Steinberg, D.K., Carlson, C.A., Bates, N.R., Johnson, R.J., Michaels, A.F., Knap, A.H., 2001. Overview of the US JGOFS Bermuda Atlantic Time-series Study (BATS): a decade-scale look at ocean biology and biogeochemistry. Deep Sea Res. Part II Top. Stud. Oceanogr. 48, 1405–1447. https://doi.org/10.1016/S0967-0645(00)00148-X.
- Stewart, G., Cochran, J.K., Xue, J., Lee, C., Wakeham, S.G., Armstrong, R.A., Masqué, P., Miquel, J.C., 2007. Exploring the connection between <sup>210</sup>Po and organic matter in the

- northwestern Mediterranean. Deep Sea Res. Part I Oceanogr. Res. Pap. 54, 415–427. https://doi.org/10.1016/j.dsr.2006.12.006.
- Stukel, M.R., Aluwihare, L.I., Barbeau, K.A., Chekalyuk, A.M., Goericke, R., Miller, A.J., Ohman, M.D., Ruacho, A., Song, H., Stephens, B.M., Landry, M.R., 2017. Mesoscale ocean fronts enhance carbon export due to gravitational sinking and subduction. Proc. Natl. Acad. Sci. USA 114, 1252–1257. https://doi.org/10.1073/pnas. 1609435114.
- Sukenik, A., Carmeli, Y., Berner, T., 1989. Regulation of fatty acid composition by irradiance level in the Eustigmatophyte *Nannochloropsis sp.* J. Phycol. 25, 686–692. https://doi.org/10.1111/j.0022-3646.1989.00686.x.
- Sun, M.-Y., Zou, L., Dai, J., Ding, H., Culp, R.A., Scranton, M.I., 2004. Molecular carbon isotopic fractionation of algal lipids during decomposition in natural oxic and anoxic seawaters. Org. Geochem. 35, 895–908. https://doi.org/10.1016/j.orggeochem. 2004.04.001.
- Tang, K.W., Jakobsen, H.H., Visser, A.W., 2001. Phaeocystis globosa (Prymnesiophyceae) and the planktonic food web: Feeding, growth, and trophic interactions among grazers. Limnol. Oceanogr. 46, 1860–1870. https://doi.org/10.4319/lo.2001.46.8.1860.
- Teshima, S.-I., 1971. Bioconversion of β-sitosterol and 24-methylcholesterol to cholesterol in marine crustacea. Comp. Biochem. Physiol. Part B Comp. Biochem. 39, 815–822. https://doi.org/10.1016/0305-0491(71)90105-2.
- Tholosan, O., Garcin, J., Bianchi, A., 1999. Effects of hydrostatic pressure on microbial activity through a 2000 m deep water column in the. NW Mediterranean Sea 183, 49–57. https://doi.org/10.3354/meps183049.
- Tolosa, I., Fiorini, S., Gasser, B., Martín, J., Miquel, J.C., 2013. Carbon sources in suspended particles and surface sediments from the Beaufort Sea revealed by molecular lipid biomarkers and compound-specific isotope analysis. Biogeosciences 10, 2061–2087. https://doi.org/10.5194/bg-10-2061-2013.
- Tolosa, I., LeBlond, N., Copin-Montégut, C., Marty, J.-C., de Mora, S., Prieur, L., 2003. Distribution of sterol and fatty alcohol biomarkers in particulate matter from the frontal structure of the Alboran Sea (S.W. Mediterranean Sea). Mar. Chem. 82, 161-183. https://doi.org/10.1016/S0304-4203(03)00051-3.
- Tolosa, I., Miquel, J.-C., Gasser, B., Raimbault, P., Goyet, C., Claustre, H., 2008. Distribution of lipid biomarkers and carbon isotope fractionation in contrasting trophic environments of the South East Pacific. Biogeosciences 5, 949–968. https://doi.org/10.5194/bg-5-949-2008.
- Tyler, P.A., 2003. Ecosystems of the Deep Oceans. Elsevier.
- Versteegh, G.J., Bosch, H.-J., De Leeuw, J.W., 1997. Potential palaeoenvironmental information of C<sub>24</sub> to C<sub>36</sub> mid-chain diols, keto-ols and mid-chain hydroxy fatty acids; a critical review. Org. Geochem. 27, 1–13. https://doi.org/1016/S0146-6380(97) 00063-6.
- Versteegh, G.J.M., Jansen, J.H.F., Schneider, R.R., De Leeuw, J.W., 2000. Mid-chain diols and keto-ols in SE atlantic sediments: a new tool for tracing past sea surface water masses? Geochim. Cosmochim. Acta 64, 1879–1892. https://doi.org/10.1016/ S0016-7037(99)00398-1.
- Vinogradov, M.E., 1968. Vertical Distribution of the Oceanic Zooplankton. Israel Prgram for Science Translations, 1970. Academia Nauk SSSR, Institute Okeanologii, Original.
- Vinogradov, M.E., Shushkina, E.A., Kukina, I.N., 1977. Structural and functional analysis of pelagic communities in equatorial upwelling. Pol. Arch. Hydrobiol 24, 503–526. Volkman, J.K., 2006. Lipid Markers for Marine Organic Matter. In: Volkman, J.K. (Ed.),
- Volkman, J.K., 2006. Lipid Markers for Marine Organic Matter. In: Volkman, J.K. (Ed.) Marine Organic Matter: Biomarkers, Isotopes and DNA. Springer-Verlag, Berlin, pp. 27–70.
- $\label{eq:Volkman} Volkman, J.K., 2003. Sterols in microorganisms. Appl. Microbiol. Biotechnol. 60, \\ 495-506. \ https://doi.org/10.1007/s00253-002-1172-8.$
- Volkman, J.K., 1986. A review of sterol markers for marine and terrigenous organic matter. Org. Geochem. 9, 83–99. https://doi.org/10.1016/0146-6380(86)90089-6.
- Volkman, J.K., Barrett, S.M., Blackburn, S.I., Mansour, M.P., Sikes, E.L., Gelin, F., 1998. Microalgal biomarkers: a review of recent research developments. Org. Geochem. 29, 1163–1179. https://doi.org/10.1016/S0146-6380(98)00062-X.
- Volkman, J.K., Barrett, S.M., Dunstan, G.A., Jeffrey, S.W., 1992. C<sub>30 C3</sub>2 alkyl diols and unsaturated alcohols in microalgae of the class Eustigmatophyceae. Org. Geochem. 18, 131–138. https://doi.org/10.1016/0146-6380(92)90150-V.
- Volkman, J.K., Eglinton, G., Corner, E.D.S., Forsberg, T.E.V., 1980a. Long-chain alkenes and alkenones in the marine coccolithophorid *Emiliania huxleyi*. Phytochemistry 19, 2619–2622. https://doi.org/10.1016/S0031-9422(00)83930-8.
- Volkman, J.K., Gatten, R.R., Sargent, J.R., 1980b. Composition and origin of milky water in the North Sea. J. Mar. Biol. Assoc. United Kingdom 60, 759. https://doi.org/10. 1017/S002531540004042X
- Volkman, J.K., Jeffrey, S.W., Nichols, P.D., Rogers, G.I., Garland3, C.D., 1989. Fatty acid and lipid composition of 10 species of microalgae used in mariculture. J. Exp. Mar. Bio. Ecol. 128, 219–240. https://doi.org/10.1016/0022-0981(89)90029-4.
- Volkman, J.K., Johns, R.B., Gillan, F.T., Perry, G.J., Bavor, H.J., 1980c. Microbial lipids of an intertidal sediment—I. Fatty acids and hydrocarbons. Geochim. Cosmochim. Acta 44, 1133–1143. https://doi.org/10.1016/0016-7037(80)90067-8.
- Volkman, J.K., Tanoue, E., 2002. Chemical and biological studies of particulate organic matter in the ocean. J. Oceanogr. 58, 265–279. https://doi.org/10.1023/ A:1015809708632.
- Wakeham, S.G., 1995. Lipid biomarkers for heterotrophic alteration of suspended particulate organic matter in oxygenated and anoxic water columns of the ocean. Deep Sea Res Part I Oceanogr. Res. Pap. 42, 1749–1771. https://doi.org/10.1016/0967-0637(95)00074-G.
- Wakeham, S.G., 1982. Organic matter from a sediment trap experiment in the equatorial North Atlantic: wax esters, steryl esters, triacylglycerols and alkyldiacylglycerols. Geochim. Cosmochim. Acta 46, 2239–2257. https://doi.org/10.1016/0016-7037(82) 00108 2

- Wakeham, S.G., Canuel, E.A., 1988. Organic geochemistry of particulate matter in the eastern tropical North Pacific Ocean: implications for particle dynamics. J. Mar. Res. 46, 183–213. https://doi.org/10.1357/002224088785113748.
- Wakeham, S.G., Canuel, E.A., 1986. Lipid composition of the pelagic crab *Pleuroncodes planipes*, its feces, and sinking particulate organic matter in the Equatorial North Pacific Ocean. Org. Geochem. 9, 331–343. https://doi.org/10.1016/0146-6380(86)
- Wakeham, S.G., Lee, C., 1989. Organic geochemistry of particulate matter in the ocean: The role of particles in oceanic sedimentary cycles. Org. Geochem. 14, 83–96. https://doi.org/10.1016/0146-6380(89)90022-3.
- Wakeham, S.G., Lee, C., Hedges, J.I., Hernes, P.J., Peterson, M.J., 1997. Molecular indicators of diagenetic status in marine organic matter. Geochim. Cosmochim. Acta 61, 5363–5369. https://doi.org/10.1016/S0016-7037(97)00312-8.
- Walker, N.D., Leben, R.R., Balasubramanian, S., 2005. Hurricane-forced upwelling and chlorophyll a enhancement within cold-core cyclones in the Gulf of Mexico. Geophys. Res. Lett. 32, 1–5. https://doi.org/10.1029/2005GL023716.

- Walsh, I., Fischer, K., Murray, D., Dymond, J., 1988. Evidence for resuspension of rebound particles from near-bottom sediment traps. Deep Sea Res Part A. Oceanogr. Res. Pap. 35, 59–70. https://doi.org/10.1016/0198-0149(88)90057-X.
- Weber, T., Cram, J.A., Leung, S.W., DeVries, T., Deutsch, C., 2016. Deep ocean nutrients imply large latitudinal variation in particle transfer efficiency. Proc. Natl. Acad. Sci. 113, 8606–8611.
- Wilson, A.M., 2016. Lateral transport of suspended particulate matter in nepheloid layers along the Irish continental margin-a case study of the Whittard Canyon, north-east Atlantic Ocean. National University of Ireland.
- Wolf, B.M., Niedzwiedzki, D.M., Magdaong, N.C.M., Roth, R., Goodenough, U., Blankenship, R.E., 2018. Characterization of a newly isolated freshwater Eustigmatophyte alga capable of utilizing far-red light as its sole light source. Photosynth. Res. 135, 177–189.
- Zeng, Y.B., 1988. Geochemical Studies of Microbial Lipids. Ph.D. Thesis. Univeristy of Bristol.